

Lake water temperature modeling in an era of climate change: data sources, models, and future prospects

Article

Published Version

Creative Commons: Attribution 4.0 (CC-BY)

Open Access

Piccolroaz, S., Zhu, S., Ladwig, R., Carrea, L. ORCID: <https://orcid.org/0000-0002-3280-2767>, Oliver, S., Piotrowski, A. P., Ptak, M., Shinohara, R., Sojka, M., Woolway, R. I. ORCID: <https://orcid.org/0000-0003-0498-7968> and Zhu, D. Z. (2024) Lake water temperature modeling in an era of climate change: data sources, models, and future prospects. *Review of Geophysics*, 62 (1). e2023RG000816. ISSN 1944-9208 doi: <https://doi.org/10.1029/2023RG000816> Available at <https://centaur.reading.ac.uk/115202/>

It is advisable to refer to the publisher's version if you intend to cite from the work. See [Guidance on citing](#).

To link to this article DOI: <http://dx.doi.org/10.1029/2023RG000816>

Publisher: Wiley

All outputs in CentAUR are protected by Intellectual Property Rights law, including copyright law. Copyright and IPR is retained by the creators or other copyright holders. Terms and conditions for use of this material are defined in the [End User Agreement](#).

www.reading.ac.uk/centaur

CentAUR

Central Archive at the University of Reading

Reading's research outputs online

Reviews of Geophysics®



INVITED ARTICLE

10.1029/2023RG000816

Lake Water Temperature Modeling in an Era of Climate Change: Data Sources, Models, and Future Prospects

S. Piccolroaz¹ , S. Zhu², R. Ladwig³ , L. Carrea⁴, S. Oliver⁵ , A. P. Piotrowski⁶, M. Ptak⁷ , R. Shinohara⁸ , M. Sojka⁹ , R. I. Woolway¹⁰ , and D. Z. Zhu¹¹ 

¹Department of Civil, Environmental and Mechanical Engineering, University of Trento, Trento, Italy, ²College of Hydraulic Science and Engineering, Yangzhou University, Yangzhou, China, ³Center for Limnology, University of Wisconsin-Madison, Madison, WI, USA, ⁴Department of Meteorology, University of Reading, Reading, UK, ⁵U.S. Geological Survey, Upper Midwest Water Science Center, Madison, WI, USA, ⁶Institute of Geophysics, Polish Academy of Sciences, Warsaw, Poland, ⁷Department of Hydrology and Water Management, Adam Mickiewicz University, Poznań, Poland, ⁸National Institute for Environmental Studies, Tsukuba, Japan, ⁹Department of Land Improvement, Environmental Development and Spatial Management, Poznań University of Life Sciences, Poznań, Poland, ¹⁰School of Ocean Sciences, Bangor University, Bangor, UK, ¹¹Department of Civil and Environmental Engineering, University of Alberta, Edmonton, AB, Canada

Key Points:

- Lake thermal dynamics are central in shaping mixing processes and the health of aquatic ecosystems, and climate change alters these dynamics
- Mathematical models are essential to understand past and project future climate change impacts on lake thermal dynamics
- This study reviews lake water temperature modeling, covering concepts, data sources, and model evaluation for applications across disciplines

Correspondence to:

S. Piccolroaz and S. Zhu,
s.piccolroaz@unitn.it;
slzhu@yzu.edu.cn

Citation:

Piccolroaz, S., Zhu, S., Ladwig, R., Carrea, L., Oliver, S., Piotrowski, A. P., et al. (2024). Lake water temperature modeling in an Era of climate change: Data sources, models, and future prospects. *Reviews of Geophysics*, 62, e2023RG000816. <https://doi.org/10.1029/2023RG000816>

Received 27 JUN 2023
Accepted 21 DEC 2023

Author Contributions:

Conceptualization: S. Piccolroaz, S. Zhu
Data curation: R. Ladwig, L. Carrea
Formal analysis: S. Piccolroaz, L. Carrea
Investigation: S. Piccolroaz, S. Zhu, R. Ladwig, A. P. Piotrowski
Methodology: S. Piccolroaz, S. Zhu, R. Ladwig, A. P. Piotrowski
Project Administration: S. Piccolroaz, S. Zhu
Software: R. Ladwig
Supervision: S. Piccolroaz
Visualization: S. Piccolroaz, L. Carrea
Writing – original draft: S. Piccolroaz, S. Zhu, R. Ladwig

Abstract Lake thermal dynamics have been considerably impacted by climate change, with potential adverse effects on aquatic ecosystems. To better understand the potential impacts of future climate change on lake thermal dynamics and related processes, the use of mathematical models is essential. In this study, we provide a comprehensive review of lake water temperature modeling. We begin by discussing the physical concepts that regulate thermal dynamics in lakes, which serve as a primer for the description of process-based models. We then provide an overview of different sources of observational water temperature data, including in situ monitoring and satellite Earth observations, used in the field of lake water temperature modeling. We classify and review the various lake water temperature models available, and then discuss model performance, including commonly used performance metrics and optimization methods. Finally, we analyze emerging modeling approaches, including forecasting, digital twins, combining process-based modeling with deep learning, evaluating structural model differences through ensemble modeling, adapted water management, and coupling of climate and lake models. This review is aimed at a diverse group of professionals working in the fields of limnology and hydrology, including ecologists, biologists, physicists, engineers, and remote sensing researchers from the private and public sectors who are interested in understanding lake water temperature modeling and its potential applications.

Plain Language Summary Lake thermal dynamics are fundamental in controlling mixing processes and have significant implications for biological and geochemical processes. Consequently, the impacts of climate change on these dynamics can have severe consequences for the health of lakes and their aquatic ecosystems. In this context, mathematical models are essential for understanding the potential effects of future climate change on lake thermal dynamics and related processes. This manuscript offers a comprehensive review of lake water temperature modeling. It covers the fundamental physical concepts that govern thermal dynamics in lakes and provides an overview of various sources of observational water temperature data, including in situ monitoring and satellite data used in these models. The study evaluates different types of lake water temperature models, including statistical, process-based, and hybrid models. It explores emerging modeling approaches such as forecasting, digital twins, combining process-based modeling with deep learning, ensemble modeling, and climate-lake models coupling. Model performance is also discussed, highlighting suggested evaluation metrics and providing a comprehensive analysis of the state-of-the-art optimization methods to assess model accuracy. This review targets researchers in limnology, hydrology, ecology, biology, physics, engineering, and remote sensing from the private and public sectors interested in lake water temperature modeling and its applications.

1. Introduction

Lakes are a major component of the hydrosphere which are able to accumulate and transfer energy and matter to and from other spheres of the environment. Lakes, especially the largest ones, have higher thermal inertia and longer residence times than those of other inland water bodies such as rivers and lagoons, and thus they act as buffers in the inland waters transport network. As such, they play an important role in the global water cycle and

© 2024. The Authors.

This is an open access article under the terms of the [Creative Commons Attribution License](https://creativecommons.org/licenses/by/4.0/), which permits use, distribution and reproduction in any medium, provided the original work is properly cited.

Writing – review & editing: S. Piccolroaz, S. Zhu, R. Ladwig, L. Carrea, S. Oliver, A. P. Piotrowski, M. Ptak, R. Shinohara, M. Sojka, R. I. Woolway, D. Z. Zhu

in regulating biodiversity, the availability and quality of water resources, and the provision of ecosystem services. In many regions of the world, lakes are of key significance in purely environmental terms, and also through their relevance for human life and socioeconomic activities. Human activities contribute to the ongoing alteration of the quality of inland water bodies. For example, over-exploitation of water resources causes the progressive, and sometimes abrupt, shrinking of lakes. This is an emergent issue especially in drylands (Klein et al., 2014; H. Liu et al., 2019) that leads to, for example, the disappearing of the Aral Sea. A decrease in lake water storage across the globe is also an effect of climate change (E. A. Webb & Liljedahl, 2023; F. Yao et al., 2023; G. Zhao et al., 2022), which has motivated a growing need for models that predict lake water levels (Ozdemir et al., 2023).

Recent studies have suggested a rapid and abrupt change in water temperature, ice cover, water quality, and hydrobiological conditions in lakes worldwide, with clear regime shifts observed in some cases (North et al., 2013; Tan et al., 2018; Van Cleave et al., 2014; W. Wang et al., 2023; Woolway, Kraemer, et al., 2020), driven by climate change. Specifically, changes in meteorological conditions (e.g., air temperature) are the most closely associated with those observed in lakes. Based on lake model projections, the anticipated evolution of climate change under various Representative Concentration Pathways (RCPs) suggests that the current trajectory will persist in the coming decades. This is true when considering the most optimistic future emission scenarios (e.g., RCP2.6), and it can be even worse under moderate to severe future emission scenarios (e.g., RCP4.5 and RCP8.5) (Golub et al., 2022; Kraemer et al., 2021; Maberly et al., 2020; Merz et al., 2023; Piccolroaz, Zhu, et al., 2021; Woolway, 2023; Woolway, Jennings, et al., 2021). Shifts in lake thermal regimes can have extensive and potentially profound impacts on lake ecosystems. Shorter winters (e.g., ice cover) and an earlier onset and strengthening of summer stratification are projected to occur this century (see e.g., Anderson et al., 2021; Fenocchi et al., 2018; Mullin et al., 2020; Piccolroaz, Zhu, et al., 2021; Shatwell et al., 2019; Woolway, Sharma, et al., 2021; Xue et al., 2022). These are expected to be accompanied by a reduction of lake turnovers and eventual mixing regime shifts (Shatwell et al., 2019; Woolway & Merchant, 2019; Wood et al., 2023), which can generate complex physical, chemical, and biological feedback mechanisms and modify the lake ecosystem functioning (Mesman et al., 2021). Deep mixing in lakes is crucial for redistributing nutrients throughout the water column, maintaining oxygen levels in deep layers and preventing a deoxygenation of bottom waters which pose a threat to aquatic fauna and can facilitate the release of phosphorus from lake sediments (Hupfer & Lewandowski, 2008). The progressive warming, depletion of dissolved oxygen, and increase of nutrient concentrations in deep layers have already been observed in numerous lakes worldwide. In many cases, these factors occur simultaneously, posing significant challenges to lake ecosystems (see e.g., Jane et al., 2023; Kong et al., 2023; North et al., 2014; Rempfer et al., 2010; Straile et al., 2003) and highlighting the importance of conducting further research in the field of lake thermal dynamics and regimes.

Water temperature is one of the most commonly used indicators to assess the impact of climate change on the physical and ecological functioning of lakes. Indeed, water temperature is one of the most widely monitored physical characteristic of lakes. Most lake temperature records start during the second half of the 20th century or in the 21st century, although for some lakes regular measurements of water temperatures are available for even a longer period (see e.g., some Austrian lakes, Dokulil et al., 2006; Livingstone & Dokulil, 2001; some lakes in the English Lake District, Feuchtmayr et al., 2012; Lake Peipsi in Estonia/Russia, Kangur et al., 2020, 2021; Lake Mendota in the USA Robertson, 2016; see also Pilla et al., 2021). The relatively large availability of lake water temperature observations is due to both (a) the relative ease and affordability of acquiring this type of measurement and (b) the central role of water temperature in controlling most of the physical and bio-chemical processes in a lake (Mollema & Antonellini, 2016; Woolway, Kraemer, et al., 2020). It is sufficient to cite that water temperature is at the basis of the classification of lakes' mixing regimes starting from the seminal contribution by Hutchinson and Löffler (1956) and its revised version by (W. M. Lewis, 1983) until more recent classifications (Kirillin & Shatwell, 2016; Yang et al., 2021). As such, water temperature is increasingly used as one of the main indicators to quantify and communicate the impact of climate change on inland water bodies.

Technological advancements have made temperature monitoring more efficient and accurate through (a) increasing availability of remote sensing data starting from the 1980s and their use for lakes (Carrea, Crétaux, et al., 2022; Layden et al., 2015; Merchant & MacCallum, 2018; Schneider & Hook, 2010; Schneider et al., 2019), with improving sensors (higher stability, better traceability chain (Smith et al., 2021), and finer spatial/temporal resolution) and refined retrieval techniques tracking uncertainties from the thermal noise of the instrument to the uncertainty in the retrieval (Carrea, Crétaux, et al., 2023), (b) easier access to low-cost sensors that promoted the building of self-made systems for in situ monitoring (Demetillo et al., 2019; Marcé et al., 2016), and (c) general

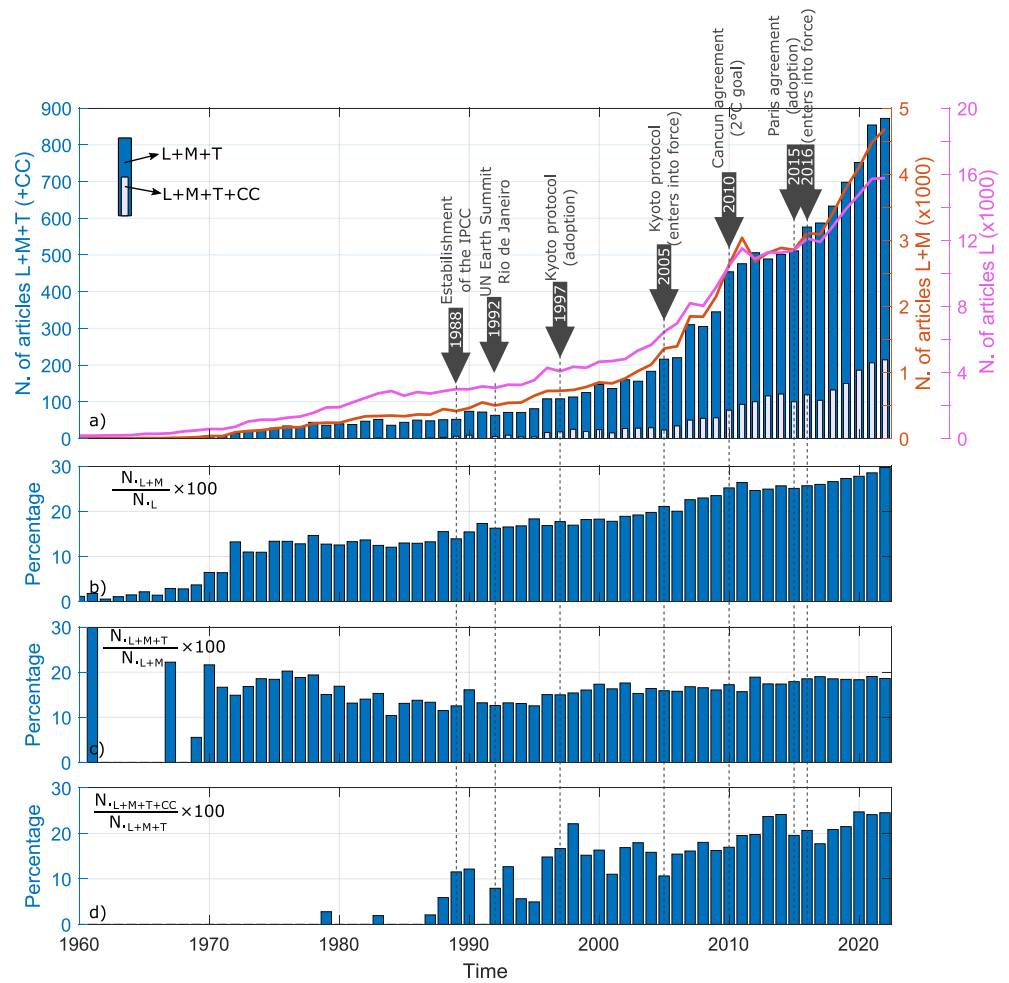


Figure 1. (a) Number of articles published per year from 1960 to 2022 containing the term “lake*” (L) or the terms “lake*” (L) and “model*” or “simulation” (M) in title, abstract and keywords, with a specific focus on those also containing the terms “temperature” (T) and “climate change” or “climatic change” (CC). The milestones in climate change mitigation and adaptation summits are also reported, including the establishment of the Intergovernmental Panel on Climate Change (IPCC), the United Nations (UN) Earth Summit, and various climate protocols and agreements. The percentages of articles dealing with modeling (L + M) relative to all lake studies (L), modeling lake temperature (L + M + T) relative to all lake modeling studies (L + M), and lake temperature modeling and climate change (L + M + T + CC) relative to all the lake temperature modeling studies (L + M + T) is also reported in subplots (b), (c), and (d). Source: Scopus, 19 April 2023.

improvement of the sensors' performance and accuracy (Sommer et al., 2013; Van Haren et al., 2001). Parallel to this, new types of instruments have been produced and are increasingly used as for example, turbulence microprofilers (Piccolroaz, Fernández-Castro, et al., 2021; Sepúlveda Steiner et al., 2021), autonomous profilers (Rainville & Pinkel, 2001; Ward et al., 2014), underwater gliders (Austin, 2013; Sepúlveda Steiner et al., 2023) and fiber-optics (Duraibabu et al., 2017; Selker et al., 2006), thus allowing a larger spectrum of possible monitoring applications. Accordingly, lake water temperature data are of different types, in terms of measurement technique (in situ sampling vs. remote sensing), temporal resolution (periodic or spot samplings data vs. continuous data) and spatial coverage (point data vs. maps passing through profiles and transects).

Exploring the dynamics of water temperature is highly beneficial for understanding past and current states of lakes and forecasting the possible trajectories lakes may take in the future. Mathematical models play a crucial and powerful role in projecting the impact of climate change on future lake mixing and thermal dynamics. Thanks to the increasing availability of data and progress in computational technology, the limnological community contributed to the development and application of a number of water temperature models. Figure 1a reports the number of scientific publications from 1960 to 2022 containing the term “lake*” (L) and those containing

also the terms “model*” or “simulation” (L + M) in title, abstract and keywords (* being a truncation wildcard operator; right y-axis). Among the latter group we identified those also containing the terms “temperature” (L + M + T, bars in the left y-axis) and “climate change” or “climatic change” (L + M + T + CC, inner bars in the left y-axis). The scientific production was limited before the 1960s, after which it underwent an exponential trend with a marked increase after mid of 2000s. The fraction of lake studies (L) containing the search words “model*” or “simulation” (L + M) shows a clear boost in the early 1970s, consistent with the introduction of the personal computer and the progress in high-performance scientific computing, followed by a steady increase (Figure 1b). In 2022 about one third of L studies included the terms “model*” or “simulation”. A similar trend has been observed in the closely related field of integrated water resource assessment and modeling, as reported by Zare et al. (2017). The fraction of L + M studies containing the search word “temperature” (L + M + T) was constantly around 15% (Figure 1c), with a small decline down to ~10% around 1980s followed by a steady increase up to 20% in the last decade. The publications that also contain the search terms “climate change” or “climatic change” (L + M + T + CC) first appeared in 1987 and become more widespread after the 1990s, consistent with the timeline of climate change mitigation and adaptation summits (Figure 1a). Since then, the percentage of these studies relative to the lake temperature modeling studies (L + M + T) has been steadily increased up to more than 20% in recent years (Figure 1d).

The available modeling studies span a wide range of applications (see e.g., T. Jia et al. (2022) for a recent review) from the hindcast of historical lake water temperature conditions (Hegerl et al., 2018; Piccolroaz et al., 2020) to the forecast of lake water temperature over seasonal (Mercado-Bettín et al., 2021) to climatological time scales (Golub et al., 2022). Indeed, depending on the type of model, water temperature simulations can cover different extents (local vs. global lakes), refer to different temporal scales (from daily to climatological time scales) and account for various spatial dimensions (from zero-dimensional lake surface water temperature (LSWT) models to fully three-dimensional hydro-thermodynamic models).

In this contribution, we review lake water temperature models, and summarize their advantages and limitations and the data sources required to drive them. Here, we distinguish between (a) models used to predict LSWT, which is increasingly used as an indicator of global warming, and (b) models to reproduce the vertical distribution of lake water temperature that describe vertical stratification and mixing, with a particular focus on one-dimensional (1D) models. In Section 2, we discuss the physics regulating thermal dynamics in lakes as a primer for the description of physical or process-based models. In Section 3, we provide an overview of the different sources of observational water temperature data used in the field of lake water temperature modeling. The classification and a detailed review of the water temperature models available in the literature is provided in Section 4. Model performance and optimization methods are discussed in Section 5, whereas emerging modeling approaches are examined in Section 6. Finally, the main conclusions are drawn in Section 7.

2. Heat Budget and Thermodynamics of Lakes

Any change in lake water temperature is determined by the imbalance in heat gains and losses of the lake, that is, by the net heat flux passing through the boundaries between the lake and the surrounding environment. The direction and magnitude of the net heat flux change over multiple time scales: from daily (day-night cycles), to seasonal (depending on the climatic conditions), and climatological (due to long-term trends). Most of the heat fluxes occur at the lake surface, between the lake and the overlying atmosphere, and are linked with natural processes. However, heat exchanges can also occur below the surface (e.g., thermal vents, groundwater-lake interactions) and may be due to anthropogenic activities (e.g., sewage inflows, selective withdrawals; see Figure 2). The net heat flux passing across the lake boundaries (H_{net} , W/m²) can be summarized as:

$$H_{net} = H_{s,net} + H_{a,net} + H_w + H_c + H_e + H_p \pm H_{i/o}, \quad (1)$$

that is the combination of net short-wave solar radiation ($H_{s,net}$), net long-wave radiation emitted from the sky ($H_{a,net}$) and from the water surface (H_w), sensible (H_c) and latent (H_e) heat fluxes, and advected fluxes due to precipitation (H_p) and inflows/outflows ($H_{i/o}$). The first two terms in the equation account for the short-wave and long-wave reflectivities (albedoes) of the water, denoted by r_s and r_a in Figure 2. Specifically, $H_{s,net}$ and $H_{a,net}$ are calculated as $(1 - r_s)H_s$ and $(1 - r_a)H_a$, respectively, where H_s and H_a are the incident radiations. We note that in the case of ice-covered lakes, the ice acts as insulation between the lake water and the atmosphere and influences surface albedo, hence it impacts the thermal dynamics of the lakes (for a more in-depth physical review,

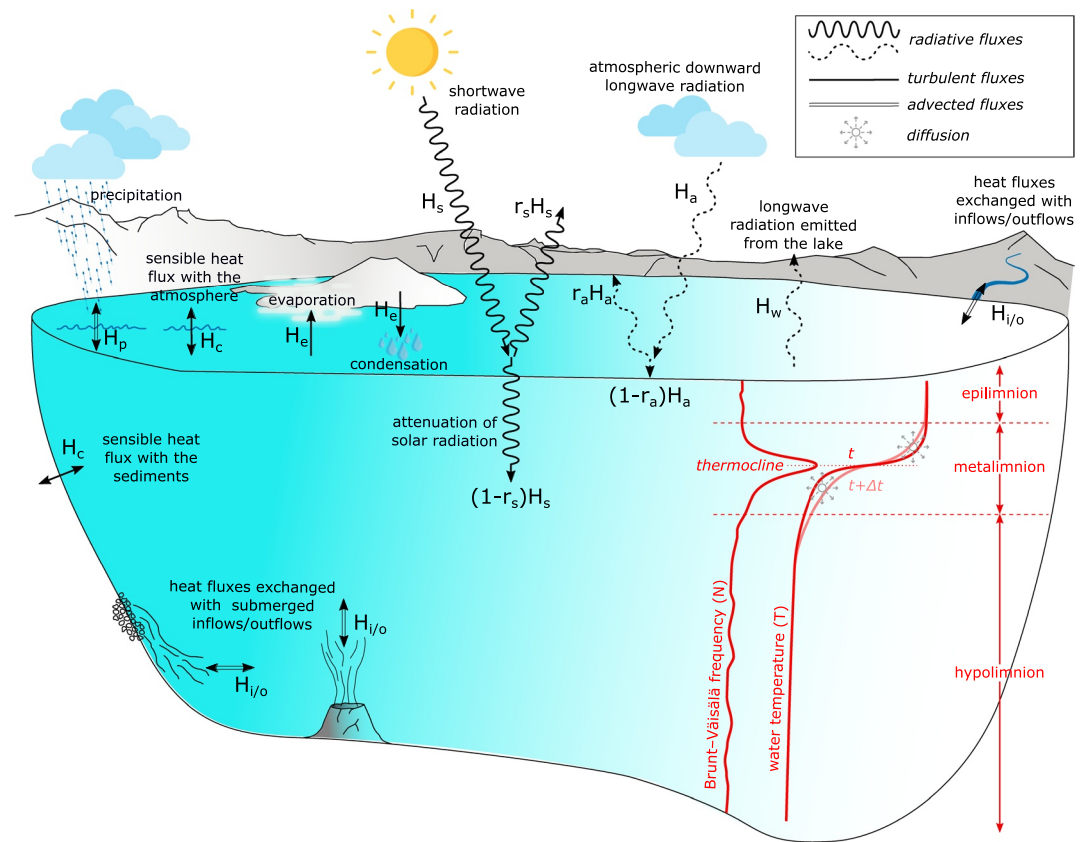


Figure 2. Schematic of the main heat flux components contributing to the heat balance of a lake. The subdivision of the lake volume into epilimnion, metalimnion and hypolimnion is also shown, assuming an hypothetical temperature profile and corresponding Brunt-Väisälä frequency profile. The lake in the schematic is inspired by Crater Lake and its Wizard Island (Oregon, USA).

please refer to Kirillin et al. (2012)). Hereafter, all heat flux components (expressed in W/m^2) are defined as positive when entering the lake (warming). The first three terms are referred to as radiative fluxes, the terms H_e and H_c as turbulent fluxes which depend on wind speed, air-water temperature difference, near surface humidity and atmospheric stability, and the last two terms as advective fluxes. All the radiative and turbulent fluxes are boundary fluxes acting at the water surface, while short-wave radiation penetrates and is attenuated through the water column thus acting as a volumetric source of heat (Bouffard & Wüest, 2019). We notice that it is a common practice to calculate all the heat flux terms in Equation 1 by dividing by the surface area of the lake A_0 , as it is there where most of the heat exchanges occur (Imboden & Wüest, 1995). This applies also to the advective heat exchanged with inflows and outflows, which can be written as:

$$H_{i/o} = \frac{1}{A_0} \rho c_p Q_{i/o} T_{i/o}, \quad (2)$$

where ρ is the density of water, c_p its heat capacity, $Q_{i/o}$ is the inflows/outflows discharge and $T_{i/o}$ its temperature. Equation 2 provides the module of $H_{i/o}$, its sign being positive for inflows and negative for outflows. The water temperature of outflows can be taken equal to the LSWT for surface outlets, and equal to lake water temperature at a given depth for withdrawals or groundwater seepage. Groundwater recharge is generally computed assuming that T_i is equal to the mean annual air temperature (Winter et al., 2003). We note that if the effect of inflows and outflows is included in the heat budget, the volume balance of the lake must be solved as well, unless it is reasonable to assume that the inflows balance the outflows (i.e., $Q_i = Q_o = Q$) and the lake does not undergo volume changes. In this case, Equation 2 can be used to evaluate the net inflows/outflows heat flux as follows: $H_{i/o,net} = \frac{1}{A_0} \rho c_p Q (T_i - T_o)$. In many practical applications, advective heat fluxes associated with inflows/outflows are neglected (Fukushima et al., 2022; Rahaghi et al., 2018), which can be a reasonable assumption for

some but, clearly, not all large lakes (Raman Vinna et al., 2018), but not for small lakes with short residence times primarily controlled by riverine and groundwater exchanges (Carmack, 1979). This is true also for the heat flux associated with precipitation (H_p), although in some cases it can be relevant (Rooney et al., 2018) depending on the rainfall intensity and temperature difference between the rain and lake. The term H_p is normally quantified by assuming the precipitation temperature to be equivalent to the wet bulb temperature at the time precipitation occurred (Sturrock et al., 1992). Finally, we note that the sensible heat flux (H_c) term also includes the heat flux exchanged by conduction at the water-sediment interface. Although this term is generally small due to the low thermal diffusivity of the lake sediments, it is important for many lakes, especially for shallow lakes (de la Fuente & Meruane, 2017), where the ratio of sediment interface-to-lake volume is larger, and in ice-covered lakes, where also the heat fluxes across the lake surface are limited thus resulting in one of the main drivers for under-ice circulation and mixing (Kirillin et al., 2012). On average, the heat transfer is from lake water to bottom sediments in summer and from bottom sediments to lake water in winter, thus adding significant thermal inertia to the water column (Fang & Stefan, 1996). However, this heat exchange is very dynamic and changes direction frequently, particularly in transparent shallow lakes and littoral areas where sediments are heated by solar radiation directly. In lakes with volcanic or tectonic origins, the water-sediment flux is primarily governed by the geothermal heat flux, which can be especially relevant (Boehrer et al., 2013; Wood et al., 2023). We refer the interested reader to (Schmid & Read, 2022) for a recent overview of the heat budget of lakes, which provides a quantitative comparison among the different heat flux components for a temperate and a tropical lake (the radiative fluxes being the dominant terms, see also Imboden and Wüest (1995)) and contains some selected references to case studies that may be of interest to deepen some aspects of the topic.

The heat flux components listed in Equation 1 can be measured directly or calculated using equations derived from well-known principles of physics (e.g., the Stefan-Boltzman law for the long-wave heat fluxes), fundamental trigonometric principles of astronomy (e.g., to calculate extraterrestrial short-wave radiation under clear sky conditions and flat topography), or extensively validated empirical relationships (e.g., the Dalton's law for the evaporative heat flux). Detailed reviews of the most established literature parameterizations used to quantify the surface heat fluxes can be found in Henderson-Sellers (1986) and J. L. Martin and McCutcheon (1999), among others, and a script for calculating the surface energy fluxes according to these and other methodologies has been provided by Woolway et al. (2015). Additionally, many lake models are published with large sections and appendices describing the details of the heat flux equations and the decision trees for their implementation (Cole & Wells, 2006; Goudsmit et al., 2002; Hamrick, 1992; Hipsey et al., 2019; Piccolroaz et al., 2013). Here, we provide only the key equations that are needed for the comprehension of the modeling sections.

Following Edinger et al. (1968), we refer to the sum of $H_{s,net}$ and $H_{a,net}$ as the absorbed radiation, which is independent of the surface water temperature T_s , and that can be measured or computed from meteorological observations (see e.g., Henderson-Sellers, 1986). All the other terms depend in different ways on T_s , air temperature, water vapor pressure, wind speed, and other variables as explained below.

The emitted long-wave radiation H_w is described by the Stefan-Boltzman's law:

$$H_w = -\epsilon_w \sigma (T_s + T_0)^4, \quad (3)$$

where T_s is the surface water temperature in °C, $T_0 = 273.15$, ϵ_w is the emissivity of water (i.e., about 0.97), and σ is the Stefan-Boltzmann constant (i.e., $5.67 \times 10^{-8} \text{ W m}^{-2} \text{ K}^{-4}$). The minus sign indicates that the heat flux is from the lake to the atmosphere. This equation can be simplified by taking the Taylor expansion of the above equation around the origin and truncating it at the second-order term since $T_s \ll T_0$, to give:

$$H_w \approx -\epsilon_w \sigma T_0^4 \left[1 + 4 \left(\frac{T_s}{T_0} \right) + 6 \left(\frac{T_s}{T_0} \right)^2 \right]. \quad (4)$$

The rate of heat loss by evaporation H_e can be expressed as a simple bulk formula:

$$H_e = -L \rho f(W) (e_s - e_a), \quad (5)$$

where L is the latent heat of evaporation, the $f(W)$ is a transfer function that can be chosen from a wide range of empirical relationships essentially depending on the wind speed W , and $(e_s - e_a)$ is the difference between the saturated vapor pressure at the surface water temperature and the actual vapor pressure at the temperature of the

air. Often, this equation is simplified by approximating the relationship between the saturation vapor pressure of water and the water temperature by a linear function of the form:

$$(e_s - e_a) = \delta_s(T_s - T_d), \quad (6)$$

where T_d represents the dew point temperature (i.e., the temperature the air needs to be cooled, at constant pressure and constant water vapor content, to become saturated with water vapor), and the slope δ of the linear approximation can be quantified using observed values of T_s and T_d and reading values of e_s and e_a from a curve of vapor pressure versus temperature.

Introducing the Bowen ratio $B = H_c/H_e = \xi \frac{T_s - T_d}{e_s - e_a}$ as the ratio between sensible and latent heat fluxes where ξ is the psychrometric constant which depends on atmospheric pressure and temperature, the heat flux by conduction is given by:

$$H_c = -L\rho\xi f(W)(T_s - T_a). \quad (7)$$

By substituting Equations 3–7 into Equation 1 and neglecting the effects of precipitation, inflows/outflows, and water-sediment exchanges, the net heat exchange can be expressed as:

$$\begin{aligned} H_{net} \approx H_{s,net} & \quad + H_{a,net} \\ - \epsilon_w \sigma T_0^4 \left[1 + 4 \left(\frac{T_s}{T_0} \right) + 6 \left(\frac{T_s}{T_0} \right)^2 \right] & \\ - L\rho f(W) [\delta_s(T_s - T_d) + \xi(T_s - T_a)] & \end{aligned} \quad (8)$$

This is an approximate estimate of H_{net} . To obtain the precise quantification of the heat fluxes contributing to H_{net} , specific coefficients and correction functions should be taken into account. For example, atmospheric stability should be considered in the estimation of the turbulent fluxes. Ideally, these coefficients and correction functions are known, but in practice, they are often case-study-dependent and need to be determined through calibration (Rahaghi et al., 2018). One way to do this is by writing the heat balance of the lake, which equates the change in time of the total heat content of the lake (HC) with the net heat flux exchanged with the surrounding environment:

$$\frac{d}{dt}(HC) = \frac{d}{dt} \int_V \rho c_p T(z, t) dV = A_0 H_{net}, \quad (9)$$

where t is time and z is the vertical coordinate, T is the water temperature of the lake, V its volume and A_0 its surface area. If water temperature profiles are available in space and time, Equation 9 can be used to tune the calibration parameters included in the different components of H_{net} (Fukushima et al., 2022; Rahaghi et al., 2018). The same heat balance can be used to quantify unknown heat flux components (Sturrock et al., 1992; Winter et al., 2003), by relying on measured water temperature profiles to calculate HC and on measurements or estimations (using equations with predefined or best guess parameters' values) of the other heat fluxes.

When the net heat flux H_{net} is known, Equation 9 can be used to evaluate the change in time of the HC of the lake. Taking V equal to the total volume of the lake, this provides the change in time of the average water temperature of the lake T_{lake} . Likewise, considering V equal to the volume of surface well-mixed layer V_s , it is possible to calculate the change in time of the average water temperature within this layer, reasonably assuming that during the stratified period vertical transfer of heat below the thermocline is inhibited (see e.g., Toffolon et al., 2022). In this case, if we assume that the heat gain/loss associated to the temporal variation of the volume of the surface well-mixed layer is of minor importance, then the volume term can be extracted from the time derivative and the change in time of water temperature in this layer (T_s) can be expressed as:

$$\frac{dT_s}{dt} = \frac{A_0}{\rho c_p V_s} H_{net} = \frac{1}{\rho c_p D_s} H_{net}, \quad (10)$$

where $D_s = V_s/A_0$ is the average depth of the surface well-mixed layer. This is the reference equation at the basis of physically-based zero-dimensional (0D) or half-dimensional (0.5D) lake temperature models (see Sections 4.1 and 4.2).

The spatial variability of water temperature is shaped by the transport and mixing processes taking place within the lake, which are primarily determined by the fluxes of mechanical energy and by lake morphology. Spatial and

temporal changes in water temperature are described by the advection-diffusion equation for temperature T that, using Einstein summation notation where repeated indices imply the summation over all the values of the index ($j = 1, 2, 3$), reads:

$$\frac{\partial T}{\partial t} + u_j \frac{\partial T}{\partial x_j} = \frac{S_T}{\rho c_p} + D \frac{\partial^2 T}{\partial x_j^2}, \quad (11)$$

where S_T is a source or sink term for heat production or consumption, u_j is the j th component of the velocity along the x_j direction, D is the molecular diffusivity of temperature, and the second term on the left-hand side represents the advective term. As all natural water bodies, lakes are turbulent environments, where the fine-scale structures of the flow embedded in the advective term of Equation 11 generates turbulent mixing that is usually much faster than molecular diffusion (Fisher et al., 1979; Imboden & Wüest, 1995). Accounting for turbulence explicitly would require solving the equations expressing conservation of mass and conservation of momentum (i.e., the Navier-Stokes equation) and the advection-diffusion equation on fine computational grids and using small time steps (Direct Numerical Simulation—DNS), to an extent that is normally prohibitive for environmental applications. A classical way to account for turbulent fluxes in a computationally affordable way is through Reynolds' decomposition, which consists in simplifying the governing equations by statistically splitting variables such as velocity and temperature into a temporal mean component (representative of the mean, large scale advection and denoted with an overbar) and a fluctuating term about the mean component (accounting for small-scale turbulent fluctuations and denoted with a prime '). For the generic variable f , the Reynolds' decomposition reads: $f = \bar{f} + f'$. By substituting each variable in Equation 11 by the sum of the mean and perturbation components and by taking the time-average of the resulting equation (we refer to classical fluid mechanics books such as e.g., Kundu & Cohen, 2012 for the details), the advection-diffusion equation for temperature can be rewritten into:

$$\frac{\partial \bar{T}}{\partial t} + u_j \frac{\partial \bar{T}}{\partial x_j} = \frac{S_T}{\rho c_p} + \frac{\partial}{\partial x_j} \left(D \frac{\partial \bar{T}}{\partial x_j} - \overline{u'_j T'} \right), \quad (12)$$

in which the rules $\overline{\bar{f}} = \bar{f}$ and $\overline{f'} = 0$ have been used. This is the advection-diffusion equation valid for the mean flow and accounting for transport of water temperature due to turbulent mixing through the non-linear term $u'_j T'$. The unknown higher-order correlations between fluctuating velocity and temperature introduced by this term can be approximated using lower-order closure schemes. The simplest approach is the use of a first-order local closure scheme according to the so-called eddy formulation where the turbulent flux of temperature is modeled as being proportional to the local gradient of the mean temperature through a positive coefficient D_j^T called eddy diffusion of temperature:

$$\overline{u'_j T'} = -D_j^T \frac{\partial \bar{T}}{\partial x_j}. \quad (13)$$

From this it follows that the turbulent fluxes of temperature, as well as of any other scalar property, flows down the local gradient of the mean temperature, analogous to molecular transport (see Fick's first law). Since the eddy diffusivity is typically much larger than its molecular counterpart, the eddy formulation allows to transform Equation 12 by neglecting molecular diffusion (but assuming it as the lower bound of D_j^T , that is $D_j^T \geq D$) into:

$$\frac{\partial \bar{T}}{\partial t} + u_j \frac{\partial \bar{T}}{\partial x_j} = \frac{S_T}{\rho c_p} + \frac{\partial}{\partial x_j} \left(D_j^T \frac{\partial \bar{T}}{\partial x_j} \right). \quad (14)$$

To solve this equation, the associated flow field is required to quantify the advective heat exchanges and determine the eddy diffusivity of temperature. This can be done by solving the three- or two-dimensional (3D or 2D) conservation of mass and momentum equations or, in many practical applications, through reducing the problem to a 1D diffusion equation along the vertical direction, neglecting advective fluxes and introducing empirical algebraic models to describe eddy diffusivity and vertical mixing (see Sections 4.3 and 4.4, respectively).

3. Water Temperature Monitoring Approaches

Water temperature is one of the most widely monitored characteristic of lakes. Typically water temperature is routinely measured by various governmental agencies, universities and companies in thousands of lakes around

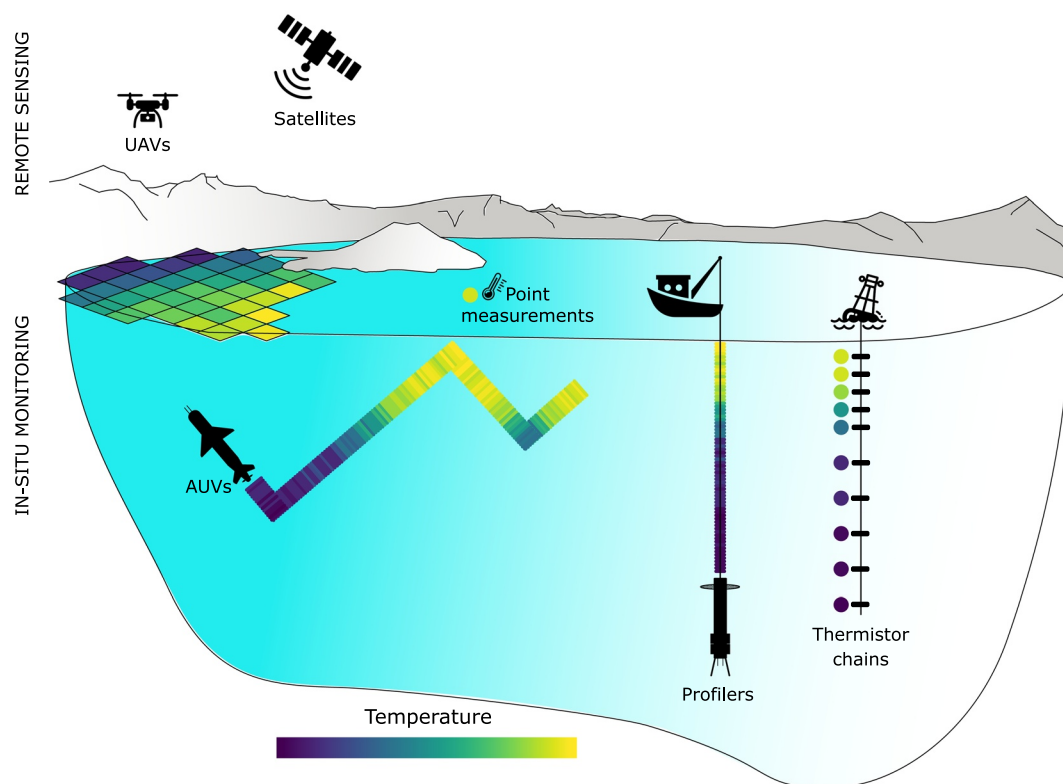


Figure 3. Overview of the main methodologies used to collect water temperature data in a lake.

the world. Water temperature records, however, are different in terms of type of collected data and the instruments used to collect them. As a first level classification, we can distinguish between *in situ* monitoring and *remote sensing* and then between *manual* and *automatic* measurements. Depending on the considered monitoring methodology, the spatial, temporal, and temperature resolutions can be different and, in general, can span different orders of magnitudes. Furthermore, the spatial and temporal coverage generally differ significantly. In this section, we present the main monitoring methodologies (Figure 3).

3.1. In Situ Monitoring

Systematic records of water temperature began in the 20th century (see e.g., Kangur et al., 2021; Livingstone & Dokulil, 2001). Historically these measurements were collected manually using mercury thermometers directly immersed (a) in the lake surface water to measure LSWT or (b) in water samples collected at depth and brought up to the boat deck (e.g., Hampton et al., 2008) or using reversing thermometers integrated in sampling bottles (e.g., Leoni et al., 2019) when collecting water temperature profiles. Historical LSWT records were often collected relatively close to the shore (e.g., Gerten & Adrian, 2000; McCormick & Fahnenstiel, 1999) and sometimes in river outlets just downstream of a lake (e.g., Austin & Colman, 2007), while full water temperature profiles were typically taken in the deepest point of a lake (e.g., Rimet et al., 2020; Salmaso et al., 2014). In order to ensure continuity and homogeneity of observations, the historical monitoring points have been typically kept unchanged throughout time. According to the global data sets and relative methodological details published by Sharma et al. (2015) for LSWT and Pilla et al. (2021) for water temperature profiles, manual sampling was typically scheduled in the morning and in the early afternoon, with a time frequency that ranged from daily to monthly with sporadic cases in which water temperature was sampled twice daily, in the morning and in the evening (Noges & Noges, 2014). Due to technological and automation advancements, mercury thermometers have been progressively replaced by digital thermometers and/or multi-parametric probes, and manual sampling replaced by automatic sampling using buoys equipped with surface sensors (e.g., Austin & Colman, 2007) or moored stations equipped with thermistor chains providing water temperature measurements at discrete depths (Tiberti et al., 2021; Valerio et al., 2012). In some cases, these moored stations are real floating laboratories, providing

space for laboratory equipment and personnel (see Wüest et al., 2021 that details the LÉXPLORE platform on Lake Geneva and a list of other lake platforms).

The introduction of a new generation of temperature sensors in place of mercury thermometers significantly improved the resolution of the measurements (from $O(0.1)$ K Niedrist et al., 2018) to $O(0.1)$ mK (Van Haren et al., 2005) and the automation of the monitoring stations increased the sampling frequency. In this case, more than reporting on the wide spectrum of possible sampling frequencies that are available nowadays (up to 1,024 Hz for microstructure purposes, see e.g., Kolås et al. (2022), but the choice is dependent on the compromise between desired resolution of the final data set and available storage capacity), it is probably more relevant commenting on the advantages introduced by automated stations in terms of limiting the well-recognized influence of weather conditions on the availability/quality of the final measurements. On the one hand manual measurements suffer from the so-called “fair weather bias,” where manual sampling is avoided or impossible in bad weather conditions, and on the other hand the quality and accuracy of these measurements, when their acquisition is logistically possible, are affected by the weather conditions (Rand et al., 2022). However, it should be noted that the availability of continuous, automatic in situ monitoring can be affected by the presence of harsh weather/climate conditions: a clear example is the removal of surface buoys from the Laurentian Great Lakes when they freeze in winter to avoid risk of damage by ice (e.g., Van Cleave et al., 2014). Automatic monitoring also allowed for installing networks of sensors within a lake (e.g., Hart & Martinez, 2006; Meinson et al., 2016) or in different lakes of a region (e.g., Vitale et al., 2018), generating spatially distributed in situ data to an extent that was improbable using manual sampling alone. However, it should be recognized that earlier examples of distributed monitoring based on manual sampling are available even for large lakes (see e.g., Izmet'eva et al., 2016 for a network of 79 stations sampled ca. annually from 1977 to 2003 in Lake Baikal, Russia).

Despite the advent of automatic measurements, manual monitoring has not been disappearing and, in many cases, it is still the only source of observations. Manual monitoring is routinely performed with CTD or multiparametric probes for research and quality control purposes. Besides routine measurements, typical manual monitoring activities include the acquisition of high frequency temperature microstructure profiles for turbulence analysis (e.g., Macintyre et al., 2021), which can also be used for investigating specific physical (e.g., Piccolroaz et al., 2019) and biological processes (e.g., Sepúlveda Steiner et al., 2019). It should be noted that in recent years there were attempts to alleviate the operational burden associated with taking this type of measurements, through the development of automatic microstructure profilers either (a) propelled by the action of waves and moving vertically along a wire (Pinkel et al., 2011) or (b) propelled by internal-battery-powered thrusters and free to drift (see e.g., the Argo float program, Roemmich & Owens, 2000 or the ASIP—Air-Sea Interaction Profiler, Ward et al., 2014) that have been used in the ocean. Buoyancy-driven Autonomous Underwater Vehicles (AUVs; also called gliders) were also traditionally developed for application in the oceans, but their limnological applications are increasing, particularly in large lakes as such as Lake Superior (Austin, 2012, 2013), Lake Tahoe (McInerney et al., 2019), and Lake Geneva (Sepúlveda Steiner et al., 2023). Gliders allow for repeated observations covering long distances over periods from days to weeks. These instruments are typically operated in “yo-yo” mode, conducting depth/distance transects with a time and spatial resolution that are difficult to attain using other manual or automatic monitoring techniques. In this respect, the use of gliders is particularly promising for the understanding of temperature related processes such as internal waves and deep intrusions, thus being particularly useful for the validation of 2D and 3D lake models. Among the emerging techniques for spatially distributed monitoring, we refer to the use of autonomously operating vessels to measure near surface water temperatures, and drones and balloons (Uncrewed Aerial Vehicles—UAVs) equipped with infrared camera for the observation of lake surface thermography (Irani Rahaghi et al., 2019). In the latter case, high resolution maps (~ 1 m) can be acquired, thus allowing to appreciate LSWT patterns at sub-pixel satellite scale (see the next section and Table 1).

3.2. Satellite Observation of LSWT

Records of LSWT based on in situ measurements are not always easily accessible, and global-scale in situ LSWT observations are rare. This is particularly the case for tropical lakes, where compared with temperate and arctic regions, long-term, in situ LSWT data sets are scarce. Furthermore, the available in situ data do not provide comprehensive coverage of entire lake surface and are limited to point measurements. Additionally, there is significant variation in the temporal coverage of data across different lakes, making it challenging to conduct global or regional studies with a high degree of certainty. In contrast, satellite observations have provided a global

Table 1
Infrared Sensors and Satellite Platforms Used to Record Lake Surface Water Temperature

Sensor	Satellite	Spectral resolution (μm)	Number of TIR bands	Spatial resolution (m)	Time resolution (days)	Coverage	Agency
MSS (LS 1–3)	Landsat 1	10.4–12.6	1	79	18	1972–1978	NASA
	Landsat 2					1975–1982	
	Landsat 3					1978–1983	
TM	Landsat 4	10.40–12.50	1	120	16	1982–2001	NASA
	Landsat 5					1984–2013	
ETM+	Landsat 7	10.31–12.36	1	60	16	1999–	NASA
TIRS	Landsat 8	10.60–11.19	2	100	16	2013–	NASA
		11.50–12.51					
TIRS-2	Landsat 9	10.60–11.19	2	100	16	2021–	NASA
		11.50–12.51					
Aster	Terra	8.125–8.475	5	90	16	1999–	NASA
		8.475–8.825					
		8.925–9.275					
		10.25–10.95					
		10.95–11.65					
MODIS	Terra	6.535–6.895	10	1,000	2	2000–	NASA
		7.175–7.475					
		8.40–8.70					
		9.58–9.88					
		10.78–11.28					
	Aqua	11.77–12.27	2	2002–	NASA		
		13.185–13.485					
		13.485–13.785					
		13.785–14.085					
		14.085–14.385					
ATSR-1	ERS-1	10.35–11.35	2	1,000	3–4	1991–2000	ESA
		11.50–12.50					
ATSR-2	ERS-2	3.55–3.93	3	1,000	3–4	1995–2003 (2011)	ESA
		10.35–11.35					
		11.50–12.50					
AATSR	ENVISAT	3.55–3.93	3	1,000	3–4	2002–2012	ESA
		10.40–11.30					
		11.50–12.50					
AVHRR/2	NOAA-10	3.55–3.93	3	1,100	0.5	1986–2001	NOAA
	NOAA-11	10.30–11.30			0.5	1988–2004	
	NOAA-12	11.40–12.40			0.5	1991–2007	
	NOAA-14				0.5	1994–2007	
	NOAA-15				0.5	1998–	
AVHRR/3	NOAA-16	3.55–3.93	3	1,090	0.5	2000–2014	NOAA
	NOAA-17	10.30–11.30			0.5	2002–2013	
	NOAA-18	11.50–12.50			0.5	2005–	
	NOAA-19				0.5	2009–	

Table 1
Continued

Sensor	Satellite	Spectral resolution (μm)	Number of TIR bands	Spatial resolution (m)	Time resolution (days)	Coverage	Agency
AVHRR/3	METOP-A	3.55–3.93	3	1,090	0.5	2006–2021	EUMETSAT
	METOP-B	10.30–11.30			0.5	2012–	
	METOP-C	11.50–12.50			0.5	2018–	
SLSTR	Sentinel-3A	3.34–4.14	3	1,000	<1.8	2016–	ESA
	Sentinel-3B	10.08–11.63			<1.8	2018–	
	Sentinel-3C	11.12–12.93			≥ 2024		
VIIRS	Suomi-NPP	3.55–3.93	4	750	0.5	2011–	NASA
		8.4–8.7					
		10.26–11.26					
		11.54–12.49					

Note. Detailed information can be found at: <https://webapps.itc.utwente.nl/sensor/>. TIR stands for thermal infrared.

archive of LSWT in recent decades, oftentimes with several passes per day, with progressively higher spatial and temporal resolution in recent years. This invaluable data source, which can rectify the latitude bias of in situ LSWT monitoring, allows for near-daily observations of LSWT over the full lake, across many lakes worldwide consistently for the same period of time, depending, of course, on the availability of cloud-free pixels.

Indeed, satellite Earth Observation data are critical for studying climate change impacts on lakes worldwide by routinely measuring LSWT from space. Satellite Earth observations have largely contributed to the availability of global lake observations in recent decades (Carrea, Crétaux, et al., 2023; MacCallum & Merchant, 2012; Schneider & Hook, 2010), and can be considered a key tool for assessing climate change impacts in lakes worldwide. LSWT is defined as an Essential Climate Variable (ECV) by the Global Climate Observing System (GCOS) (GCOS-244, 2022). To be considered an ECV, a variable must meet three primary criteria: (a) that the variable in question is critical for characterizing the climate system and its changes; (b) observing and deriving the variable on a global scale is technically feasible using proven and scientifically sound methods; and (c) generating and archiving data on the variable is affordable, mainly relying on coordinated observing systems using proven technology. LSWT meets these criteria, largely owing to recent developments in satellite technology and processing methods, which have made the characterization of LSWT from space more comprehensive and quantitatively robust, overcoming the lack of a standardization of observations that characterizes long-term ground-based observational data. Though satellite observations have greatly expanded our ability to monitor lake temperature across the globe, it is not without challenges. Efforts investigating lake responses to climatic variations need to be grounded in a sustainable and systematic way.

Lake water temperature is measured from satellite by an instrument called a radiometer, but not directly. The quantity measured by the radiometer is the radiant flux (energy emitted per unit time) emitted by the surface of the lake water per unit solid angle and unit projected area. This quantity is called radiance and the temperature is then inferred through mathematical inversion (Rodgers, 2000). To retrieve LSWT, radiances are measured for frequency bands in the infrared (but also microwave) region of the electromagnetic spectrum. In these frequency bands, the atmosphere is almost transparent and when no clouds are present, the radiances measured by the satellite are related to the energy emitted by the surface water and ultimately to the temperature of the water. Using an infrared radiometer operating at wavelengths across 3.7–12 μm , the water temperature is sensed at a depth of 10–20 μm , depending on the local energy flux through the surface of the water. This depth is within the so-called “skin layer.” This skin layer is the molecular boundary between a turbulent water surface and a turbulent atmosphere. Below the skin layer, water temperatures then transition to what is commonly referred to as the “bulk” temperature. This bulk layer temperature is comparable to that measured conventionally using floating thermometers or instruments mounted on in situ monitoring stations. The bulk temperature is consistently warmer than the skin temperature, typically by a few tenths of a degree, but the difference between the two can also be much higher (Hondzo et al., 2022; Hook et al., 2003; Wilson et al., 2013). This temperature difference

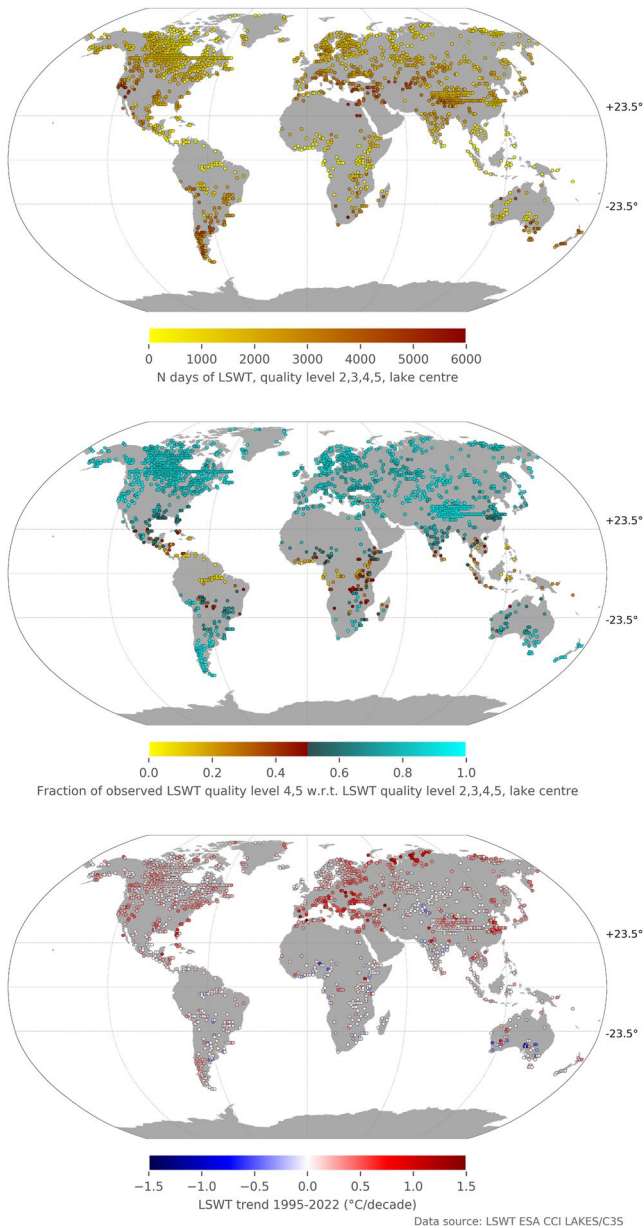


Figure 4. (a) Number of days when a lake surface water temperature (LSWT) observation at the lake center (as defined in Carrea et al. (2015)) is present in the timeseries over the 1995–2022 period in the European Space Agency-Climate Change Initiative Lakes LSWT data set v2.0.2 (Carrea, Crétaux, et al., 2022) extended for the European Union Copernicus Climate Change Service (Carrea et al., 2020). Note that the number of days in the period 1995–2022 with satellite coverage over the 2024 lakes is 9,757. Observations associated to quality level 1 (bad data) have been discarded as they should never be used. (b) Fraction of daytime LSWT of quality levels 4 and 5 in relation to the total number of available observations (quality levels ≥ 2) shown in subplot (a). LSWTs of quality levels 4 and 5 are the only ones which should be safely used. (c) LSWT trend for 1976 lakes calculated over the 1995–2022 period. Note that to avoid overlapping in high density areas, the dot has been plotted at the latitude of the lake center but the longitude has been shifted.

between the skin and bulk temperature is commonly known as the cool skin effect (Fairall et al., 1996; Minnett et al., 2011), the magnitude of which is influenced by the air-water surface heat fluxes (Hondzo et al., 2022; Wilson et al., 2013). The cool skin effect also varies considerably at diurnal timescales (Hook et al., 2003). In brief, nighttime skin temperature retrievals are considered to provide better accuracy than daytime data when compared with bulk temperatures due to, among other things, the absence of solar heating (Hook et al., 2003). At depths of a meter or more below the lake surface a bulk temperature measurement can differ from the skin layer by a few degrees Celsius, depending on the depth and variability of the diurnal mixed layer (Imberger, 1985). Although the cool skin effect in lakes leads to oftentimes noticeable differences between bulk temperatures and those measured from satellite Earth observations, skin surface temperatures are nonetheless tightly coupled to temporal variations in bulk lake surface temperature, particularly over long timescales. In turn, these global observations have been used extensively to observe climate change signals in lakes.

For several decades, satellite Earth observation have provided continuous data for observing spatial and temporal variations of LSWT worldwide (see Table 1 and T. Jia et al., 2022 for a recent review). Most studies have been based on moderate spatial resolution high radiometric quality meteorological sensors, with a pixel size of approximately 1 km, including MODerate resolution Imaging Spectroradiometer (MODIS), Along Track Scanning Radiometer (ATSR), and Sea and Land Surface Temperature Radiometer (SLSTR), at up to daily time scales (Carrea, Crétaux, et al., 2023; MacCallum & Merchant, 2012; Reinart & Reinhold, 2008; Schneider et al., 2009). These have been heavily relied upon to estimate LSWT in recent years, as well as to investigate lake responses to climate change. However, their application to small sized lakes is limited due to their relatively moderate spatial resolution, resulting in most global scale studies being restricted to the largest lakes of the world (Carrea, Crétaux, et al., 2023; MacCallum & Merchant, 2012; Schneider & Hook, 2010). In contrast, Landsat satellites could provide useful information of LSWT for both large and small lakes worldwide. The strength of Landsat includes its high spatial and radiometric resolution, and long-term continuous record. However, the 16-day revisit time, which can be longer due to cloud cover, limits the applicability of Landsat for tracking sub-seasonal patterns in surface water temperature. This can be particularly problematic for some parts of the world where cloud cover is common (see Figure 4 and relative discussion below), thus limiting the reliability of estimated changes in LSWT. Furthermore, Landsat offers two infrared channels only from Landsat 8 onwards in the series, which do observe at 100 m resolution. However, currently no mature LSWT method or product of the accuracy required by users for climate related purposes (of order 0.5 K or better; GCOS-245, 2022; Schaeffer et al., 2018) is available for Landsat data. Future developments are aiming to improve high resolution LSWT retrievals.

Some of the first studies investigating the impact of climate change on global LSWT via satellite Earth observation focused on a central within-lake region (Schneider & Hook, 2010). This central region, often defined relative to a maximum distance from land and based on 3×3 arrays of $\sim 1 \text{ km}^2$, was chosen to provide a balance between sampling a relatively large surface area and conservatively avoiding any potential bias by including shoreline pixels, which would result in contamination of the LSWT retrieval. Subsequent studies that were able to investigate spatially resolved LSWT, and provide pixel-based information, calculated both average LSWT (i.e., averages across

all pixels within a water body) (MacCallum & Merchant, 2012; Woolway & Merchant, 2017) and within-lake thermal patterns, as well as their responses to climate change (Calamita et al., 2021; Mason et al., 2016; Woolway & Merchant, 2018; Zhong et al., 2016). Specifically, studies that have investigated spatially resolved observations of LSWT demonstrated considerable within-lake warming patterns, with warming rates often differing at sub-basin scales (Kraemer et al., 2015; Mason et al., 2016; Zhong et al., 2016). The Laurentian Great Lakes, for example, show clear intra-lake warming patterns, often associated with shortening winter ice cover as well as other geophysical factors, such as bathymetry (Calamita et al., 2021; Mason et al., 2016; Toffolon et al., 2020; Zhong et al., 2016). In particular, higher summer warming rates have been reported over the deepest parts of the Laurentian Great Lakes. Similar responses have also been reported in other lakes throughout the Northern Hemisphere (Woolway & Merchant, 2018). Such analyses of spatially resolved LSWTs have been pivotal in improving our understanding of within-lake thermal responses to climate change and the underlying mechanisms.

LSWT from satellite and measured on-site are used in climate reports, such as the State of the Climate Report released every year by the Bulletin of the American Society (see for example Carrea, Merchant, et al., 2023), where the lake-average warm-season temperature anomalies of the year are reported in the context of the anomalies across the full extension in time of the satellite data record. Satellites provide consistent data in space and time, which allow us to understand where water bodies are more drastically impacted by global climate change. The latest published version of LSWT data set (Carrea et al., 2020; Carrea, Crétau, et al., 2022; Carrea, Crétau, et al., 2023; Carrea, Merchant, et al., 2023) from satellites is currently provided for a period of 25 years (with harmonisation across different instruments), with regular updates aiming to increase the temporal coverage of the record, and with future releases that will include improvements of the data set/coverage. The LSWTs of 2,024 lakes (selected within the European Space Agency-ESA Climate Change Initiative-CCI project, Carrea, Merchant, & Simis, 2022) are available at a spatial resolution of about 1 km, on regular grid, with an estimation of the uncertainty and a confidence level (quality level), and they are validated against in situ data. The LSWT data set has been created utilising only daytime imagery as it was coupled with a threshold-based water detection algorithm that does not rely on a solid prior to classify water/non-water pixels. The time resolution and spatial coverage of satellite data depends, among other factors, on the cloud/ice cover, since radiances that are affected by clouds/ice differ from clear-sky radiances (Merchant et al., 2019). Figure 4a illustrates the total number of available observations at the lake centre (Carrea et al., 2015), which exclude LSWT measurements at a quality level equal to 1 and days without LSWT values due to various factors such as cloud cover, ice cover, polar night, among others. We note that we excluded quality level 1 (bad data) from the count as they should never be used (Carrea, Crétau, et al., 2023). The tropical area is known to be affected by clouds, as confirmed by the figure, which clearly shows that data availability for lakes located at equatorial latitudes is lower in comparison to other regions. A low number of days with observations is appreciable also in the Arctics, which is primarily attributed to polar nights, which restrict LSWT daytime observations, and ice cover. Likewise, the frequency of observations decreases towards higher latitudes and in the Tibetan Plateau due to ice cover, while in Australia because the selected lakes are very likely experiencing drying out conditions. Figure 4b shows the fraction of LSWT with good/best quality levels, specifically quality levels 4 and 5, recommended for climate applications, for each lake with respect to the total number of available observations reported in Figure 4a. The map clearly indicates that the tropics have the lowest fraction of observations of good quality, primarily due to factors such as thin clouds and high density of low water vapor, which make the retrieval of LSWT more complex.

Despite the inherent data gaps in satellite observations, they remain highly valuable for describing where climate change is currently impacting water bodies most substantially. This is primarily due to the consistent global coverage provided by a limited number of instruments, whose characteristics are well-known and closely monitored during their orbital operation. Figure 4c shows LSWT trends computed from 1995 to 2022 of the lake-average warm-season LSWT anomalies. The warm season is defined as July-August-September for the northern hemisphere, January-February-March for the southern hemisphere and the whole year for the tropics (region between the ± 23.5 parallels). Only the acceptable/best quality levels LSWT data have been used to compute the trends for 1978 lakes (out of the ESA CCI 2024 for which a sufficient number of observations was available). From Figure 4c it can be clearly seen that lakes in southern and eastern Europe, in the Middle East, eastern China, and in some regions in the Arctics are warming faster than the lakes in the other regions. Overall, the majority of lakes, approximately 85%, exhibit a warming trend. However, there are a few regions, particularly in the southern hemisphere and in Central Asia, where this warming pattern is less prevalent.

Satellite Earth observation data are also often used to validate LSWT simulations in climate change assessments. For example, satellite-derived LSWTs have been used to validate lake models, which were then applied in the

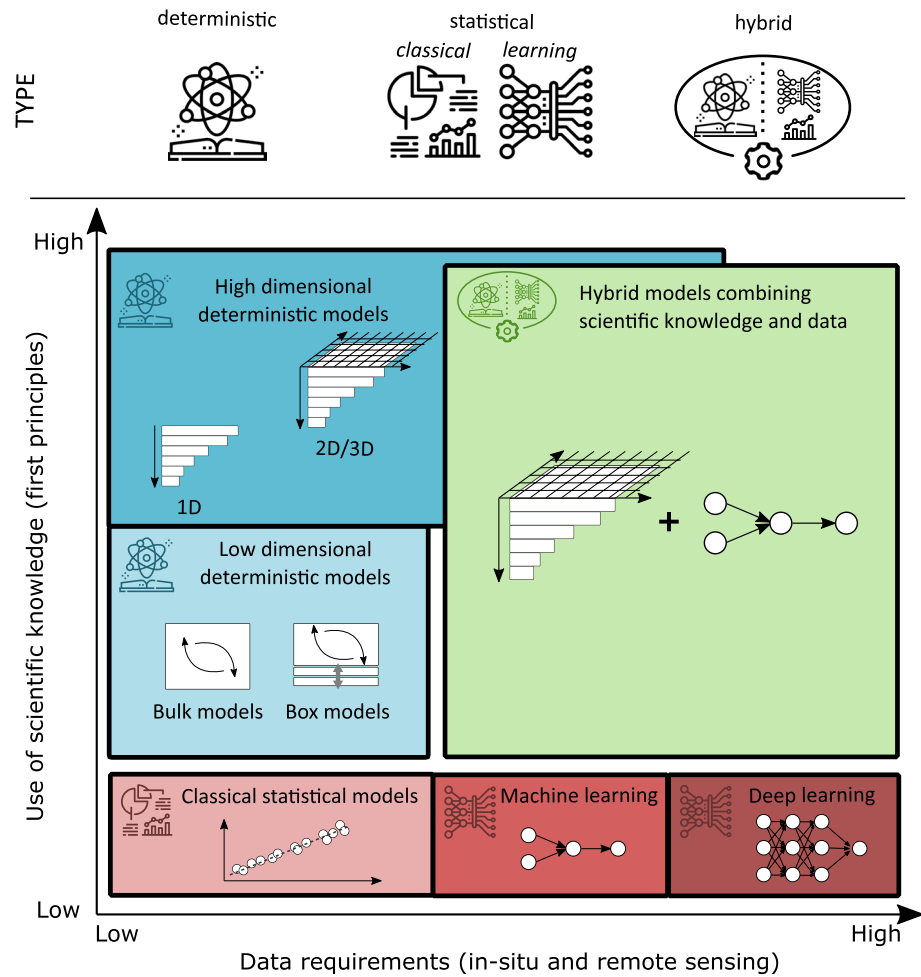


Figure 5. Classification of lake temperature models based on model type and scientific knowledge versus data information requirements (adapted from Karpatne et al. (2017)).

analysis of seasonal cycles (Maberly et al., 2020), the onset of summer stratification and overturning behavior (Fichot et al., 2019; Woolway, Jennings, et al., 2021), and climate-induced alterations in lake mixing regimes (Woolway & Merchant, 2019). However, it's important to note that if the error in satellite-derived surface temperatures (e.g., Schaeffer et al., 2018) is greater than the predictive error from models, then satellite Earth observations are less useful for validating simulations (e.g., Willard, Read, et al., 2022).

4. Classification of Lake Temperature Models

For many decades, two major types of models have been used to simulate lake temperatures: statistical models based on regressions, and deterministic models. More recently, two other groups of models have been developed, namely machine learning (ML) models, and hybrid models that combine statistical or ML approaches with process-based approaches. These different models can be represented on a two-dimensional plane, where one axis measures the amount of data needed to run a model and the other measures the scientific knowledge required to represent the underlying processes (see Figure 5, modified from Karpatne et al. (2017)). The combination of statistical and ML models belongs to the realm of data-driven models, which directly distill critical information from data sets to elucidate system behavior and relationships among variables. Conversely, deterministic models require the formulation of first principles and relationships among variables, according to empirically or theoretically derived laws. When scientific knowledge is limited, deterministic models may require simplifying assumptions that can reduce their performance and make it difficult to interpret the results. Similarly, when data are scarce, data science models may struggle to learn as well as extrapolate from the data, and identify relationships

among variables. In this regard, hybrid models combine the available sources of information, leveraging available data while being grounded on the underlying scientific knowledge (Karpatne et al., 2017).

Statistical models have the advantages of being simple and generally requiring little data for their use. These models provide mathematical relationships between forcing variables and the target variable (water temperature), without inferring the mechanistic connections among them. For this reason, their performance is highly dependent on the case study and quality of data at hand, and their use may be questionable when applied with input variables going beyond the limits used for model calibration, as for example, in climate changes studies (Piccolroaz et al., 2018) or when extreme events are of interest (Jankowski et al., 2006; Shinohara et al., 2023). These models require little or no scientific knowledge about the simulated processes, making them accessible to a wider range of users.

The boundary between statistical models and *ML* is a topic of current debate (see e.g., Bzdok, 2017; Bzdok et al., 2018; Wikle & Zammit-Mangion, 2023), and one may consider the two types of models belonging to the same macro-group. The main difference between classical statistics and ML methods can be found in the degree of automation (which is lower for statistical models), complexity, and in the number of assumptions that are needed to solve a problem (which is higher for statistical models). Deep learning methods are generally regarded as a subset of ML, and have been combined with both statistical models (Shlezinger et al., 2023; Wikle & Zammit-Mangion, 2023) and physical models (Read et al., 2019; Reichstein et al., 2019; Y. Zhu et al., 2023). Deep learning models have limited assumptions on the data and processes that are to be modeled, and can use a large amount of information. However, they cannot be treated as a panacea for solving any task, as they can learn spurious relationships and make bad predictions outside of observed conditions, can demand a lot of computational resources (Menghani, 2023), and can sometimes be less accurate than process-based or simpler statistical models (Gamage & Samarabandu, 2020; Korbmacher & Todeaux, 2022; Rajula et al., 2020; H. Zhao et al., 2022).

Deterministic models, also referred to as mechanistic, process-based or theory-based models (see e.g., Soares and do Carmo Calijuri, 2021) simulate the fundamental processes relevant for lake water temperature, including the accurate quantification of the different energy fluxes involved. The development of these conceptual models requires an understanding of the fundamental processes involved and the ability to represent them mathematically. Depending on the complexity of the processes involved, these models may require a significant amount of diverse data for their proper functioning, which may not always be available with sufficient spatial and temporal coverage.

Hybrid models are somewhat in between process-based and statistical models (in its wider sense, including classical statistics, statistical learning, data-driven optimization, up to deep learning). These models combine first principle-based models with data-driven models into a joint architecture (Kurz et al., 2022) and aim at preserving some of the physical realism of process-based models, while allowing for the flexibility, simplicity, and performance of data-driven models. Hybrid models do not necessarily use more knowledge or data, but combine the benefits of process-based and statistical models, placing them at a level equal to or below the highest data and knowledge use scenarios (Figure 5).

Models can also be classified according to the number of spatial dimensions that they can solve, ranging from zero-dimensional (0D) to three-dimensional (3D) models (see Figure 6). The choice of the best model to use depends upon the processes that are investigated and the morphological characteristics of the lake at hand and is often constrained by the type and quality of available data. In this respect, we refer the interested reader to the study by Ishikawa et al. (2022) for a detailed comparison among models with different dimensions (from 1D to 3D) in relation to their ability in simulating, among others, thermal stratification in a medium-sized drinking-water reservoir. Here, we provide a description of each category of model along with references to the most relevant literature on the topic, with a particular focus on 0D and 1D models passing through 0.5D models.

4.1. 0D Models

0D models (also termed bulk models) are used for modeling either LSWT or the vertically homogeneous water temperature of a lake assuming complete mixing throughout the water column (e.g., in shallow lakes). Depending on the spatial representativeness of the data used for model calibration, 0D models can be used to model spatially-averaged or local lake water temperature. In all cases, this category of models does not consider any spatial variability in either horizontal or vertical direction. These models generally belong to the category

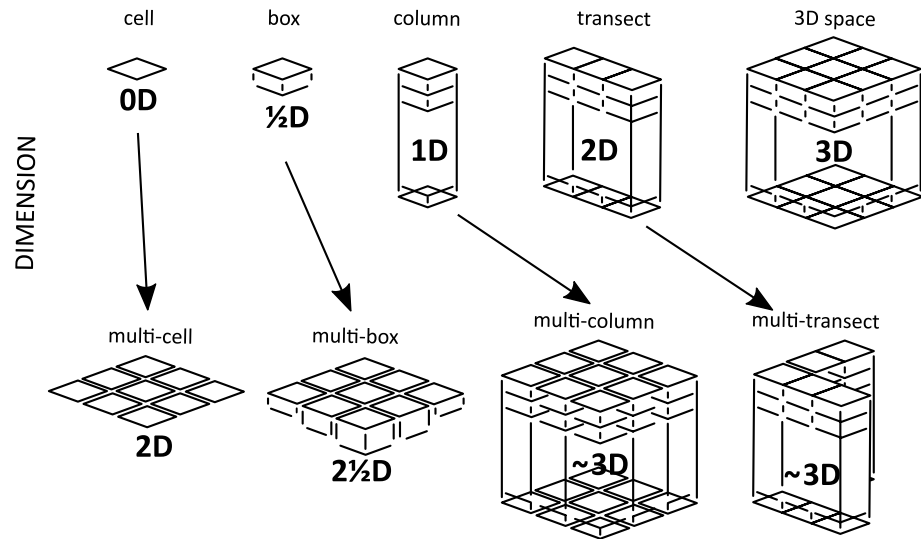


Figure 6. Classification of lake temperature models according to the number of spatial dimensions solved.

of statistical models (e.g., Sharma et al., 2008; Willard, Read, et al., 2022), although there are examples of hybrid 0D models (e.g., Bilello, 1964; Kettle et al., 2004). Furthermore, since such models are typically designed for the purpose of predicting LSWT, according to the notation already introduced in Equation 10, in the following we will denote water temperature as T_s . This can be interpreted as the temperature of the surface well-mixed layer (i.e., the epilimnion, see Figure 2) normally measured from ships, buoys, or moored stations at depths ranging from centimeters to a couple of meters below the lake surface (bulk temperature) or as the temperature of the thin surface layer on the order of 10 μm generally measured by infrared radiometers (skin temperature; see Section 3.2).

4.1.1. Climatological Models

An example of 0D statistical models are sinusoidal models fitted to observed data, which are able to capture LSWT seasonality and the timing of maximum and minimum temperatures, but limited to the climatological mean only, thus neglecting any inter-annual variability. These models can be first-order models based on a sine-cosine pair with annual periodicity (Flaim et al., 2016) or higher-order models with additional sine-cosine pairs characterized by sub-annual periodicity (Minns et al., 2018):

$$T_s = \beta_0 + \sum_{i=1}^n \left(\beta_{s,i} \sin\left(\text{DOY} \frac{2\pi}{365}\right) + \beta_{c,i} \cos\left(\text{DOY} \frac{2\pi}{365}\right) \right), \quad (15)$$

where β denotes a generic model parameter both here and throughout the rest of the text, DOY refers to the day of the year, and n is the number of sine-cosine pairs. Likewise, certain authors proposed models founded on the complementary error function erfc (Hutorowicz, 2020), which take the form:

$$T_s = \beta_0 + \beta_1 \text{erfc} \left[\left(\frac{\text{DOY} - \beta_2}{\beta_3} \right)^2 \right]. \quad (16)$$

However, one may prefer to consider the climatological year obtained by averaging the temperature for each DOY as a better, first-approximation model of the water temperature seasonality. Expanding upon these basic models, a more sophisticated, yet still simple, statistical 0D model is the three part, trapezoidal-like model proposed by Trumpickas et al. (2009) consisting of linear warming through the spring, a plateau in mid-summer, and linear cooling in fall. Besides being lake-specific, the model parameters are year-specific, allowing to determine the relationships between model parameters and climate variables (e.g., air temperature). These relationships can be used to draw preliminary climate-change-related considerations in the context of expected climate scenarios.

4.1.2. Regression Models

Moving toward more advanced statistical OD models, we can refer to statistical models that utilize multivariate regressions to establish the correlation between water temperature and one or more predictors. These models allow for a deeper understanding of the seasonality and inter-annual variability of water temperature. A generic multivariate regression model can be represented as:

$$T_s = \beta_0 + \beta_1 x_1 + \beta_2 x_2 + \dots + \beta_N x_N + \epsilon \quad (17)$$

where x_1, x_2, \dots, x_N are the independent variables (the predictors), $\beta_0, \beta_1, \beta_2, \dots, \beta_N$ are the regression coefficients, and ϵ is the error term. Previous studies found that water temperature can be effectively explained by utilizing a combination of different predictors. The most commonly used predictors include meteorological variables like air temperature, dew point temperature, solar radiation, wind speed, wind direction and precipitation (Hondzo & Stefan, 1993). Geographical information such as latitude, longitude and elevation are additional factors that have been considered, particularly when the objective is to set-up a multi-lake modeling framework specifically tailored to a specific region (e.g., Bachmann et al., 2019; Livingstone et al., 1999; Sabás et al., 2021). Lake morphological variables such as lake area, volume, depth, and shape have been shown to be important factors affecting water temperature dynamics (e.g., Calamita et al., 2021; Edmundson & Mazumder, 2002; Kettle et al., 2004; Toffolon et al., 2014; Woolway et al., 2016), and as such have been considered as relevant predictors in several statistical models (Edmundson & Mazumder, 2002; Sharma et al., 2008; Shuter et al., 1983; Snucins & Gunn, 2000). In accordance with the climate-morphometry-typology hierarchical framework, as proposed by Edmundson and Mazumder (2002) to describe the thermal properties of Alaskan lakes, another significant set of predictors pertains to water quality and chemistry (Rose et al., 2016). These may include parameters such as Secchi depth (a measure of water clarity, introduced by Italian priest and scientist Pietro Angelo Secchi in the mid-19th century, determined by lowering a standard disk into the water until it is no longer visible, then measuring the depth at which it disappears), turbidity, water color, and dissolved organic carbon, which are examples of parameters frequently employed as predictors in previous studies (e.g., Minns et al., 2018; Snucins & Gunn, 2000). A generic multivariate regression model can either be linear, where all predictors are assumed to have a linear relationship with the response variable, or non-linear, allowing for more complex relationships between predictors and the response variable. In some cases, quadratic or higher order terms, logarithmic or exponential functions, or other transformations of the predictors may also be included in the model (e.g., Minns et al., 2018; Sharma et al., 2008).

Many studies, from regional (e.g., Livingstone & Lotter, 1998; Woolway, Jennings, & Carrea, 2020) to worldwide (e.g., Schmid et al., 2014; S. Wang et al., 2021; Winslow et al., 2018) applications, have consistently demonstrated a significant relationship between air and water temperatures. This has motivated the development of numerous simple linear regression models that utilize air temperature alone to predict water temperature values on a daily (e.g., Bachmann et al., 2019; Matuszek & Shuter, 1996), monthly (e.g., McCombie, 1959), and annual (e.g., Shuter et al., 1983) basis, or to predict peak summer temperatures (Minns et al., 2018; Sharma et al., 2007). In deep lakes characterized by clear hysteresis cycles between air and water temperatures, the impact of the lake's thermal inertia is addressed indirectly by estimating separate seasonal regressions of air-water temperature relationships for each branch of the hysteresis loop (M. S. Webb, 1974). Alternatively, linear regressions can be used to estimate monthly means of surface water temperature from monthly means of measured air temperature data (Lathrop et al., 2019; McCombie, 1959). In some cases, linear regressions are substituted by non-linear functions such as the logistic function that is given by:

$$T_s = \beta_0 + \frac{\beta_1 - \beta_0}{1 + \exp(\beta_2(\beta_3 - T_a))}, \quad (18)$$

where T_a is air temperature. This model has been widely applied in studies on stream water temperature forecasting (Mohseni & Stefan, 1999; Piccolroaz et al., 2016; S. Zhu et al., 2018), but has also been applied to LSWT forecasting, (Roberts et al., 2017; S. Zhu, Ptak, Choiński, & Wu, 2020; S. Zhu, Ptak, Yaseen, et al., 2020). While the logistic model generally offers better performance compared to linear regression models for extreme upper and lower values, its applicability is reasonably restricted to the case of shallow lakes that, similar to rivers, exhibit a small thermal inertia and thus weak (or absent) hysteresis cycles between air and water temperatures.

4.1.3. Autoregressive Models

In some cases, particularly when thermal inertia is high and water temperature reacts to air temperature changes with a damped and delayed response, autoregressive models that account for the previous predicted values have been used (e.g., Håkanson, 1996; Kettle et al., 2004; Ottosson & Abrahamsson, 1998; Prats & Danis, 2019). For example, to estimate the hypolimnion temperature, Prats and Danis (2019) used an autoregressive model based on an exponential smoothing function of the epilimnion temperature, which in turn was modeled through an exponential smoothing function of air temperature based on the model proposed by Kettle et al. (2004) that is presented below (see *Hybrid models*). In this context, it is worth noting that second-order Markov models have been successfully employed for modeling river water temperature (Caissie et al., 2001; Cluis, 1972). Although such systems exhibit lower thermal inertia than lakes, there is potential for these models to be applicable in lake systems. In this type of model, water temperature is represented as the sum of two terms. In parallel with the Reynolds notation introduced earlier, these two terms can be understood as the mean annual component, denoted as \bar{T} , and a residual (or fluctuating) component, denoted as T' , such that $T = \bar{T} + T'$. The mean annual component is described by a sinusoidal model of the type shown in Equation 15. The residual component is obtained by subtracting the actual water temperatures from the annual component, and this series are subsequently used to calibrate a stochastic second-order Markov model of the type:

$$T'_s(t) = \gamma_1 T_s(t - \Delta t) + \gamma_2 T_s(t - 2\Delta t) + \gamma_3 T'_a(t), \quad (19)$$

where $T'_a(t)$ is the residual of air temperature with respect to its corresponding annual component evaluated according to a sinusoidal model as done for water temperature, and γ denotes a generic model parameter. More specifically, γ_1 and γ_2 are related to the autocorrelation coefficients for a lag of Δt and $2\Delta t$, respectively (Caissie et al., 2001; Cluis, 1972), where Δt is generally assumed equal to one day.

4.1.4. Bayesian Models

Bayesian regression models extend standard regression models and use Bayes' theorem to infer the probability distribution of the parameters. The posterior distribution is obtained by combining the prior distribution, which represents our prior beliefs about the parameters, and the likelihood of the data, which represents the probability of obtaining the observed data given the parameter values. This approach allows for modeling uncertainty in the parameters and provides a probabilistic framework for making predictions. More specifically, the prior distribution represents our initial beliefs or guesses about the probability distribution of the model parameters before observing any data. The posterior distribution, in contrast, incorporates both the prior distribution and the likelihood of the data, resulting in an updated probability distribution of the model parameters that accounts for both the prior information and the information contained in the observed data. In general, probability distributions are built using Monte Carlo simulations.

Bayesian modeling allows for a hierarchical approach that can be applied to analyze complex data structures. This approach is based on a sequential procedure with more than one model structure in the hierarchy, allowing for estimation of the parameters and prior distributions for each level using the observed data. In this way, each model structure builds upon the previous model's results, incorporating informative priors that leverage additional sources of information and enable the use of past knowledge in the analysis. As an example, Christianson et al. (2019) implemented a sequential procedure with three models in hierarchy to predict sub-daily LSWT of high altitude lakes of the Southern Rocky Mountains (U.S.A). The first-level model described daily and seasonal variation in LSWT by combining sine and cosine functions and a linear term dependent on lake surface area. Here, vague priors were employed initially, assuming normal distributions, while in subsequent steps the means and covariance results from the previous model were utilized for all previously introduced parameters. In the second-level model, the effect of elevation was added to account for the wide range of variability of the studied lakes. Finally, the third-level model has been built on the second one by adding a term dependent on the year and considering an unknown sampling time, yielding to the full equation written below:

$$T_s = \beta_0 + \beta_1 \sin\left(2\pi \frac{t}{24}\right) + \beta_2 \cos\left(2\pi \frac{t}{24}\right) + \beta_3 \sin\left(2\pi \frac{DOY}{365}\right) + \beta_4 \cos\left(2\pi \frac{DOY}{365}\right) + \beta_5 A_0 + \beta_6 Elev + \beta_7 Year, \quad (20)$$

where A_0 is lake surface area, $Elev$ is the lake elevation, and $Year$ is the year of observation. In this case, not only did the complexity of the model increase moving through the hierarchy, but the authors also used different data

sets with increasingly larger but more sparse (i.e., less densely sampled in time and space) observations at each level.

4.1.5. Machine Learning

ML models are now a popular tool for water quality modeling (Appling et al., 2022). Studies that used ML for lake temperature modeling can be divided into two groups: shallow and deep ML models. The shallow ML models used in the literature include artificial neural networks (Di Nunno et al., 2023; Heddum et al., 2020; W. C. Liu & Chen, 2012; Saber et al., 2020; S. Zhu, Ptak, Yaseen, et al., 2020; S. Zhu et al., 2023), support vector regression (Quan et al., 2020), adaptive neuro-fuzzy inference system (Yousefi & Toffolon, 2022), and decision trees (Heddum et al., 2020; Yousefi & Toffolon, 2022). Most deep ML models use recurrent neural networks, for example, long short-term memory (LSTM) models (X. Jia et al., 2021; Read et al., 2019; L. Wang et al., 2022; Willard, Read, et al., 2022; Yousefi & Toffolon, 2022) to replicate the memory of the thermal system.

The majority of studies using ML for lake temperature prediction have focused on surface predictions (e.g., Di Nunno et al., 2023; Hao et al., 2023; Heddum et al., 2020; Quan et al., 2020; Saber et al., 2020; Sharma et al., 2008; Yousefi & Toffolon, 2022; Willard, Read, et al., 2022; S. Zhu, Ptak, Yaseen, et al., 2020; S. Zhu et al., 2023), but some have also simulated depth-resolved lake water temperatures (e.g., Read et al., 2019; Willard et al., 2021). Among these studies, Yousefi and Toffolon (2022) compared nine ML models including both shallow and deep models for the forecasting of LSWT and evaluated the best input predictors. The results showed that none of the nine ML models performed significantly better, and that the best input predictors are air temperature and day of the year. The analysis also showed that including the air temperature from previous days as inputs in the ML models improved prediction performance, as this helped to retain the historical context of the forcing conditions.

ML has the potential to improve modeling of lake water temperature at broad spatial scales through several mechanisms. ML models can leverage information across thousands of lakes to improve predictions. Willard, Read, et al. (2022) used LSTM-based deep learning to estimate LSWT for 185,549 lakes in the conterminous United States, and the results showed that a global deep learning model substantially improves predictive accuracy compared to a prior empirical model and a debiased process-based approach. For temperature profiles, Willard et al. (2021) proposed a meta-transfer learning method, which predicts transfer performance from candidate source models to unmonitored target lakes using lake attributes. This work showed that information from lakes that are similar (e.g., similarity in maximum depth) can be successfully transferred between well- and unmonitored systems, and that hybrid deep learning and process-based models (described in the next paragraph) transferred better than process-based models. An additional challenge for broad scale modeling is that process-based models often require information about lake characteristics (e.g., bathymetry, water clarity) for parameterization that are not known for most lakes. ML techniques are flexible where you can exclude certain parameters that are not available at large extents. For example, Willard, Read, et al. (2022) did not use depth or water clarity despite the known importance in predicting temperature across lakes. In fact, ML methods can be used to learn about the lake characteristics themselves from the observational temperature data set. For example, LSTM and inversion techniques have been combined to build models that can predict both dynamic lake temperatures and infer static features of lakes that are important for making temperature predictions across lakes (e.g., lake depths; Tayal et al., 2022).

4.1.6. Hybrid Models

Hybrid 0D models generally rely on the fundamental zero-dimensional heat budget Equation 9. As shown in Equation 10 and the corresponding text, applying this heat balance to the well-mixed layer yields the time evolution of the water temperature averaged over the corresponding volume. A simplified way to account for the right-hand-side of the equation is through assuming that the heat flux is predominantly controlled by the sensible heat exchange, so that:

$$\frac{dT_s}{dt} = \eta(T_a - T_s), \quad (21)$$

where T_a is air temperature, and η is a heat exchange coefficient having dimension of inverse time. This simple model was first proposed by Rodhe (1952) and has been applied to the Baltic Sea to predict the timing of ice formation, which was simply computed as the time when the water temperature T_s drops below 0°C. Since then,

the same model has been used in numerous other locations, as for example, Canadian rivers, lakes, and bays (Bilello, 1964), Lake Mendota in USA (Robertson et al., 1992), as well as lakes in Greenland (Kettle et al., 2004) and other regions. In this model η is constant, therefore the effects of seasonality on the heat exchange coefficient and of stratification (i.e., varying volume in Equation 10) are neglected. Equation 21 can be solved numerically or, as done in the aforementioned works, integrated over time, rearranged and solved iteratively (see Rodhe (1952) and Bilello (1964) for the mathematical treatment) to obtain:

$$T_s(t) = (1 - e^{-\eta\Delta t})T_a(t) + e^{-\eta\Delta t}T_s(t - \Delta t), \quad (22)$$

where Δt is the integration time interval, normally assumed equal to one day. This equation suggests that if T_a is constant in time, the temperature in the surface well-mixed layer T_s tends to approach it exponentially.

Following Kettle et al. (2004), this equation can be rewritten assuming that water temperature is related to air temperature through a smoothing function f , such that $T_s(t) = f(T_a(t))$, yielding to:

$$f(T_a(t)) = \alpha T_a(t) + (1 - \alpha)f(T_a(t - \Delta t)), \quad (23)$$

where $\alpha = (1 - e^{-\eta\Delta t})$ is a smoothing parameter that has the effect of reducing the variance of air temperature and introducing a time delay in the thermal response of the lake. In this way, the model includes an autoregression component thus accounting for the thermal inertia of the lake. To enhance the model's applicability to lakes where factors beyond the temperature difference between air and water may influence the system, an extended version incorporates theoretical short-wave solar radiation H_s as an additional component (Kettle et al., 2004):

$$T_s(t) = \beta_0 + \beta_1 f(T_a) + \beta_2 H_s, \quad (24)$$

where the term H_s can refer to the theoretical clear-sky radiation (see e.g., Annear & Wells, 2007 for an overview of models to calculate it), as proposed by the authors, be represented as a sinusoidal fit to average daily solar radiation data (Prats & Danis, 2019), or be assigned directly based on measured data. The model parameters in Equation 24 and the smoothing parameter α are specific to each lake and should be calibrated by fitting the model to the corresponding observational data. In the study by Kettle et al. (2004), scaling relationships were discovered between these model parameters and lake area and maximum depth, which led to the creation of a regional model for predicting summer LSWT in lakes located in southwest Greenland.

4.1.7. Equilibrium Temperature Models

Edinger et al. (1968) introduced the concept of equilibrium temperature T_{eq} , defined as the surface water temperature at which the net heat flux H_{net} exchanged at the lake's surface would be zero. The equilibrium temperature can be therefore calculated from Equation 1 by setting H_{net} to zero, substituting T_s with T_{eq} in the heat fluxes terms depending on LSWT, and solving for T_{eq} . Before doing so, let us obtain the equation for H_{net} by subtracting Equation 8 in the case when $H_{net} = 0$ and $T_s = T_{eq}$, from the case when $H_{net} \neq 0$. This yields:

$$H_{net} = 4\epsilon_w\sigma T_0^3(T_{eq} - T_s) + 6\epsilon_w\sigma T_0^2(T_{eq}^2 - T_s^2) + L\rho f(W)[T_{eq}(\delta + \xi) - T_s(\delta + \xi)], \quad (25)$$

where we assumed that since the difference between T_{eq} and T_s is generally small for averaging periods larger than daily, it is reasonable to assume $\delta_{eq} = \delta_s = \delta$. This equation can be linearized by neglecting the second term on the right-hand-side, usually contributing by less than 10% of the total H_{net} (Edinger et al., 1968; Eggers & Tetzlaff, 1978), to give:

$$H_{net} = [4\epsilon_w\sigma T_0^3 + L\rho f(W)(\delta + \xi)](T_{eq} - T_s) = K_{eq}(T_{eq} - T_s), \quad (26)$$

where the heat exchange coefficient K_{eq} in this equation is defined by the terms within the square brackets. With this definition of K_{eq} , the equilibrium temperature can be computed from Equation 8 with $H_{net} = 0$, by setting $T_s = T_{eq}$ and $\delta_{eq} = \delta$, and neglecting higher order terms:

$$T_{eq} = \frac{H_{s,net} + H_{a,net} - \epsilon_w\sigma T_0^4}{K_{eq}} + \left[\frac{K_{eq} - 4\epsilon_w\sigma T_0^3}{K_{eq}(\delta + \xi)} \right] (\xi T_a + \delta T_d). \quad (27)$$

In addition, by substituting Equation 26 into Equation 10 for the time evolution of T_s in the well-mixed surface layer, one obtains:

$$\frac{dT_s}{dt} = \frac{K_{eq}}{\rho c_p D_s} (T_{eq} - T_s) = \eta_{eq} (T_{eq} - T_s). \quad (28)$$

We note that this equation is formally equivalent to Equation 21 and that $\eta_{eq} = \frac{K_{eq}}{\rho c_p D_s}$ has the same meaning as the coefficient η in that equation. Hence from a mathematical point of view the solutions provided in Equation 22 holds true also in this case, once T_a and η have been replaced by T_{eq} and η_{eq} , respectively. However, these two equations differ substantially in their physical interpretation, since in the latter the heat exchange between a water body and the atmosphere is proportional to the difference between LSWT and the equilibrium temperature, rather than the difference between LSWT and the air temperature. We note that the equilibrium temperature would be the same as the air temperature only if heat were exchanged solely through conduction and convection ($H_{net} = H_c$). However, this is usually not the case although it is the assumption underlying the model proposed by Rodhe (1952), as shown above.

LSWT models based on the concept of the equilibrium temperature are grounded in the fundamental physical principles that control the lake's thermodynamics. Indeed, solving the system of Equations 27 and 28 corresponds to solving the heat budget of a lake, which can be done numerically by considering either constant or variable η_{eq} and D_s through time. However, in some previous applications, the problem has been simplified by solving Equation 28 using a sinusoidal function to describe T_{eq} , obtained by fitting the values from Equation 27 using a sinusoidal regression (which has been proven to explain most of the variance of T_{eq} ; Livingstone & Imboden, 1989). This approach allowed for gaining insight on the effects of meteorological factors on water temperatures (Edinger et al., 1968; Livingstone & Imboden, 1989), and for quantifying the average and the amplitude of sub-daily LSWT in the form of a simple sine wave (Eggers & Tetzlaff, 1978). In some other applications, T_{eq} computed according to Equation 27 or considering other assumptions to simplify the heat flux terms has been used as a proxy for LSWT to investigate the thermal sensitivity of lakes to changes in meteorological forcing variables (Schmid et al., 2014).

4.2. 0.5D Models

0.5D models (also termed box models, according to the wide literature in ocean science; see e.g., Welander, 1982) are intermediate between 0D and 1D models, in that they model water temperature within a time-varying upper well-mixed layer, thus allowing for including the effect of stratification and vertical mixing. This type of models can be coupled with one underlying layer considering it decoupled from the upper well-mixed layer (as e.g., in *air2water*, Piccolroaz et al., 2013) or coupled through simple temperature-depth parameterizations (as e.g., in FLake, Mironov et al., 2010). Similar to 0D models, depending on the spatial representativeness of the data used for model calibration, 0.5D models can be used to model spatially-averaged or local lake water temperature.

The *air2water* model is an example of a 0.5D hybrid model for LSWT prediction that combines the simplicity and parsimony of statistical models with the high performance of more complex deterministic models, thanks to its physically based derivation (Piccolroaz, 2016; Piccolroaz et al., 2013; Toffolon et al., 2014). The model solves the volume-integrated, zero-dimensional heat equation applied to the well-mixed surface volume of the lake as described in Equation 10. In this case, the net heat flux H_{net} is mathematically simplified through linearization using Taylor expansion and with air temperature serving as a proxy for the integrated effects of relevant processes and fluxes. The result is a simple ordinary differential equation that depends on air temperature, LSWT, and model parameters summarizing the main climatic and thermophysical properties of the lake. This equation is not fundamentally different from Equation 28 and reads:

$$\frac{dT_s}{dt} = \frac{1}{\delta} \left\{ a_1 + a_2 T_a - a_3 T_s + a_5 \left[2\pi \left(\frac{t}{T_y} - a_6 \right) \right] \right\}, \quad (29)$$

where a_1, \dots, a_6 are model parameters and $\delta = V_s/V_{lake} = D_s/D_{mean}$ is the dimensionless depth (or volume) of the well-mixed surface layer relative to the lake mean depth D_{mean} (total volume V_{lake}). The inclusion of δ provides a significant advantage for *air2water* over purely regressive models. In fact δ is described by a time-dependent function that explicitly accounts for the significant role of vertical stratification on lake thermal dynamics:

$$\delta = \begin{cases} \exp\left(-\frac{T_s - T_h}{a_4}\right), & \text{if } T_s \geq T_h \\ \exp\left(\frac{T_s - T_h}{a_7}\right) + \exp\left(-\frac{T_s}{a_8}\right), & \text{if } T_s < T_h \end{cases} \quad (30)$$

where T_h is the temperature of the hypolimnion (i.e., the deep layer, see Figure 2), which can be assumed equal to the minimum (maximum) surface temperature registered during the year for warm (cold) monomictic lakes that mix once per year, or equal to the temperature of maximum density (temperature of maximum density varies with salt content and is approx. 4°C in freshwater lakes at the atmospheric pressure) for the case of dimictic lakes that circulate twice a year. Although the definition of δ as implemented in the *air2water* model is empirical, the comparison between simulated and observed values of δ for Lakes Constance and Superior showed good agreement (Piccolroaz et al., 2015; Toffolon et al., 2014). Furthermore, a recent analysis by Toffolon et al. (2022) using a 1D physically-based model confirmed that δ decreases exponentially over time. However, the study suggests that a potential improvement could be achieved by considering different exponential decay parameters for the warming and cooling periods. Similarly, it has been suggested that at least for some lakes the model may better follow observations when T_h is considered to be another model parameter to be calibrated, instead of being fixed as described above (Piotrowski et al., 2022). In addition to distinguishing *air2water* from standard regression models, the inclusion of a time-varying δ also allows this model to be classified as 0.5D, because it simulates the temporal evolution of the epilimnion. Besides the 8-parameter full model, alternative versions of the model also exist: one with 6 parameters, where δ equals 1 during inverse stratification (i.e., when $T_s < T_h$), and another with 4 parameters where the sinusoidal term in Equation 29 is neglected. The first simplification was reasonable in a wide range of cases (Piccolroaz et al., 2013), and implies a mild effect of reverse stratification (i.e., parameter a_7) and the possible insulating effect of ice cover (see the fictitious increase of delta through the term depending on parameter a_8) on the resulting LSWT dynamics. The second simplification is particularly reasonable, especially when the air temperature and LSWT cycles are almost sinusoidal, in which case the third sinusoidal term would be redundant: the sum of sinusoidal functions with the same frequency but different amplitude and phase yields another sinusoid with different amplitude and phase but the same frequency.

FLake (Freshwater Lake model) is another example of a widely used 0.5D lake model capable of predicting the vertical temperature structure and mixing conditions in lakes of various depths on a time scale from a few hours to many years (Mironov, 2008; Mironov et al., 2010). The model is based on two dynamic layers: an upper mixed layer and a thermocline layer in which the water temperature is parameterized using the concept of self-similarity of the temperature-depth curve, meaning that the characteristic shape of the temperature profile is conserved irrespective of the depth of this layer. The model is written in terms of potential water temperature Θ that is the temperature a parcel of water would have if it were moved adiabatically (i.e., without exchange of heat) to a reference pressure, normally at the surface (see e.g., Imboden & Wüest, 1995). According to the two-layer parameterization of FLake, the time evolution of the potential water temperature profile is given by:

$$\Theta = \begin{cases} \Theta_s, & \text{if } 0 < z < D_s \\ \Theta_s - (\Theta_s - \Theta_b)\phi(\zeta), & \text{if } D_{lake} \leq z \leq D_s \end{cases} \quad (31)$$

where $\Theta = \Theta(z, t)$, z is the vertical coordinate, $\Theta_s(t)$ and $\Theta_b(t)$ are the potential water temperatures in the surface well-mixed layer of depth D_s and at the very bottom (i.e., $z = D_{lake}$), and $\phi(\zeta)$ is the dimensionless “universal” shape function describing the self-similar temperature profile in the thermocline. The shape function used in the FLake model is a fourth order polynomial in the dimensionless depth $\zeta = \frac{z - D_s(t)}{D_{lake} - D_s(t)}$ and depends on a shape coefficient C varying in time to account for the effect of mixed-layer deepening, stationary state, or retreat (Mironov, 2008). The same self-similarity theory is used to describe the temperature profile of the lake ice, snow, and active upper layer of bottom sediments. While this approach relies on “verifiable empiricism,” it still incorporates much of the essential physics, thus offering a good compromise between physical realism and computational economy (Mironov et al., 2010). However, because FLake does not allow for the hypolimnion layer below the thermocline, a virtual bottom at 40–60 m is used in simulations, instead of the real lake depth (Martynov et al., 2010). In FLake the upper layer is assumed to be well mixed and vertically uniform. The depth of this layer (D_s) is dynamically parameterized through an entrainment equation for the depth of a convectively mixed layer and a relaxation-type equation for the depth of a wind-mixed layer in stable and neutral stratification, as well as accounting for volumetric solar radiation absorption. The set of equations used in this parameterization along with all details for their comprehension can be found in Mironov (2008) and in the Appendix of Mironov et al. (2010). We refer interested readers to those previous studies for a detailed explanation. Although the FLake model is commonly referred to as a bulk model, it is classified as a box model in the classification scheme used

in this review because the model solves for the time-dependent depth of the well-mixed layer. FLake has been implemented within the weather prediction model COSMO (Mironov et al., 2010) and coupled in one-way (Gula & Peltier, 2012) and two-way (Mallard et al., 2014) model configurations to the Weather Research and Forecasting (WRF) model, which demonstrated a good performance with respect to the lake surface temperature and to the freeze-up of lakes and the ice break-up. The interested reader can refer to the FLake model website (<http://www.flake.igb-berlin.de/>) for downloading the code and for the relevant documentation.

4.3. 1D Models

1D models (also termed column models) allow the simulation of water temperature vertical profiles. 1D models can be applied either at the deepest point of a lake considering its hypsometric curve (variable area over depth) or, particularly when the detailed bathymetry is not available, on shape assumptions, for example, assuming an equivalent cylinder in which lakes have constant area equal to the surface area and depth equal to the lake's mean depth, or a simplified cone if only surface area and depth are known. 1D models can be used as lake-averaged or single station models depending on the observations used for model calibration (i.e., horizontally averaged vs. local). The first case is more appropriate for small and deep lakes where lateral variability is less important than the vertical one. In either case, this should be explicitly clarified when presenting the results to avoid misinterpretations (Henderson-Sellers, 1984).

1D lake models are based on the assumption that mixing processes happen rapidly on the horizontal axis, making horizontal density gradients negligible. This allows the focus on the vertical axis of the water column for transport and mixing processes. Various criteria for the validity of the 1D assumption have been proposed. Generally, the 1D assumption requires a mostly stably stratified water column which can be validated by calculating the dimensionless Wedderburn number or Lake Number (Imberger & Patterson, 1989; Patterson et al., 1984). The Lake Number (LN) quantifies the dynamic stability of the water column and is defined as the ratio of the momentum of stabilizing forces (resulting from stratification) to the momentum of the destabilizing forces due to wind. Long periods characterized by $LN \gg 1$ can be used as a preliminary basic validation of the 1D model assumption (Bruce et al., 2018)

$$LN = \frac{St\beta}{\rho u_*^2 z_v} \quad (32)$$

where St is the Schmidt stability, β is the angle of the metalimnion surface to the lake bottom (that can be approximated as $\beta = D_m / \sqrt{A_0}$, where D_m is the depth of the thermocline and A_0 is the lake surface area), u_* is the wind friction velocity, and z_v is the center of volume depth. While we refer to classical limnological textbooks for the details on the definitions of St and z_v , we specify that the wind shear velocity u_* can be quantified as:

$$u_*^2 = \frac{\rho_a}{\rho} C_D U_{10}^2 \quad (33)$$

where ρ_a and ρ are air and water density (in the latter case, the density of the surface water), C_D is the drag coefficient for momentum, and U_{10}^2 is wind velocity measured at 10 m above the lake surface. Generally, the use of 1D lake models in reservoirs is not a common practice, especially when the geometry is intricate and marked by a dendritic pattern (see also Section 4.4). Further, the 1D assumption is generally valid for lakes that are not affected by the effects of Earth's rotation on the internal flow field, although there are several examples of 1D lake models applied to large lakes (see e.g., Fenocchi et al., 2019; Gaudard et al., 2019; Goyette & Perroud, 2012; Piccolroaz & Toffolon, 2013; Wood et al., 2023). This can be verified by calculating the Rossby radius and is mostly valid for small and medium-sized water bodies. It should be noted that turbulence-based 1D models (see below for the definition), as for example, Simstrat (Goudsmit et al., 2002) and LAKE 2.0 (Stepanenko et al., 2016) account for the effects of the Coriolis force in their hydrodynamic calculations and can generally be used for lakes regardless of size.

The key equation at the basis of 1D lake models is the vertical water temperature transport equation. This equation can be formulated starting from Equation 14 by focusing only on vertical processes and neglecting the vertical advection term to give:

$$\frac{\partial T}{\partial t} = \frac{S_r}{\rho c_p} + \frac{\partial}{\partial z} \left(D_z^T \frac{\partial T}{\partial z} \right), \quad (34)$$

where $D_z^T(z, t)$ is the vertical eddy diffusivity (that, we recall, has a lower bound determined by the value of molecular diffusivity D). In this equation we replaced $j = 3$ with z , z being the depth hence defined as positive downwards, and omitted the overbar that denotes averaging. This equation can be rewritten making explicit the dominant heat source/sink terms and accounting for the lake's hypsography:

$$\frac{\partial T}{\partial t} = -\frac{1}{\rho c_p} \frac{\partial I}{\partial z} + \frac{H_{sed}}{A \rho c_p} \frac{\partial A}{\partial z} + \frac{S_T}{\rho c_p} + \frac{1}{A} \frac{\partial}{\partial z} \left(A D_z^T \frac{\partial T}{\partial z} \right) \quad (35)$$

where $I(z, t)$ represents the internal heat generation due to penetrative solar radiation, $H_{sed}(z, t)$ is the heat flux at the water-sediment interface (defined to be positive if heat flows from the sediments into the water), S_T denotes other sink/source terms, and $A(z)$ is the lake area. The penetrative solar radiation I is governed by the water clarity and, in general, is described through an exponential approximation of the Beer-Lambert attenuation law as follows:

$$I(z) = I_0 \exp(-k_d z), \quad (36)$$

where $I_0 = H_{s,net}$ is the available solar radiation at the lake surface and k_d is the light extinction coefficient. It should be noted that, in general, the light extinction coefficient is not constant and varies as a function of the wavelength across the light spectrum (Bouffard et al., 2019). However, for simplicity, a monochromatic source is often assumed, and a constant value of k_d is frequently empirically estimated as a function of the Secchi depth (Subin et al., 2012). In general, k_d is on the order of 1 m^{-1} for turbid lakes and 0.1 m^{-1} for clear lakes (Bouffard & Wüest, 2019). In some cases, a fraction β_s of the available solar radiation associated with wavelengths in the red end of the solar spectrum (wavelengths $>700 \text{ nm}$), is allowed to be absorbed within the surface layer z_a . In such cases, Equation 36 is adjusted by defining $I_0 = (1 - \beta_s) H_{s,net}$ and applying it for depths $z \geq z_a$, with the component of I_0 absorbed within the uppermost z_a layer being accounted for within the source term per unit volume S_T . The fraction β_s accounts for approximately 40%–50% of the total energy, which is absorbed within a surface layer $z_a \sim 0.6 \text{ m}$ (Henderson-Sellers, 1986). We note that in shallow/clear lakes the portion of penetrating solar radiation reaching the bottom is absorbed in the top layer of sediments, although it can be partially reflected back and either absorbed in the layers above or released to the atmosphere, increasing the lake albedo (Subin et al., 2012).

In order to solve Equation 35 an upper, surface boundary condition of the Neumann type is generally assumed with the form of:

$$\rho c_p \left(-D_z^T \frac{\partial T}{\partial z} \right) \Big|_{z=0} = H_{net} - H_{s,net}, \quad (37)$$

where H_{net} is the net heat flux exchange (positive when directed from the atmosphere toward the lake) between atmosphere and water column given by Equation 8, where the effects of precipitation, inflows/outflows, and water-sediment exchanges were excluded. The net shortwave radiation $H_{s,net}$ is removed from the right-hand-side because, as noted above, it is already included in Equation 35 as a separate production term. Similarly, the contributions of precipitation, inflow/outflows, and water-sediment exchanges are regarded as additional source/sink terms in Equation 35. The right-hand side of Equation 37 includes only long-wave and non-radiative fluxes exchanged at the lake-atmosphere interface, which are absorbed within the uppermost 1–2 mm of the water column (Henderson-Sellers, 1986). This thickness is smaller than the depth of surface layers typically considered in lake models, thus justifying its application as a Neumann-type boundary condition.

The bottom boundary condition, is already introduced in Equation 35 as the term $\frac{H_{sed}}{A \rho c_p} \frac{\partial A}{\partial z}$, which accounts for the water-sediment heat flux through approximating the water-sediment interface areas by the difference in horizontal areas between two consecutive depths according to the bathymetry of the lake (Goudsmit et al., 2002; Saloranta & Andersen, 2007). In general, this heat flux varies with depth and can be assigned if it is known, particularly when it is predominantly influenced by the upward geothermal flux (Gaudard et al., 2019; Piccolroaz & Toffolon, 2013), or modeled by taking into account sediment layers through the following heat conduction equation:

$$H_{sed} = \lambda_{sed} \frac{dT_{sed}}{dz_{sed}} \quad (38)$$

where λ_{sed} is the thermal conductivity, T_{sed} the temperature, and z_{sed} the depth of the sediments (see e.g., the MyLake model in Saloranta and Andersen (2007)). We recall that the water-sediment heat flux H_{sed} is defined as positive when directed toward the water column. The effect of H_{sed} is often neglected (adiabatic boundary

conditions at the sides), but it should always be considered in long-term climatic simulations (de la Fuente & Meruane, 2017).

Ice and snow dynamics, and their impact on vertical heat fluxes, are mostly handled in a separate algorithm for 1D water temperature models. Here, more detailed descriptions of different algorithms can be found in H. Yao et al. (2014) and U. G. Kobler and Schmid (2019). Water temperature models differ in their ability to simulate a set of multiple variables, for example, black ice (congelation ice), white ice (snow ice) and/or snow thickness, the respective effects on atmosphere-water exchanges, and if ice growth can happen on top or below the ice-water interface. As the plethora of different ice algorithms makes a comprehensive description challenging, we will briefly describe the popular ice and snow algorithm of the MyLake model (Saloranta & Andersen, 2007) in this paragraph, which is also incorporated into Simstrat (Goudsmit et al., 2002) and GOTM (Burchard et al., 1999), which will be presented regarding their water temperature modeling approach in more details below. The MyLake ice and snow algorithm considers the dynamics of black ice, white ice as well as snow. Here, ice thickness changes when air temperature is below the freezing point and is quantified using Stefan's law:

$$h_{ice} = \sqrt{h_{ice}^2 + \frac{2\lambda_{ice}}{\rho_{ice}L_f}(T_f - T_{ice})\Delta t} \quad (39)$$

where h_{ice} is ice thickness, λ_{ice} is thermal conductivity of ice, ρ_{ice} is ice density, L_f is latent heat of freezing, T_f is water temperature at the freezing point ($T_f = 0^\circ\text{C}$), and T_{ice} is the temperature of the ice surface (Leppäranta, 1993). Snow thickness is a function of precipitation, and white ice forms whenever the weight of snow exceeds the buoyancy capacity of the ice layer. Ice cover causes the surface layer to stay at constant freezing point temperatures, and heat diffusing into this layer is used for melting. Ice and snow thickness further affect the albedo regarding incoming short-wave radiation.

Two prominent formulations for 1D water temperature modeling have been established (Ford & Stefan, 1980; Perroud et al., 2009) based on how they simulate vertical transport. Both types of 1D models apply the 1D water temperature transport Equation 35 but individual models differ regarding their turbulent closure schemes which eventually results in different formulations for deriving the eddy diffusion coefficient D_z^T . The first type estimates eddy diffusivity coefficients based on empirical or physically-based relationships. These models include integral energy models (also called mixed-layer models) as well as eddy-diffusion models. The other type are turbulence-based models that use additional equations to quantify turbulent transport of turbulent kinetic energy (TKE, k) and of its rate of dissipation (ϵ) (Rodi, 1984).

In most cases, integral energy models apply the TKE by wind shear directly to calculate the mixed layer depth without focus on vertical transport of TKE (Ford & Stefan, 1980). The transport below the mixed layer depth is modeled solving Equation 35 with D_z^T estimated using empirical relationships, mostly based on parameterizations related to the gradient Richardson number defined as the ratio between local gradients of buoyancy (stabilizing) and shear (causing turbulent mixing):

$$Ri = \frac{g}{\rho} \frac{\partial\rho/\partial z}{(\partial u/\partial z)^2} = \frac{N^2}{S^2} \quad (40)$$

where u is the horizontal velocity, N is the Brunt-Väisälä or buoyancy frequency $N = \sqrt{\frac{g}{\rho} \frac{\partial\rho}{\partial z}}$, and S represents local shear (note that the vertical coordinate z is defined as positive downwards). In a simple form, the eddy diffusivity can be related to buoyancy effects as:

$$D_z^T = D_{z0}^T (1 + aRi^b)^c \quad (41)$$

where D_{z0}^T is the diffusivity at neutral stratification ($Ri = 0$), b and c are empirical coefficients that vary across a wide range according to the several relationships available in the literature (Henderson-Sellers, 1982; Munk & Anderson, 1948; Pacanowski & Philander, 1981). An example is the approach following Henderson-Sellers (1985), in which turbulent diffusivity is also parameterized based on the gradient Richardson number, see Equation 40, and is used to quantify vertical mixing over the full vertical axis (e.g., in the so-called Hostetler-type models, after Hostetler and Bartlein (1990)). This turbulent diffusivity model does not estimate a mixed layer depth from the external available kinetic energy and can be classified as eddy-diffusion model. It differs from turbulence-based

models as it does not use additional calculations to account for turbulent energy production and dissipation. Therefore, methodologically and technically, models *sensu* Henderson-Sellers (1985) are closer to integral energy models than turbulence-based models.

On the other hand, turbulence-based models quantify directly the production, transport and dissipation of TKE along the entire water column and have thereby a mechanistic basis for analyzing vertical turbulent transport and shear. Two-equation turbulence models like the $k - \epsilon$ model or the Mellor-Yamada model relate the TKE, k , to its dissipation rate, ϵ , using a characteristic length scale

$$L \sim k^{3/2} \epsilon^{-1} \quad (42)$$

and thereby introducing two additional equations for calculating the 1D water temperature transport (Burchard & Baumert, 1995; Burchard et al., 1998; Rodi, 1987).

Several 1D lake models have been proposed by the scientific community, including widely used modeling software such as Advanced Lake Biogeochemistry Model (ALBM, Tan et al., 2015), DYNAMIC RESERVOIR SIMULATION MODEL (DYRESM, Imberger & Patterson, 1981; Yeates & Imberger, 2003), General Lake Model (GLM, Hipsey et al., 2019), General Ocean Turbulence Model (GOTM, Burchard et al., 1999), the Hostetler model (Hostetler & Bartlein, 1990), LAKE 2.0 (Stepanenko et al., 2016), Multi-year Lake simulation model (MyLake, Saloranta & Andersen, 2007), Simstrat (Gaudard et al., 2017; Goudsmit et al., 2002), CLM4-LISSS (Subin et al., 2012), LAKEoneD (K. Jöhnk & Umlauf, 2001; K. D. Jöhnk et al., 2008), MINLAKE96 (Fang & Stefan, 1996), Weather Research and Forecasting-Lake (WRF-Lake, Gu et al., 2015), and customized lake models developed for investigating specific lakes conditions, for example, deep ventilation due to thermobaric instability (Piccolroaz & Toffolon, 2013), temperature patterns in turbid lakes (Fukushima et al., 2022). All these 1D modeling tools, see also F. Wang et al. (2019) for a similar list, provide lake-averaged projections.

GLM, MyLake, and MINLAKE96 are examples of integral energy models in which the depth of the mixed layer is determined, and then the available external kinetic energy is compared to the internal potential energy of the water column to entrain denser water into the mixed layer (although specific formulations of the integral energy comparison vary, see i.e., Ford and Stefan (1980)). Integral energy models assume that the mixed surface layer is a perfectly mixed slab with constant temperature over depth and are based on early works of bulk mixed layer depth assumptions by for example, Kraus and Turner (1967). Generally, the external amount of TKE in such models mostly represents the external wind shear stress, but can also include convective overturn, shear production between layers and Kelvin-Helmholtz billowing (see Hipsey et al. (2019) for such an implementation). For surface layer mixing to occur, the TKE budget must be higher than the potential energy in the water column which is needed to lift up denser water from below the mixed layer and into the newly formed mixed layer, as well as in some formulations to account for the energy consumption by previously mentioned Kelvin-Helmholtz billowing. In other words, the lake is divided into a series of layers that are successively mixed downward until the available TKE is no longer sufficient to mix the next deeper layer. As an example for an integral energy scheme, we highlight here the approach *sensu* Herb and Stefan (2004) (neglecting the effects of the macrophyte vegetation reducing wind mixing) which is based on MINLAKE96. The external kinetic energy per unit area KE is parameterized based on surface wind velocity as:

$$KE = \tau u_* \Delta t \quad (43)$$

where τ is surface turbulent shear stress, u_* is surface shear velocity, and Δt is the model time step. Potential energy PE at layer i (with the reference at the surface) is:

$$PE_i = g z_i (z_{i+1} - z_{cm}) \Delta \rho \quad (44)$$

where z_i is the mean depth of the i th layer, z_{cm} is the center of mass of the mixed layer, and $\Delta \rho$ is the density change from the mixed layer to the layer $i + 1$ (Herb & Stefan, 2004). At each model time step, the depth of the mixed layer is iteratively calculated until the condition $PE_{i+1} > KE$ is met. All these models apply an empirical parameterization of the eddy diffusivity, D_z^T , related to buoyancy effects and therefore to the Brunt-Väisälä frequency to model mixing below the mixed layer, hence in the thermocline:

$$\text{GLM (Weinstock, 1981): } D_z^T = \frac{C_{HYP} \epsilon_{TKE}}{N^2 + 0.6 k_{TKE}^2 u_*^2} \quad (45)$$

$$\text{MyLake, MINLAKE96 (Hondzo \& Stefan, 1993): } D_z^T = a_k (N^2)^{-0.43} \quad (46)$$

GLM uses the Weinstock derivation which relates the eddy diffusivity to water column stability and rate of turbulent dissipation, in which C_{HYP} is a constant coefficient for the mixing efficiency, ε_{TKE} is a simplified approximation of turbulent dissipation rate based on the dissipation by inflows and wind, k_{TKE} is the turbulence energy containing wavenumber, and u_* is the wind shear velocity (Weinstock, 1981). We note that in GLM, k_{TKE} is empirically parameterized based on lake morphometry and stratification (Hipsev et al., 2019). MyLake and MINLAKE96 relate the eddy diffusivity to an empirically measured relationship of diffusivity values to the buoyancy frequency, where a_k is a parameterization of the lake surface area (Hondzo & Stefan, 1993).

WRF-Lake, ALBM, and the Hostetler model are examples of models based on the previously mentioned formulation after Henderson-Sellers (1985) which can be considered as eddy-diffusion-based models. The depth of the surface mixed layer is not calculated directly from external KE but solved for solely through turbulent diffusion, in which the eddy diffusivity coefficient is related to the gradient Richardson number, and employing a mixing scheme to adjust water temperature instabilities by mixing instantaneously and recursively adjacent water layers until the temperature difference is less than a small specified-value:

$$\text{ALBM, WRF-Lake; Hostetler (Henderson-Sellers, 1985): } D_z^T = \frac{\kappa u_* z}{\sigma_{t,0}} e^{-k_* z} (1 + 37 Ri^2)^{-1} \quad (47)$$

where κ is the von Karman's constant, $\sigma_{t,0}$ is the neutral value of the turbulent Prandtl number (normally assumed equal to 1 according to the Reynolds analogy), and k_* is a latitudinally dependent parameter of the Ekman profile (see also Hostetler and Bartlein (1990)). k_* can be quantified as:

$$k_* = 6.6 \sqrt{\sin \phi} U_2^{-1.84} \quad (48)$$

where ϕ is the latitude of the lake, and U_2 is wind speed 2 m above the water surface. The turbulent Prandtl number is defined as:

$$\sigma_t = \nu_z / D_z^T \quad (49)$$

where ν_z is the kinematic eddy viscosity along the z direction.

Simstrat, LAKE 2.0, LAKEoneD, and GOTM are examples for turbulence-based models that apply the $k - \varepsilon$ two-equation turbulence model to quantify production, transport and dissipation rates of TKE. These type of models add two more equations of the general form:

$$\frac{\partial k}{\partial t} = \frac{1}{A} \frac{\partial}{\partial z} \left(A D_z^k \frac{\partial k}{\partial z} \right) + P + B - \varepsilon, \quad (50)$$

$$\frac{\partial \varepsilon}{\partial t} = \frac{1}{A} \frac{\partial}{\partial z} \left(A D_z^\varepsilon \frac{\partial \varepsilon}{\partial z} \right) + \frac{\varepsilon}{k} (c_{\varepsilon,1} P + c_{\varepsilon,3} B - c_{\varepsilon,2} \varepsilon), \quad (51)$$

in which k and ε are related to the turbulent diffusivities of TKE and TKE dissipation (D_z^k and D_z^ε , respectively), the TKE production due to shear (P), and the production and dissipation of TKE related to buoyancy (B) (Goudsmit et al., 2002; Rodi, 1984). The empirical constants $c_{\varepsilon,1}$, $c_{\varepsilon,2}$, and $c_{\varepsilon,3}$ are fitted using field or experimental data. The eddy viscosity can be calculated as $\nu_z = c_\mu \frac{k^2}{\varepsilon}$, where c_μ is an empirical coefficient based on flow experiments (Rodi, 1984). In the standard $k - \varepsilon$ model, the eddy diffusivity coefficient D_z^T is related to the turbulence kinetic energy k and dissipation rate ε through the turbulent Prandtl number σ_t , which was introduced earlier: $D_z^T = \frac{\nu_z}{\sigma_t} = \frac{c_\mu k^2}{\sigma_t \varepsilon}$. Similarly, $D_z^k = \frac{c_\mu k^2}{\sigma_k \varepsilon}$ and $D_z^\varepsilon = \frac{c_\mu k^2}{\sigma_\varepsilon \varepsilon}$, where σ_k and σ_ε are model constants (Goudsmit et al., 2002). According to the Reynolds analogy, the turbulent Prandtl number σ_t is typically assumed to be equal to $\sigma_t = \sigma_{t,0} = 1.0$ in neutrally stratified environments. On the other hand, in stable stratification environments, it may be a calibration parameter (Boegman et al., 2001) or a function of the Richardson number (Venayagamoorthy & Stretch, 2010).

These four highlighted 1D turbulence-based models all apply a fixed numerical grid with the grid layers having a constant thickness over the course of a simulation. Turbulence-based models may also include the horizontal velocity components over the vertical axis through which they account for the effects of the Coriolis force on the vertical flow field. Because turbulence-based models have a mechanistic representation of momentum as well as

production and dissipation of TKE, they can be used to directly compare model projections with measured quantities of TKE and shear stress. This enables them to have a greater generality than integral energy models which rely on specific assumptions about how external TKE affects the heat budget inside the water column.

Due to their low computational costs and the availability of long-term monitoring data typically measured at a lake's deepest site, vertical 1D water temperature models are prominently used for lake modeling. Their main applications are regarding physical limnological investigations, for example, projecting changes in lake mixing and stratification, quantifying vertical heat transport, guiding lake and reservoir management, and investigating the thermal habitat of different species. A typical application is to use 1D lake models in projecting climate change effects on lake systems (e.g., Ayala et al., 2020; Fenocchi et al., 2018; U. G. Kobler & Schmid, 2019; Magee & Wu, 2017; Moras et al., 2019; Piccolroaz & Toffolon, 2018; Robertson & Ragotzkie, 1990; Woolway, Jennings, et al., 2021; Wood et al., 2023), as, due to low computational costs, they can project long-term effects in a low time frame. Their application for climate change projections is especially advisable as 1D lake models can sufficiently replicate the dynamics of lake systems regarding stratification, ice formation and mixing compared with higher dimensional models (Ishikawa et al., 2022), and upscaling is technically feasible due to low computational demands. 1D lake models are also frequently used to evaluate the effect of meteorological extreme events on in-lake mixing and heat transport (e.g., Bueche et al., 2017; Mesman et al., 2021; Perga et al., 2018; Shinohara et al., 2023). Further, 1D lake models are frequently used for quantifying heat and mass transport in water bodies and therefore to infer and adapt water management (e.g., Barbosa et al., 2021; Ladwig et al., 2018; Mi et al., 2018; Olsson, 2022; Soares et al., 2019; Weber et al., 2017). Also, important ecological information like the thermal habitat or the solubility of gases can be inferred from the vertical distribution of water temperature (e.g., Butcher et al., 2015; Magee et al., 2019). 1D water temperature models can be easily coupled, or in some cases are already internally coupled, to aquatic ecosystem models (AEM3Ds) to project changes in water quality and ecosystem dynamics (e.g., Andersen et al., 2022; Kong et al., 2023; Ladwig, Hanson, et al., 2021; Salk et al., 2022). In most cases, there is a one-way coupling between the thermodynamics and the AEM3D, in which the projected vertical diffusivity coefficient is used to infer the transport of water quality variables. Two-way couplings exist, notably when the light attenuation by dissolved and particulate matter is projected from the water quality model and fed-back to the thermodynamic model for calculating the internal heat generation.

4.4. 2D and 3D Models

2D models are used to simulate lake transects (length-depth), typically, but not necessarily, lying along the longitudinal and lateral directions of a curvilinear coordinates system. This type of model is particularly suitable for application in fjord lakes, deep-valley reservoirs, and elongated lakes in general (e.g., Kim & Choi, 2021; Lindenschmidt et al., 2019; Mi et al., 2020; Ulloa et al., 2022). Besides temperature and other scalars, 2D models normally solve also the bi-dimensional flow field. One of the most widely used 2D models is the CE-QUAL-W2 model, which is a longitudinal/vertical hydrodynamic and water quality model developed and maintained by US Army Corps of Engineers and Portland State University (Cole & Wells, 2006). The model is laterally averaged, assuming that lateral variations in velocities, temperatures, and constituents are negligible. For this reason, it is best suited for relatively long and narrow water bodies characterized by longitudinal and vertical water quality gradients. The CE-QUAL-W2 model uses fixed computation grids with a static bathymetric surface onto which longitudinal segments and vertical layers are mapped, and the hydrodynamic and water temperature computations are performed at the intersections of these segments and layers. The model user can choose among several different turbulence closure schemes, ranging from Richardson number based parameterizations to the $k - \epsilon$ model, the latter being the turbulence closure recommended by the developers. These models quantify the eddy vertical viscosity ν_z , which is then used to calculate the vertical thermal eddy diffusivity D_z^T assuming a default constant value of the turbulent Prandtl number $\sigma_t = 7$. The value of $\sigma_t = 7$ is commonly accepted for laminar flows in freshwater. However, previous sensitivity analyses of the CE-QUAL-W2 model have shown that optimal values for this parameter are smaller, as expected in turbulent flows where the parameter approaches unity (Boegman et al., 2001). The model also requires the definition of a horizontal diffusion coefficient, which, according to the approach proposed by Okubo (1971), is linearly proportional to the lateral grid spacing through a coefficient.

3D models are utilized to reconstruct the full thermo-hydrodynamics of a lake. These models are commonly used in large water bodies or when a detailed simulation of specific processes is required. Like 2D models, 3D models simulate not only temperature and other scalar values but also the flow field, resulting in the most physically realistic and complete simulation of the processes occurring in a water body. Parallel to a better representation

of the processes, also the complexity, computational cost, and data requirements increase compared to simpler models. Several 3D models are used to simulate the thermodynamics of lakes, many of which are also used in the oceanography community. Delft3D, an open-source integrated modeling suite (Deltare, 2023), is an example widely used by limnologists. It simulates two-dimensional flow (in either the horizontal or vertical plane) and three-dimensional flow (through the Delft3D-FLOW module), as well as sediment transport, morphology, waves, water quality, and ecology through other specific modules of the modeling suite. This model has been successfully applied in several physical and ecological lake studies (e.g., Amadori et al., 2021; Guo et al., 2023b; Schwindt et al., 2023; Soulignac et al., 2019) and is at the basis of an online platform providing lake observations and three-dimensional numerical simulations in near real-time with short-term forecasts and data assimilation (Baracchini, Wüest, & Bouffard, 2020). Another example is MITgcm (Massachusetts Institute of Technology General Circulation Model, Adcroft et al., 1997), whose hydrodynamic kernel is used to drive both atmospheric and oceanic models and that includes physical and biogeochemical parameterizations of key atmospheric and oceanic processes. This model has been recently applied also to lake modeling (e.g., Safin et al., 2022). The ELCOM model (Estuary and Lake COmputer Model, Hodges et al., 2000), adapted from the TRIM model (Casulli & Cheng, 1992) with the inclusion, among the other modifications, of a mixed-layer turbulence closure, is another well-known 3D hydrodynamics model that has been widely applied for simulating processes in lakes and reservoirs. ELCOM is often coupled with the biogeochemical model Computational Aquatic Ecosystem DYNAMICS Model (CAEDYM, Hamilton & Schladow, 1997), the coupled model being known as (AEM3D) and being used for water quality analyses including water temperature and stratification forecasting (Lin et al., 2022). Finally, among many others here we mention Environmental Fluid Dynamics Code (EFDC, Hamrick, 1992) that can be used to simulate aquatic systems in 1D, 2D, and 3D and has been applied to simulate thermal structures and dynamics in many lakes worldwide (e.g., Arifin et al., 2016; Hui et al., 2018; Khazaei et al., 2023; Y. Li et al., 2010).

Compared with the above discussed 1D and 2D models, 3D models are closer to reality as they can model the thermal dynamics in the longitudinal, lateral, and vertical directions. However, they need more computational efforts due to their higher complexity and, in principle, require spatially distributed forcing variables to impose the boundary conditions and spatially distributed observations for their validation. In fact, the proper assessment of any 3D lake model would require a comparison of simulated and observed velocity fields at several locations. However, even 3D models may produce unrealistic scenarios, especially when the calibration of their parameters was improperly or unsuccessfully conducted (Schwindt et al., 2023). Moreover, available measurements are often limited to water temperature profiles and velocity measurements are generally scarce or absent, thus limiting the application of 3D models. In some cases, however, in absence of velocity measurement a consistent reproduction of the 3D lake dynamics may be tempted, by distilling information across diverse spatial and temporal scales from a heterogeneous set of water temperature data alone (Amadori et al., 2021).

In absence of sufficient information or computational power required to run a 3D model, lower dimensionality models can be used to obtain quasi-3D simulations (see Figure 6). For example, the CE-QUAL-W2 model can be applied in a quasi-3D manner by discretizing the computational domain into different branches. This approach is particularly useful when modeling dendritic lakes, which is typical of reservoirs with several side arms (Cole & Wells, 2006). Likewise, there are examples of 1D models applied in a spatially distributed domain thus obtaining a so-called multi-column lake model, which can be assumed as a quasi-3D representation of a lake (e.g., Gaillard et al., 2022; Martynov et al., 2010; Subin et al., 2012; Sugiyama et al., 2018). This approach does not allow for the simulation of the lake's hydrodynamics and hence of horizontal heat advection but has been proven to be a good (and more economic) alternative to full 3D models to simulate the horizontal and vertical spatial thermal patterns of large lakes over seasonal time scales (Gaillard et al., 2022). Also 0D and 0.5D models can be applied in a distributed framework to obtain 2D and 2.5D representation of a lake, respectively, in terms of horizontal spatial patterns of LSWT, in the second case including the estimate of the well-mixed layer depth (see e.g., Calamita et al., 2021).

5. Model Performance

5.1. Performance Metrics

To evaluate the performance of environmental models, including water temperature models, a large number of performance metrics has been proposed in the literature. The most used performance metrics span from standard residual criteria, to correlation and model efficiency measures, and are summarized in Table 2. For other common

Table 2

List of the Most Used Performance Metrics (See e.g., Bennett et al., 2013; Hipsey et al., 2020 for Additional Metrics and Further Details)

Name	Formula	Notes
Mean Error (ME) or Bias	$\frac{1}{N} \sum_{i=1}^N (M_i - O_i)$	Calculates if the model over/underestimates observations. Values close to zero does not necessarily indicate low error due to cancellation
Mean Absolute Error (MAE)	$\frac{1}{N} \sum_{i=1}^N M_i - O_i $	Similar to ME except absolute values are used instead. It is not affected by cancellation
Mean Square Error (MSE)	$\frac{1}{N} \sum_{i=1}^N (M_i - O_i)^2$	Similar to ME but in data units squared. It is not affected by cancellation and squaring the data penalizes more higher error values
Root Mean Square Error (RMSE)	$\sqrt{\frac{1}{N} \sum_{i=1}^N (M_i - O_i)^2}$	The squared root of MSE. It facilitates interpretation since it is in the same data units. Often referred to as Root Mean Square Deviation (RMSD)
Absolute Maximum Error (AME)	$\max M_i - O_i $	Indicates the largest error
Mean Relative Mean Error or Bias (MRME)	$\frac{1}{N} \sum_{i=1}^N \left(\frac{M_i - O_i}{O_i + \epsilon} \right)$	Relative equivalent of ME. This metric increases the weighting of errors related to low measurement values. The same normalization approach is commonly applied to MAE. ϵ is a small value to avoid division by 0 when $O_i = 0$
Normalized Mean Error or Bias (NME)	$\frac{\frac{1}{N} \sum_{i=1}^N (M_i - O_i)}{\bar{O}}$	Normalized equivalent of ME. Normalization can be obtained also dividing by the standard deviation or range of variability of observations. The same normalization approach can be applied to MAE, MSE and RMSE
Correlation Coefficient (Corr or r)	$\frac{\sum_{i=1}^N (M_i - \bar{M})(O_i - \bar{O})}{\sqrt{\sum_{i=1}^N (M_i - \bar{M})^2} \sqrt{\sum_{i=1}^N (O_i - \bar{O})^2}}$	Pearson correlation coefficient, which measures the linear correlation of the observed and modeled values. The squared of the Pearson correlation coefficient is called coefficient of determination (r^2) and estimates the fraction of the variance in O that is explained by M in a simple linear regression
Nash Sutcliffe Efficiency (NSE)	$1 - \frac{\sum_{i=1}^N (M_i - O_i)^2}{\sum_{i=1}^N (O_i - \bar{O})^2}$	A normalized statistic that evaluates the relative magnitude of the residual variance compared to the observed data variance (Nash & Sutcliffe, 1970). $NSE = 1$ indicates perfect fitting while $NSE = 0$ indicates that the model performs as accurate as the mean of the observed data. $NSE < 0.5$ is associated to unsatisfactory performance (Moriassi et al., 2007). When \bar{O} is substituted with the climatological year, we refer to the modified version NSE^* , which is especially useful in the presence of significant seasonal patterns
Akaike Information Criterion (AIC)	$N \ln(RMSE) + 2k$	A metric that weights the RMSE based on the N number of observations used in calibration and k number of model parameters. AIC is aimed at finding the most parsimonious model and preventing over-fitting (Akaike, 1974)
Bayesian Information Criterion (BIC)	$N \ln(RMSE) + k \ln(N)$	Similar to AIC (Schwarz, 1978)

Note. The terms M_i and O_i indicate simulated and observed values, respectively; $i = 1, \dots, N$ indicates time index and N is the total number of observations; the bar symbol (\bar{M} and \bar{O}) refers to the time average of the time series.

performance metrics we refer the interested reader to previous reviews specifically focused on presenting these metrics with their strengths and weaknesses (Bennett et al., 2013; Moriassi et al., 2007). Likewise, we refer to the work by Hipsey et al. (2020) for a comprehensive list of performance metrics specifically tailored to the case of aquatic ecosystem modeling, which includes a section dedicated to physical models of aquatic systems. In that study, the authors proposed a four levels framework for model validation, combining: conceptual accuracy (Level 0), state accuracy (Level 1), process accuracy (Level 2), and accuracy in capturing system behavior (Level 3). The conceptual validation of a model is a needed prerequisite (Level 0) that is implicitly ensured when developing a new model, but often taken for granted when applying an existing model. Process validation (Level 2) and system validation (Level 3) are seldom undertaken (Hipsey et al., 2020) as they require richer available data sets than are generally available; the comparison of simulated state variables with observations (Level 1) is the predominant approach available in the literature (Hipsey et al., 2020). Examples of higher validation levels may include model performance metrics to assess the simulated heat fluxes and turbulent mixing intensity within the water column against for example, turbulence measurements (Level 2) or the simulated water age and eddy structures against estimates from geochemical tracers and thermal satellite images, respectively (Level 3). These higher levels of model validation are restricted to 1D/2D models (Level 2) and 3D models (Level 3).

Level 1 validation is generally undertaken by direct comparison of time-series of water temperature. The vast majority of cases use point measurements or vertical profiles, but more recently, LSWT derived from satellites have been used to evaluate the horizontal performance of 3D models (e.g., Amadori et al., 2021; Baracchini, Chu,

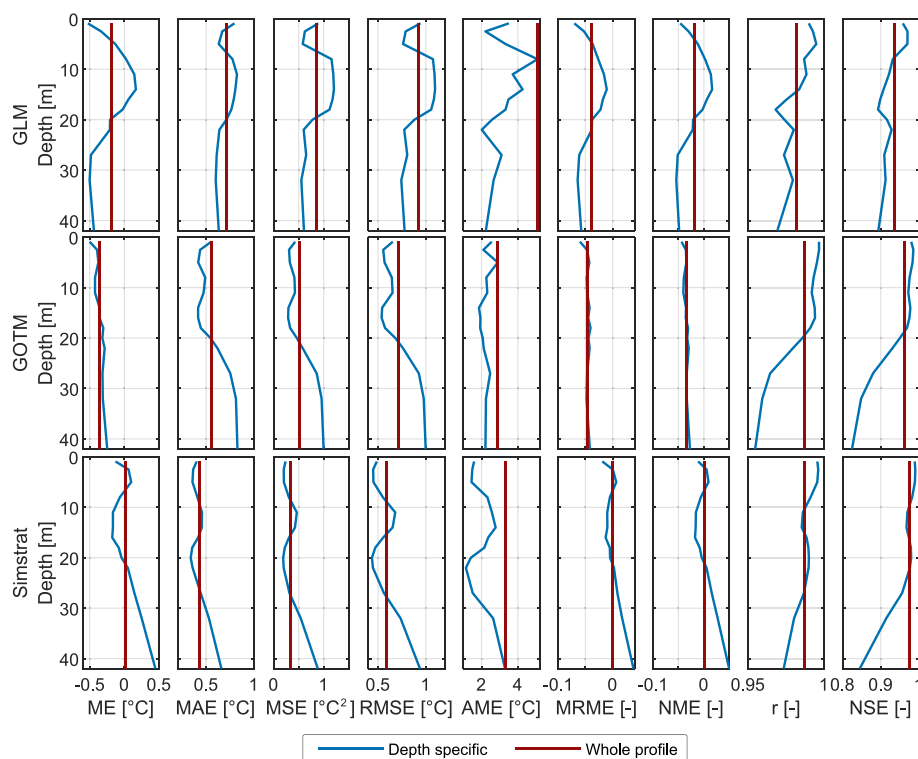


Figure 7. Depth-specific distribution of some key performance metrics for the 1D models the General Lake Model, General Ocean Turbulence Model, and Simstrat, obtained over a 2-year period in Lake Feeagh (Ireland) utilizing the R package *LakeEnsemblR*. The values of the same metrics evaluated using all the available data are also shown (vertical lines). Please refer to Table 2 for a detailed explanation of the metrics used.

et al., 2020; Mao & Xia, 2020) and 2D multi-box models (Calamita et al., 2021). In some cases, the limitations of using point measurements with low spatial representativeness can be alleviated by distilling the information across multiple temporal scales (typically from hourly to seasonally, depending on the frequency and duration of the time series) using wavelet analysis or other signal decomposition strategies and comparing the power spectra resulting from observations and simulations (e.g., Amadori et al., 2021; Kara et al., 2012). Likewise, the informativeness of vertical temperature profiles can be used beyond direct comparison of predicted and observed values by comparing derived indices of thermal stratification intensity such as the Schmidt stability (e.g., Bruce et al., 2018) or the Lake Number, or indicators of stratification phenology such as the mixed layer and thermocline depths (e.g., Bayer et al., 2013; Bruce et al., 2018), stratification onset and break-up (e.g., Woolway, Sharma, et al., 2021), or ice cover duration (e.g., Piccolroaz, Zhu, et al., 2021). This approach partially accomplishes a Level 2 model validation.

When assessing model performance using observed temperature profiles, we recommend evaluating depth-specific or layer-specific metrics in addition to the metrics calculated for the entire profile, which is the common standard. To properly interpret the model errors relative to the depth-specific variance of observations, we also suggest using normalized model efficiency performance criteria such as NSE (see Table 2 for the definition of all performance metrics). For instance, the same residual error in the epilimnion, which is typically characterized by larger observational variance, or in the hypolimnion, which is typically associated with much smaller variance, does not have the same meaning and if not normalized it may lead to incorrect conclusions (Amadori et al., 2021; Feldbauer et al., 2022; Wood et al., 2023). The usefulness of evaluating depth-specific metrics clearly emerges from Figure 7 (that will be discussed in more detail in Section 6.4), where for the 1D lake model GLM has a similar RMSE in the epilimnion or in the hypolimnion (around 0.75–0.80°C at 5 and below 20 m depth) is associated to different NSE values (around 0.97 and <0.93, respectively). We note that for metrics such as ME, MAE, MSE, and MRME the overall values obtained considering all the available data correspond to taking the average of the depth-specific metrics, if the sample sizes at different depths are the same. When assessing the performance of a model in simulating time series with prominent seasonal patterns, such as LSWT, it may be preferable to use NSE* instead of NSE (see Table 2)

to better understand how well the model captures dynamics that are not part of the seasonal component (Piccolroaz et al., 2016; Schaeffli & Gupta, 2007). In this case, it is worth noting that $NSE^* = 1$ indicates perfect model fitting, just like NSE. However, $NSE^* = 0$ implies that the model performs as well as assuming the mean year of measurements, which is different from $NSE = 0$ that indicates the model performs as well as assuming the mean observed value.

Particularly when evaluating the performance of 0D and 0.5D statistical or hybrid models, it is recommended to use information theory and the corresponding scores to rank models based on a trade-off between goodness of fit and model parsimony (i.e., number of model parameters, see Table 2). The main examples of these scores are the Akaike Information Criterion (AIC, Akaike, 1974) and the Bayesian Information Criteria (BIC, Schwarz, 1978). These information criteria have been successfully adopted in several studies (e.g., Piotrowski et al., 2021; Toffolon et al., 2022; Woolway, Sharma, et al., 2021). However, we note that the choice of the performance metric may not be sufficient to evaluate the reliability of a model to predict the investigated processes. It must be coupled with appropriate calibration procedures that are appropriate for the model and for the physical processes that are approximated by the model (Triana et al., 2019), as is further discussed in the next section.

The degree to which a model is validated depends on the choice of the number and type of performance metrics to be adopted. This choice is often guided by the background and experience of the modeler and is not immune from a general desire to report favorably on the performance of the model (Hipsey et al., 2020). This subjectivity and possible bias in model validation could be overcome by the adoption of assessment standards based on universally accepted performance criteria, which however is still lacking but is highly desired to facilitate inter-comparison of different model approaches. An unspoken rule that seems to be tacitly accepted by modelers is the combined use of multiple performance metrics. In fact, each performance metric generally measures only specific aspects of a model's performance thus single performance criterion may lead to counterproductive or biased results such as favoring models that do not reproduce important features of a system (Bennett et al., 2013).

5.2. Calibration/Optimization Methods

The majority of computational models in different fields of science have some parameters that need to be calibrated/optimized, hereafter referred to as optimized, often by fitting them to empirical-based data. There are, however, contradictory conceptual, or ideological, approaches to optimization. According to some researchers, optimization is merely a technique to make the model empirically adequate, even if it does not necessarily make it reliable for making predictions of any kind (Oreskes et al., 1994). Although such an approach may seem ideologically tempting at first, it is empirical confirmation that allows scientists to trust any theory or model. For example, the lack of empirical confirmation makes some fundamental issues, like the theoretical discussion on the existence of multiverse (Ellis, 2008) or on the real existence of pure mathematical objects (Abbott, 2013) at best on the edge of science. Although optimization of models can limit the validity of the research that is made using such models, fitting some model parameters to empirical data is often unavoidable and makes a process-driven model a semi-empirical model (Gupta et al., 2006). However, existing literature provides evidence that enhancing the realism of a model can, in some cases, diminish the necessity for extensive model calibration (e.g., Gharari et al., 2014; Guinot & Gourbesville, 2003).

There are generally four main ways to perform optimization of water temperature models. Some prefer manual calibration, in which user modifies the values of parameters based on expert knowledge. Although this approach is still sometimes recommended (Yu et al., 2022), it can be highly inefficient in terms of both time needed and effects obtained. Nonetheless, manual calibration is frequently used for computationally demanding, 2D (Diogo et al., 2008; Ishikawa et al., 2022; Zouabi-Aloui et al., 2015) and 3D (Castelletti et al., 2010; Hodges & Dallimore, 2001; Hui et al., 2018; B. Martin et al., 2013; Missaghi & Hondzo, 2010; Preston et al., 2014; Soullignac et al., 2017) thermo-hydrodynamic lake or reservoir models. The other approach is using gradient, or second-order derivative-based algorithms (Battiti, 1992; Levenberg, 1944), which are often fast and accurate in finding the local optimum. However, such algorithms generally converge to the closest local solution and require the model to be differentiable; both issues pose important limitations for lake water temperature models. The examples of application of such algorithms include mainly ML tools (Saber et al., 2020; S. Zhu, Ptak, Yaseen, et al., 2020). The third group of methods is composed of so-called metaheuristic optimization algorithms (Del Ser et al., 2019), which are optimization algorithms inspired by natural or artificial systems to fine-tune model parameters and achieve an optimal fit to observed data, and can be applied for calibration of almost any kind of lake water temperature models (e.g., Afshar et al., 2011; Piccolroaz et al., 2013; Piotrowski et al., 2022;

Shabani et al., 2021; Xia et al., 2021; Yousefi & Toffolon, 2022; S. Zhu et al., 2021). The use of metaheuristic algorithms in calibrating environmental models is encouraged in Maier et al. (2019). Finally, Markov Chain Monte Carlo (MCMC) algorithms (Andrieu et al., 2010; Braak, 2006; Vrugt et al., 2013) that iteratively generate samples of parameter values from a probability distribution, are mainly used for calibration of 3D models (e.g., Hipsey et al., 2019; Safin et al., 2022).

Some early LSWT modeling studies claim that water temperature models may not need calibration to each specific lake, as their parameters are relatively easily generalized to different water bodies (Hondzo & Stefan, 1993). For example, generalizations may be made based on links between model parameters, location and bathymetry of the lake (Fang & Stefan, 2009). However, studies on large numbers of lakes have shown that the lack of lake-specific calibration decreases the performance of water temperature model simulations (Read et al., 2014). Recently, lake-specific features were used to transfer trained process-guided deep learning models of water temperature from observed to unobserved systems via a meta-model (Willard et al., 2021). This work highlights the flexibility of deep learning to leverage information across lakes, but also confirms the importance of lake features in the prediction of lake water temperature at broad scales. Currently, most lake water temperature models are being calibrated for each specific case.

In our opinion, model calibration methods should be explicitly described, as previous studies showed that the choice of calibration method may be a crucial factor affecting the performance of lake water temperature modeling (Piotrowski et al., 2023; S. Zhu et al., 2021). The choice of the calibration method should always depend on the model and user requirements (Maier et al., 2019; Osaba et al., 2021; Weise et al., 2012). If the objective function is differentiable and the problem is unimodal (or have a few local optima with solutions of similar quality), gradient-based methods are a good choice. If the problem is not differentiable, but low-dimensional and its fitness landscape have a simple shape, one may try manual calibration. If the problem may have many local minima of diverse quality, metaheuristics or MCMC algorithms should be used. Specifically, when one wants to address the problem of parameter uncertainty, MCMC are often the best options. When a single solution is to be found for a highly-dimensional model, metaheuristics are the advisable tools. Other factors that should be taken into account include computational complexity (computationally demanding models may require gradient-based methods or surrogate-based heuristics Jin (2011), see also Xia et al. (2021) for a case focused on limnology) and the number of objectives (if one wants to fit the model to more than one criteria, multi-objective algorithms are needed).

There are also some technical points that are often neglected, but may highly affect the final outcome of the calibration procedure. First, one has to repeat calibration of the model a number of times because most calibration algorithms are stochastic in the sense that they include some randomness in their operators. As a result, two different simulations may produce two different results, hence a number of simulations is needed to summarize the quality of solutions. Additionally, even if the calibration procedure is purely deterministic, if the model is not unimodal (hence have more than a single optimum), the solution finally found may depend on the location of the initial solutions. Again, multiple simulations from different initial solutions is needed. After performing a number of simulations, some statistics on the quality of solutions should be reported. The importance of repeated simulations has been pointed out in the optimization literature (Vecsek et al., 2017), but also in limnological research (Yousefi & Toffolon, 2022).

The second important technical point that needs to be addressed in calibration is the careful choice of the algorithm's control parameters. It is often overlooked that nearly every calibration algorithm has its own set of control parameters, and some of these parameters can significantly affect performance. The simplest example is population size in evolutionary algorithms (Eiben et al., 1999; Piotrowski et al., 2020), but various kinds of control parameters exist in almost any optimization algorithm, including MCMC, metaheuristics, and gradient-based techniques. Before running an algorithm one should decide whether to use the "classical" (e.g., suggested by the authors of the particular procedure) control parameters, or perform pre-tuning (C. Huang et al., 2020). Pre-tuning is advisable for a novel application of particular optimizer, but as tuning is computationally demanding, in most cases authors prefer to rely on the suggested control parameters. However, this may lead to sub-optimal performance of the method if the recommendations were produced using a different use-case.

The third technical issue to consider when calibrating lake temperature models relates to the stopping criteria that are to be used for the algorithm. In the case of gradient-based methods, these are rather simple to set, but for metaheuristics or MCMC methods the choice of stopping conditions is more subjective and may highly affect the results (e.g., Even-Dar et al., 2006; Piotrowski et al., 2017; Sergeev et al., 2018). Modelers should ensure the

computational time allowed for the optimizer would be sufficient to find solutions of appropriate quality, otherwise the performance of the calibrated model may be affected. Finally, it should be remembered that developing the universally “best” calibration method is impossible (Wolpert & MacReady, 1997), and that the performance of various algorithms may highly differ for the specific problem. For a more general guide on the application of optimization algorithms, we refer the interested readers to Handberg and Campante (2011), Weise et al. (2012), Shahriari et al. (2016), Maier et al. (2019), Osaba et al. (2021), and Ma et al. (2023) for more details.

6. Emerging Modeling Approaches and Future Directions

6.1. Forecasting

Forecasting of water quality and ecological variables is needed for projecting future changes, validating our modeling tools and informing water management (Dietze et al., 2018). There has been a recent focus on either near-term or seasonal forecasts of water temperature. Thomas et al. (2020) developed the real-time iterative water temperature forecasting system Forecasting Lake and Reservoir Dynamics (FLARE) which consists of a data assimilation procedure and an ensemble-based forecasting algorithm to create 16-day forecasts of water temperature (using GLM) with uncertainty. A near-term forecasting study on six lakes across the United States revealed that the accuracy of water temperature forecasts depended on lake depth as well as water clarity (Thomas et al., 2020). Recently, the National Ecological Observatory Network (NEON) Ecological Forecasting Challenge created an open-data framework to advance theory in ecology by near-term forecasting of ecological variables, including water temperature (Thomas et al., 2022). There are also examples of near-term forecasting applications including data assimilation that use 3D hydrodynamics models in large lakes, that is, Lake Geneva (Baracchini, Wüest, & Bouffard, 2020) or Lake Erie (Lin et al., 2022). In both cases, the simulations results are published on user-friendly data visualization web-platform open the public and are expected to support governmental agencies in charge of the water resources management and policy making (see <http://meteolakes.ch> and <https://coastlines.engineering.queensu.ca/>). For seasonal forecasts, Mercado-Bettín et al. (2021) used GLM and GOTM for two lake systems to explore how temperature forecasts vary across different hydrologic models and climate input data. Clayer et al. (2023) further coupled these lake models with hydrological models forced with seasonal meteorological forecast ensembles to provide probabilistic predictions of seasonal anomalies in lake water temperature and ice-off. The concept of using forecasting to improve modeling theory can be an opportunity in water temperature modeling to improve existing algorithms and compare alternative model concepts (A. S. Lewis et al., 2022; Carey et al., 2022).

6.2. Digital Twins

A digital twin is a virtual representation of a physical “real” lake. The concept of a digital twin is commonly applied in other fields like water resource management and hydrology (e.g., Henriksen et al., 2023; Ramos et al., 2023; Rigon et al., 2022), but has not been extensively applied to lakes. As part of the Digital Earth (X. Li et al., 2023), the digital twin of lakes has the potential to be a strategic resource for decision-making, enabling timely interventions that can yield improved results. For instance, it can assist in assessing the impact of climate change on lake thermal dynamics and identifying feasible mitigation measures. To develop a digital twin for the study of lake thermal dynamics, four foundational elements are needed: (a) the physical twin, namely the lake itself, (b) data sets, which includes all available observations, (c) the digital twin, which includes one or more lake models with access to the data sets and modeling results to support well-timed decision-making; and (d) incorporation of decision-support tools, which include visualization capabilities and customizable digital interfaces. With the development of the digital twin of lakes, we can further answer “what if” questions, for example, what if the lake experiences extreme events (e.g., heatwaves) or human-induced alterations (e.g., selective withdrawals)? How will this impact the lake thermal dynamics (e.g., stratification and mixing) and water quality? What can be done to mitigate the negative impacts? Engaging in the creation of digital twin models for lakes represents a strategic and pioneering approach with promising prospects for scientific advancement.

6.3. Combining Process-Based Modeling With Deep Learning

ML models are more flexible compared to process-based models as they do not require the mathematical structure that represents physical processes. Though ML models have proven their efficiency and accuracy in lake water temperature modeling (see the literature cited in Section 4.1), they lack clear physical meaning, which

can lead to poor performance when predicting in out-of-bounds conditions such as future climate scenarios or in the large majority of lakes that are rarely or never monitored. To overcome this issue, coupling ML models (e.g., deep learning) with theory (physical laws) in various model architectures and methods have been proposed (Willard, Read, et al., 2022). For example, Read et al. (2019) proposed a hybrid modeling framework for the prediction of lake water temperature profiles. Three aspects of knowledge or theory were included in this modeling framework: temporal awareness in the form of an LSTM, enforcement of physical laws through model penalties when predictions violated conservation of energy, and pretraining with simulated water temperature from a process-based model. These methods have been shown to outperform process-based models and pure deep learning methods (Read et al., 2019; X. Jia et al., 2021). These and other hybrid models have led to the emergence of a new modeling approach often referred to as Knowledge-Guided Machine Learning (KGML), in which deep learning neural networks and physics-based models are combined to leverage their complementary strengths and improve the modeling of physical processes (Appling et al., 2022; Chen et al., 2023; X. Jia et al., 2019; Willard, Jia, et al., 2022). Furthermore, ML has the potential to assist in calibrating process-driven models and identifying the aspects or algorithms that may be lacking in these models.

6.4. Evaluating Structural Model Differences Through Ensemble Modeling

Water temperature modeling studies routinely compare the predictions and performance of different models (e.g., Heddam et al., 2020; Sharma et al., 2008; Yousefi & Toffolon, 2022; S. Zhu, Ptak, Yaseen, et al., 2020). For example, Yousefi and Toffolon (2022) compared nine ML models including both shallow and deep ones for the forecasting of LSWT, and the results showed that none of the nine ML models clearly prevails. In a recent study, Di Nunno et al. (2023) demonstrated that ensemble models, created by stacking multiple ML algorithms, can enhance the predictive performance of individual ML algorithms when forecasting LSWT. Likewise, Almeida et al. (2022) compared the prediction capabilities of FLake and the Hostetler models in reproducing LSWT against a ML algorithm in 24 reservoirs where temperature dynamics are substantially affected by inflows/outflows. They found that ML models may outperform process-based physical models in terms of both accuracy and computational cost when long-term observations were available. However, because these inter-comparisons were conducted on a limited number of lakes/reservoirs, they could not claim which modeling approach was the best. This is particularly true considering that, generally speaking, the choice of the best model depends on the specific process at hand and results from a compromise between model performance, data requirements, and computational cost. Furthermore, the performance of any model relies on the user's knowledge of the model and ability to calibrate or train it. However, it is challenging for scientists to be experts in the implementation of every model. Therefore, it is advisable to approach model comparison studies with caution in this regard.

Ensemble modeling is the state-of-the-art technique to conduct structural model comparison studies of 1D process-based models and evaluate the uncertainty around future projections. An early ensemble modeling initiative was the LakeMIP project which was initiated in 2008. During the first phase, several 1D models were compared, including a completely mixed model, FLake, Hostetler, CLM4-LISSS, MINLAKE96, LAKE, Simstrat, and LAKEoneD. The models were evaluated by using data from a shallow, turbid lake in Germany. The results showed that all eight models generally captured diurnal and seasonal variability of LSWT reasonably well. However, some models were not able to realistically reproduce temperature stratification in summer (Stepanenko et al., 2013). Further, Stepanenko et al. (2014) compared five of the eight models (FLake, CLM4-LISSS, LAKE, LAKEoneD, and Simstrat) in a small boreal lake and Thiery et al. (2014) compared seven of the eight models in a large, deep tropical lake. These ensemble modeling studies improved the ability to project future water temperature and thermal structure of lakes at global or regional scales, while further improvement is still needed to better serve the community regarding the impact of climate change on lake ecosystems (e.g., water quality, lake biogeochemistry). An emerging issue of ensemble modeling is that the computational implementation is quite challenging and time-consuming in case of setting up and running multiple lake models as emphasized in Soares and do Carmo Calijuri (2021), which might need better cooperation within the scientific community. To facilitate and ease the use of ensemble modeling, and to create a common framework for ensemble modeling of 1D process-based lake models, the R package *LakeEnsemblR* was developed by Moore et al. (2021). Users of *LakeEnsemblR* can run ensembles of 1D lake models (FLake, GLM, GOTM, Simstrat, MyLake) from the same input data, and the results are compiled in a single output file (Moore et al., 2021). Example ensemble studies include the evaluation of a lake's physical properties (Lake Kinneret, Israel) using an ensemble of 1D hydrodynamic lake models (Gal et al., 2020); an ensemble of vertical 1D hydrodynamic lake models used to calculate

water temperature, stratification, and ice cover for the reservoir Lichtenberg in Germany (Feldbauer et al., 2022); and the impact of increased winter salt loads on spring overturn and summer stratification evaluated using an ensemble approach (Ladwig, Rock, & Dugan, 2021).

As an example, we used *LakeEnsemblR* to simulate the thermal structure of Lough Feeagh (Ireland) over a period of 2 years. The lake has a surface area of 3.9 km², a surface elevation of 11 m, a mean depth of 14 m, and a maximum depth of 46 m. The results are shown in Figure 7 for the three 1D lake models GLM, GOTM, and Simstrat, and refer to the calibration period running all models on an hourly time step. Figure 7 illustrates the distribution of various performance metrics throughout the water column, showcasing the evaluation of each metric at specific depths. We also calculated the same metrics across all depths (red lines in Figure 7) to emphasize the importance of considering depth-specific metrics to better understand the strengths and weaknesses of each model (see Section 5.1 and Table 2 for a detailed explanation of each metric). Overall, both methods of calculating performance metrics lead to similar conclusions for this lake: (a) Simstrat outperforms GLM and GOTM, (b) GLM exhibits lower overall performance with the highest error at the depth of the metalimnion but also overall smaller performance differences between the epilimnion and hypolimnion, (c) Simstrat and GOTM clearly demonstrate a decline in performance in the hypolimnion compared to the epilimnion. Generally, model performance degrades the further a grid cell is located away from the surface boundary conditions. Especially integral energy models (i.e., GLM) have shortcomings replicating heat transport at the location of the highest density gradient, hence the metalimnion. In this example, turbulence-based models (i.e., GOTM and Simstrat) performed better at the metalimnion, but their performance deteriorated in the hypolimnion.

A framework for ensemble modeling of climate change impacts on lakes worldwide has been established through the lake sector initiative in the Inter-Sectoral Impact Model Intercomparison Project (ISIMIP, Golub et al., 2022). The framework included 11 lake models and observed data for lakes worldwide, which permits lake thermal studies at a global scale. The ISIMIP results highlighted the potential impacts of future climate change, such as increased summer stratification periods (Woolway, Sharma, et al., 2021), a global future increase in methane production (Jansen et al., 2022), a decrease of winter ice thickness in lakes in the Northern hemisphere (Grant et al., 2021), increased future intensity of heatwaves acting on the lake surface (S. Wang et al., 2021), and the magnitude of global heat uptake in inland waters (Vanderkelen et al., 2020). Multi-lake-model simulations are increasingly used to obtain robust assessments of freshwater ecosystem responses to climate change. A key challenge for understanding historic and future change in the thermal structure of lakes is to quantify the contribution of natural versus human-induced external forcing. With large ensemble simulations (i.e., a set of projections starting from different initial conditions but produced with a single model and identical external forcing), the human-induced and naturally varying variations in lake temperature can be quantified (Deser et al., 2020). Most notably, using large ensembles, one can investigate the anthropogenic and natural variability components of lake temperature changes, enabling (a) identification of the anthropogenic signal itself and (b) a timescale over which such changes will emerge over natural variability (Woolway et al., 2022). Recent studies have highlighted the benefit of using large ensemble simulations to investigate lake ice responses to natural and anthropogenic drivers (L. Huang et al., 2022), but future studies could also consider evaluating lake temperature responses to climate change within a large ensemble.

6.5. Adaptive Water Management

In reservoirs, the transport of mass, dissolved or suspended compounds, and overall energy is affected by the presence of a dam. Upstream-downstream transfers of water mass and properties, including water temperature, is often complex to quantify and to model due to the existence of withdrawals, diversions and inflows. Selective withdrawals, for example, are structures allowing the release of water from different depths in the reservoirs and are used to meet downstream water temperature and, more generally, water quality targets and mitigate undesirably warm or undesirably cool peak events (i.e., thermopeaking). A common way to operate a selective withdrawal system is by releasing warmer water from a shallower depth to mitigate the impact of cold and abrupt peak flow during the period of hydropower generation in summer compared to the case of a fixed hypolimnetic withdrawal, which is the most common situation (Kim & Choi, 2021). Another more sophisticated alternative is to modulate the use of the different withdrawals distributed along the water column during the year, which can relieve the impact of climate warming on downstream river water temperatures in summer and the consequent decline of cold water species' habitats but at the cost of warmer stream temperatures in winter (Rheinheimer et al., 2015). In

any case, a proper design of a selective withdrawal system requires knowledge of depth-specific thermal dynamics of the reservoir, which can be obtained with one of the modeling tools discussed above (in many previous studies the 2D lake model CE-QUAL-W2 has been used). The modeling of selective withdrawal not only allows to optimize its operation to meet the downstream temperature targets but provides a quantification of the impact of these operations on stratification, mixing, and water flow in the reservoir, which have obvious implications for its ecology and environment. Some research suggests that a deep withdrawal decreases the strength of summer stratification, thus improving oxygen availability and reducing the accumulation of nutrients in the hypolimnion (Duka et al., 2021; U. Kobler et al., 2018) (note that e.g., Weber et al., 2017 highlighted how withdrawal from the epilimnion on the other hand strengthened thermal stratification and decreased hypolimnetic oxygen availability). However, complexities of the reservoir regulation scenarios make this finding difficult to generalize. The different types of control structures (e.g., stoplog gate, temperature-control curtain; He et al., 2023), and the peculiarities of each hydropower network, are often complicated by the presence of a cascade of reservoirs (H. Wang et al., 2023) or pumped-storage plants (U. Kobler et al., 2018). The release of water from a reservoir (e.g., for power generation, dam spills) can cause the displacement of fish from the reservoir, a process known as fish entrainment. Fish entrainment can directly result in injury or death of individuals, as well as reduce the abundance of upstream populations and increase the abundance of downstream populations (Coutant & Whitney, 2000). The seasonal temperature stratification and fish habit use of the reservoir result in different entrainment vulnerability for fish species. Recommendations were provided for the reservoir operators to maximize operations while mitigating and compensating for fish entrainment. In this respect, lake modeling is a valuable tool to support the design and operation of reservoirs characterized by selective withdrawals and pumped-storage plants, which could be considered when carrying out environmental impact assessments for an effective management of the water resources.

6.6. Coupling of Climate and Lake Models

To investigate the impact of climate change on the thermal dynamics of lakes, it is essential to couple climate and lake models, which can be achieved through one-way or two-way coupling. In one-way coupling, time series of climate variables that are relevant for lake thermal dynamics, such as air temperature, are extracted and used as inputs for the lake model to simulate future lake thermal conditions (see e.g., Fang & Stefan, 1996; Gula & Peltier, 2012; Mi et al., 2020; Sterckx et al., 2023). In one-way coupling, downscaled meteorological forcing from global circulation or regional climate models is often required, which can be obtained using various methods available in the literature, such as the change factor method (Piccolroaz, Zhu, et al., 2021), empirical-statistical approaches (Gutiérrez et al., 2019), and deep learning methods (Baño Medina et al., 2022). Our ability to understand future lake conditions has improved as climate modeling and downscaling techniques have improved in recent decades (Alizadeh, 2022). However, large uncertainty remains in some future climate features (e.g., precipitation) that will impact lake thermodynamics (Alizadeh, 2022; Lopez-Cantu et al., 2020). Further, it is important to recognize that while connecting lake temperature models to climate projections can help us understand future lake conditions, both data-driven and process-based models can perform poorly when trying to predict in previously unseen conditions (e.g., Sungmin et al., 2020). One advantage of data-driven models is their flexibility to incorporate and learn from a wider range of data that might help inform the model on how lakes might respond to future change (e.g., data from multiple lakes across latitudes that might represent future conditions). Carefully considering evaluation criteria and model setup is critical for predicting responses to climate change (Madsen et al., 2014).

While one-way coupling is the simplest and most widely used approach, it only considers the impact of climate change on lake thermal dynamics and does not account for feedbacks from lakes to the atmosphere. As a result, important interactions between the two systems may not be captured. Two-way coupling solves this issue by fully integrating the climate and lake models, enabling the feedback impact of lake thermal processes on regional climate to be considered (Guo et al., 2022; Mallard et al., 2014). A typical example of two-way coupling is given by the models *sensu* Henderson-Sellers (1985), and other examples have been implemented in the Community Land surface Model (CLM-Lake) (Oleson et al., 2013), Common Land Model (CoLM-Lake) (Dai et al., 2018), Community Earth System Model (CESM-LISS) (Lawrence et al., 2019; Subin et al., 2012), and the Weather Research and Forecast model (WRF-Lake) (Gu et al., 2015). Two way coupling has been widely used to study lake/reservoir thermal dynamics, lake ice coverage, lake-atmosphere interactions, and climate change effects on lakes (see e.g., Guo et al., 2022, 2023a; Gu et al., 2015; F. Wang et al., 2019; Wu et al., 2020; X. Wang

et al., 2023; Xiao et al., 2016). Another example is the FLake model, which has been coupled in one-way with ERA40 reanalysis data (Martynov et al., 2010) and WRF (Gula & Peltier, 2012), and incorporated as a lake parameterization scheme into the Consortium for Small-scale Modeling—COSMO model (Mironov et al., 2010) and coupled in two-way model configurations with WRF (Mallard et al., 2014).

FLake and Hostetler models have been successfully coupled with the Canadian Regional Climate Model—CRCM5, demonstrating that considering lakes in simulated climate can have a significant impact, as shown by comparing multi-decadal simulations with and without lakes. The models have performed well in simulating temperate subgrid lakes and large shallow lakes, especially for FLake (Martynov et al., 2012). However, the performance of both 1D lake models in large deep lakes has been relatively poor due to the lack of representation of 3D processes such as upwelling and downwelling, horizontal circulation, and thermal bar formation. In this regard, efforts have been made in the last decades to fully couple 3D lake models with climate models for regional studies, especially because large and deep lakes exhibit substantial seasonal lags in temperature and fluxes compared to other landscapes (León et al., 2007). Multi-column 1D lake models for example, based on Hostetler (Notaro et al., 2013) and Simstrat (Gaillard et al., 2022), have been proposed as computationally-efficient alternatives to full 3D lake models. Multi-column models consider 1D flat-bottom columns distributed spatially across a 2D domain and neglect horizontal heat and mass transport, thus achieving a first level spatially-resolved representation of 3D thermal dynamics. However, recent studies in the Great Lakes region have overcome these limitations by proposing a two-way coupled 3D lake-ice-climate modeling system called the Great Lakes-Atmosphere Regional Model, which significantly outperformed previous coupled 1D simulations (Xue et al., 2017). This system has also been used to provide high-resolution ensemble projections of climate change, highlighting its potential for regional climate studies (Xue et al., 2022).

7. Conclusions

This review offers a valuable resource for scientists working in limnology and hydrology who seek to understand lake water temperature modeling and its potential applications. It provides an overview of the subject matter and highlights important considerations for future research and application, making it useful for both seasoned modelers and those new to the field. The review covered the physics governing thermal dynamics in lakes, different sources of observational water temperature data, available lake water temperature models, model performance evaluation, and emerging modeling approaches. Based on our analysis we identified some key areas that future efforts could prioritize, including improving forecasting capabilities also through the development of digital twins of lakes, evaluating lake water temperature responses to climate change using large ensemble models and advancing toward two-way coupling between 3D lake and climate models, and adopting universally accepted performance criteria for model assessment and inter-comparison of different model approaches. Overall, this review emphasizes the importance of mathematical modeling as an essential tool for understanding how various factors, including climate change, affect lake thermal dynamics and related processes.

Data Availability Statement

The data used to create Figure 7 and the scripts used to generate it are available at Piccolroaz et al. (2024).

The ESA CCI LAKES dataset v2.0.2 used to prepare Figure 4 can be freely downloaded at the CEDA (Centre for Environmental Data Analysis) archive <https://catalogue.ceda.ac.uk/uuid/a07deacaffb8453e93d57ee214676304> and future versions are planned to become available. The ESA CCI LAKES dataset includes lake surface water temperature in addition to lake ice cover, lake water leaving reflectance, lake water level and extent. Tools to download the data are available at the github repository https://github.com/cci-lakes/lakes_cci_tools.

References

- Abbott, D. (2013). The reasonable ineffectiveness of mathematics [point of view]. *Proceedings of the IEEE*, 101(10), 2147–2153. <https://doi.org/10.1109/JPROC.2013.2274907>
- Aderoft, A., Hill, C., & Marshall, J. (1997). Representation of topography by shaved cells in a height coordinate ocean model. *Monthly Weather Review*, 125(9), 2293–2315. [https://doi.org/10.1175/1520-0493\(1997\)125<2293:ROTBSC>2.0.CO;2](https://doi.org/10.1175/1520-0493(1997)125<2293:ROTBSC>2.0.CO;2)
- Afshar, A., Kazemi, H., & Saadatpour, M. (2011). Particle swarm optimization for automatic calibration of large scale water quality model (CE-QUAL-W2): Application to karkheh reservoir, Iran. *Water Resources Management*, 25(10), 2613–2632. <https://doi.org/10.1007/s11269-011-9829-7>

Acknowledgments

SP acknowledges the Italian Ministry of Universities and Research (MUR), in the framework of the project DICAM-EXC (Departments of Excellence 2023–2027, Grant L232/2016). SZ acknowledges the funding support provided by the National Natural Science Foundation of China (No. 52109099) and the Natural Science Foundation of the Jiangsu Higher Education Institutions of China (22KJB170023). RL was supported by a University of Wisconsin-Madison (UW-Madison) Integrative Biology Postdoctoral Fellowship Fund, a United States National Science Foundation (NSF) Advances in Biological Informatics (ABI) development grant (#DBI 1759865), UW-Madison Data Science Initiative grant, and NSF Harnessing the Data Revolution (HDR) Grant (#1934633). AP was supported within the Institute of Geophysics Polish Academy of Sciences statutory activities by Ministry of Education and Science of Poland, No. 3841/E-41/2023. The European Space Agency (ESA) Climate Change Initiative (CCI)—New Essential Climate Variables (ECVs) for Lakes (grant reference 4000125030/18/I-NB) has provided the majority of support for the creation of the lake surface water temperature (LSWT) data set used in the satellite Earth observation section. The Copernicus Climate Change Service (C3S) support is also acknowledged for the extensions and dissemination of the ESA CCI LSWT data set. Any use of trade, firm, or product names is for descriptive purposes only and does not imply endorsement by the U.S. Government.

- Akaike, H. (1974). A new look at the statistical model identification. *IEEE Transactions on Automatic Control*, 19(6), 716–723. <https://doi.org/10.1109/TAC.1974.1100705>
- Alizadeh, O. (2022). Advances and challenges in climate modeling. *Climatic Change*, 170(1–2), 18. <https://doi.org/10.1007/s10584-021-03298-4>
- Almeida, M. C., Shevchuk, Y., Kirillin, G., Soares, P. M. M., Cardoso, R. M., Matos, J. P., et al. (2022). Modelling reservoir surface temperatures for regional and global climate models: A multi-model study on the inflow and level variation effects. *Geoscientific Model Development*, 15(1), 173–197. <https://doi.org/10.5194/gmd-15-173-2022>
- Amadori, M., Giovannini, L., Toffolon, M., Piccolroaz, S., Zardi, D., Bresciani, M., et al. (2021). Multi-scale evaluation of a 3D lake model forced by an atmospheric model against standard monitoring data. *Environmental Modelling & Software*, 139, 105017. <https://doi.org/10.1016/j.envsoft.2021.105017>
- Andersen, T. K., Nielsen, A., Jeppesen, E., Bolding, K., Johansson, L. S., Søndergaard, M., & Trolle, D. (2022). Simulating shifting ecological states in a restored, shallow lake with multiple single-model ensembles: Lake Arreskov, Denmark. *Environmental Modelling & Software*, 156, 105501. <https://doi.org/10.1016/j.envsoft.2022.105501>
- Anderson, E. J., Stow, C. A., Gronewold, A. D., Mason, L. A., McCormick, M. J., Qian, S. S., et al. (2021). Seasonal overturn and stratification changes drive deep-water warming in one of Earth's largest lakes. *Nature Communications*, 12(1), 1688. <https://doi.org/10.1038/s41467-021-21971-1>
- Andrieu, C., Doucet, A., & Holenstein, R. (2010). Particle Markov Chain Monte Carlo methods. *Journal of the Royal Statistical Society*, 72(3), 269–342. <https://doi.org/10.1111/j.1467-9868.2009.00736.x>
- Annear, R. L., & Wells, S. A. (2007). A comparison of five models for estimating clear-sky solar radiation. *Water Resources Research*, 43(10), W10415. <https://doi.org/10.1029/2006WR005055>
- Appling, A. P., Oliver, S. K., Read, J. S., Sadler, J. M., & Zwart, J. A. (2022). Machine learning for understanding inland water quantity, quality, and ecology. In T. Mehner & K. Tockner (Eds.), *Encyclopedia of inland waters* (2nd ed., pp. 585–606). Elsevier. <https://doi.org/10.1016/B978-0-12-819166-8.00121-3>
- Arifin, R. R., James, S. C., de Alwis Pitts, D. A., Hamlet, A. F., Sharma, A., & Fernando, H. J. (2016). Simulating the thermal behavior in Lake Ontario using EFDC. *Journal of Great Lakes Research*, 42(3), 511–523. <https://doi.org/10.1016/j.jglr.2016.03.011>
- Austin, J. A. (2012). Resolving a persistent offshore surface temperature maximum in Lake Superior using an autonomous underwater glider. *Aquatic Ecosystem Health and Management*, 15(3), 316–321. <https://doi.org/10.1080/14634988.2012.711212>
- Austin, J. A. (2013). The potential for autonomous underwater gliders in large lake research. *Journal of Great Lakes Research*, 39, 8–13. <https://doi.org/10.1016/j.jglr.2013.01.004>
- Austin, J. A., & Colman, S. M. (2007). Lake superior summer water temperatures are increasing more rapidly than regional air temperatures: A positive ice-albedo feedback. *Geophysical Research Letters*, 34(6), 8–13. <https://doi.org/10.1029/2006GL029021>
- Ayala, A. I., Moras, S., & Pierson, D. C. (2020). Simulations of future changes in thermal structure of lake Erken: Proof of concept for ISIMIP2b lake sector local simulation strategy. *Hydrology and Earth System Sciences*, 24(6), 3311–3330. <https://doi.org/10.5194/hess-24-3311-2020>
- Bachmann, R. W., Sharma, S., Canfield, D. E., & Lecours, V. (2019). The distribution and prediction of summer near-surface water temperatures in lakes of the coterminous United States and Southern Canada. *Geosciences*, 9(7), 296. <https://doi.org/10.3390/geosciences9070296>
- Baño Medina, J., Manzananas, R., Cimadevilla, E., Fernández, J., González-Abad, J., Cofiño, A. S., & Gutiérrez, J. M. (2022). Downscaling multi-model climate projection ensembles with deep learning (DeepESD): Contribution to CORDEX EUR-44. *Geoscientific Model Development*, 15(17), 6747–6758. <https://doi.org/10.5194/gmd-15-6747-2022>
- Baracchini, T., Chu, P. Y., Šukys, J., Lieberherr, G., Wunderle, S., Wüest, A., & Bouffard, D. (2020). Data assimilation of in situ and satellite remote sensing data to 3d hydrodynamic lake models: A case study using Delft3D-FLOW v4.03 and OpenDA v2.4. *Geoscientific Model Development*, 13(3), 1267–1284. <https://doi.org/10.5194/gmd-13-1267-2020>
- Baracchini, T., Wüest, A., & Bouffard, D. (2020). MeteoLakes: An operational online three-dimensional forecasting platform for lake hydrodynamics. *Water Research*, 172, 115529. <https://doi.org/10.1016/j.watres.2020.115529>
- Barbosa, C. C., do Carmo Calijuri, M., Dos Santos, A. C. A., Ladwig, R., de Oliveira, L. F. A., & Buarque, A. C. S. (2021). Future projections of water level and thermal regime changes of a multipurpose subtropical reservoir (Sao Paulo, Brazil). *Science of the Total Environment*, 770, 144741. <https://doi.org/10.1016/j.scitotenv.2020.144741>
- Battiti, R. (1992). First-and second-order methods for learning: Between steepest descent and Newton's method. *Neural Computation*, 4(2), 141–166. <https://doi.org/10.1162/neco.1992.4.2.141>
- Bayer, T., Burns, C., & Schallenberg, M. (2013). Application of a numerical model to predict impacts of climate change on water temperatures in two deep, oligotrophic lakes in New Zealand. *Hydrobiologia*, 713(1), 53–71. <https://doi.org/10.1007/s10750-013-1492-y>
- Bennett, N. D., Croke, B. F., Guariso, G., Guillaume, J. H., Hamilton, S. H., Jakeman, A. J., et al. (2013). Characterising performance of environmental models. *Environmental Modelling & Software*, 40, 1–20. <https://doi.org/10.1016/j.envsoft.2012.09.011>
- Bilello, M. A. (1964). Method for predicting river and lake ice formation. *Journal of Applied Meteorology and Climatology*, 3(1), 38–44. [https://doi.org/10.1175/1520-0450\(1964\)003<0038:MFPRAL>2.0.CO;2](https://doi.org/10.1175/1520-0450(1964)003<0038:MFPRAL>2.0.CO;2)
- Boegman, L., Loewen, M. R., Hamblin, P. F., & Culver, D. A. (2001). Application of a two-dimensional hydrodynamic reservoir model to Lake Erie. *Canadian Journal of Fisheries and Aquatic Sciences*, 58(5), 858–869. <https://doi.org/10.1139/f01-035>
- Boehrer, B., Fukuyama, R., & Chikita, K. A. (2013). Geothermal heat flux into deep caldera lakes shikotsu, kuttara, tazawa and towada. *Limnology*, 14(2), 129–134. <https://doi.org/10.1007/s10201-013-0399-7>
- Bouffard, D., & Wüest, A. (2019). Convection in lakes. *Annual Review of Fluid Mechanics*, 51(1), 189–215. <https://doi.org/10.1146/annurev-fluid-010518-040506>
- Bouffard, D., Zdorovenova, G., Bogdanov, S., Efreanova, T., Lavanchy, S., Palshin, N., et al. (2019). Under-ice convection dynamics in a boreal lake. *Inland Waters*, 9(2), 142–161. <https://doi.org/10.1080/20442041.2018.1533356>
- Braak, C. J. F. T. (2006). A Markov chain Monte Carlo version of the genetic algorithm differential evolution: Easy Bayesian computing for real parameter spaces. *Statistics and Computing*, 16(3), 239–249. <https://doi.org/10.1007/s11222-006-8769-1>
- Bruce, L. C., Frassl, M. A., Arhonditsis, G. B., Gal, G., Hamilton, D. P., Hanson, P. C., et al. (2018). A multi-lake comparative analysis of the general lake model (GLM): Stress-testing across a global observatory network. *Environmental Modelling & Software*, 102, 274–291. <https://doi.org/10.1016/j.envsoft.2017.11.016>
- Bueche, T., Hamilton, D. P., & Vetter, M. (2017). Using the general lake model (GLM) to simulate water temperatures and ice cover of a medium-sized lake: A case study of lake Ammersee, Germany. *Environmental Earth Sciences*, 76(13), 1–14. <https://doi.org/10.1007/s12665-017-6790-7>
- Burchard, H., & Baumert, H. (1995). On the performance of a mixed-layer model based on the κ - ϵ turbulence closure. *Journal of Geophysical Research*, 100(C5), 8523–8540. <https://doi.org/10.1029/94JC03229>

- Burchard, H., Bolding, K., & Villarreal, M. R. (1999). *GOTM, a General Ocean Turbulence model: Theory, implementation and test cases*. Space Applications Institute.
- Burchard, H., Petersen, O., & Rippeth, T. P. (1998). Comparing the performance of the mellor-yamada and the κ - ϵ two-equation turbulence models. *Journal of Geophysical Research*, *103*(C5), 10543–10554. <https://doi.org/10.1029/98jc00261>
- Butcher, J. B., Nover, D., Johnson, T. E., & Clark, C. M. (2015). Sensitivity of lake thermal and mixing dynamics to climate change. *Climatic Change*, *129*(1), 295–305. <https://doi.org/10.1007/s10584-015-1326-1>
- Bzdok, D. (2017). Classical statistics and statistical learning in imaging neuroscience. *Frontiers in Neuroscience*, *11*, 543. <https://doi.org/10.3389/fnins.2017.00543>
- Bzdok, D., Altman, N., & Krzywinski, M. (2018). Statistics versus machine learning. *Nature Methods*, *15*(4), 233–234. <https://doi.org/10.1038/nmeth.4642>
- Caissie, D., El-Jabi, N., & Satish, M. G. (2001). Modelling of maximum daily water temperatures in a small stream using air temperatures. *Journal of Hydrology*, *251*(1), 14–28. [https://doi.org/10.1016/S0022-1694\(01\)00427-9](https://doi.org/10.1016/S0022-1694(01)00427-9)
- Calamita, E., Vanzo, D., Wehrli, B., & Schmid, M. (2021). Lake modeling reveals management opportunities for improving water quality downstream of transboundary tropical dams. *Water Resources Research*, *57*(4), e2020WR027465. <https://doi.org/10.1029/2020WR027465>
- Carey, C. C., Woelmer, W. M., Lofton, M. E., Figueiredo, R. J., Bookout, B. J., Corrigan, R. S., et al. (2022). Advancing lake and reservoir water quality management with near-term, iterative ecological forecasting. *Inland Waters*, *12*(1), 107–120. <https://doi.org/10.1080/20442041.2020.1816421>
- Carmack, E. C. (1979). Combined influence of inflow and lake temperatures on spring circulation in a riverine lake. *Journal of Physical Oceanography*, *9*(2), 422–434. [https://doi.org/10.1175/1520-0485\(1979\)009<0422:CIOIAL>2.0.CO;2](https://doi.org/10.1175/1520-0485(1979)009<0422:CIOIAL>2.0.CO;2)
- Carrea, L., Crétaux, J., Liu, X., Wu, Y., Bergé-Nguyen, M., Calmettes, B., et al. (2022). *ESA lakes climate change initiative (Lakes_cci): Lake products. Version 2.0.2*. Centre for Environmental Data Analysis Didcot, UK. <https://doi.org/10.5285/ab8d21568c81491fbb9a300c36884af>
- Carrea, L., Crétaux, J.-F., Liu, X., Wu, Y., Calmettes, B., Duguay, C. R., et al. (2023). Satellite-derived multivariate world-wide lake physical variable timeseries for climate studies. *Scientific Data*, *10*(1), 30. <https://doi.org/10.1038/s41597-022-01889-z>
- Carrea, L., Embury, O., & Merchant, C. J. (2015). Datasets related to in-land water for limnology and remote sensing applications: Distance-to-land, distance-to-water, water-body identifier and lake-centre co-ordinates. *Geoscience Data Journal*, *2*(2), 83–97. <https://doi.org/10.1002/gdj3.32>
- Carrea, L., Merchant, C., Cretaux, J.-F., Dukulil, T. M., Dugan, H. A., Gibbes, B., et al. (2023). Lake surface water temperature in [state of the climate in 2022]. *Bulletin of the American Meteorological Society*, *104*(9), S28–S30. <https://doi.org/10.1175/2023BAMSStateoftheClimate.1>
- Carrea, L., Merchant, C., & Embury, O. (2020). *Copernicus climate change Service, climate data Store, (2020): Lake surface water temperature from 1995 to present derived from satellite observation*. Copernicus Climate Change Service (C3S) Climate Data Store (CDS). <https://doi.org/10.24381/cds.d36187ac>
- Carrea, L., Merchant, C., & Simis, S. (2022). Lake mask and distance to land dataset of 2024 lakes for the European Space Agency Climate Change Initiative Lakes v2 (version 2.0.1) [Dataset]. Zenodo. <https://doi.org/10.5281/zenodo.6699376>
- Castelletti, A., Pianosi, F., Soncini-Sessa, R., & Antenucci, J. (2010). A multiobjective response surface approach for improved water quality planning in lakes and reservoirs. *Water Resources Research*, *46*(6), 73. <https://doi.org/10.1029/2009WR008389>
- Casulli, V., & Cheng, R. T. (1992). Semi-implicit finite difference methods for three-dimensional shallow water flow. *International Journal for Numerical Methods in Fluids*, *15*(6), 629–648. <https://doi.org/10.1002/flid.1650150602>
- Chen, C., Zhang, H., Shi, W., Zhang, W., & Xue, Y. (2023). A novel paradigm for integrating physics-based numerical and machine learning models: A case study of eco-hydrological model. *Environmental Modelling & Software*, *163*, 105669. <https://doi.org/10.1016/j.envsoft.2023.105669>
- Christianson, K. R., Johnson, B. M., Hooten, M. B., & Roberts, J. J. (2019). Estimating lake–climate responses from sparse data: An application to high elevation lakes. *Limnology & Oceanography*, *64*(3), 1371–1385. <https://doi.org/10.1002/lno.11121>
- Clayer, F., Jackson-Blake, L., Mercado-Bettin, D., Shikhani, M., French, A., Moore, T., et al. (2023). Sources of skill in lake temperature, discharge and ice-off seasonal forecasting tools. *Hydrology and Earth System Sciences*, *27*(6), 1361–1381. <https://doi.org/10.5194/hess-27-1361-2023>
- Cluis, D. A. (1972). Relationship between stream water temperature and ambient air temperature: A simple autoregressive model for mean daily stream water temperature fluctuations. *Hydrology Research*, *3*(2), 65–71. <https://doi.org/10.2166/nh.1972.0004>
- Cole, T. M., & Wells, S. A. (2006). CE-QUAL-W2: A two-dimensional, laterally averaged, hydrodynamic and water quality model, version 3.5 (technical report).
- Coutant, C. C., & Whitney, R. R. (2000). Fish behavior in relation to passage through hydropower turbines: A review. *Transactions of the American Fisheries Society*, *129*(2), 351–380. [https://doi.org/10.1577/15488659\(2000\)129<0351:FBIRTP>2.0.CO;2](https://doi.org/10.1577/15488659(2000)129<0351:FBIRTP>2.0.CO;2)
- Dai, Y., Wei, N., Huang, A., Zhu, S., Wei, S., Yuan, H., et al. (2018). The lake scheme of the common land model and its performance evaluation. *Chinese Science Bulletin*, *63*(28–29), 3002–3021. <https://doi.org/10.1360/N972018-00609>
- de la Fuente, A., & Meruane, C. (2017). Dimensionless numbers for classifying the thermodynamics regimes that determine water temperature in shallow lakes and wetlands. *Environmental Fluid Mechanics*, *17*(6), 1081–1098. <https://doi.org/10.1007/s10652-017-9536-x>
- Del Ser, J., Osaba, E., Molina, D., Yang, X. S., Salcedo-Sanz, S., Camacho, D., et al. (2019). Bio-inspired computation: Where we stand and what's next. *Swarm and Evolutionary Computation*, *48*, 220–250. <https://doi.org/10.1016/j.swevo.2019.04.008>
- Deltares. (2023). Delft3D-FLOW user manual, version 4.05 [Computer software manual]. Deltares. Retrieved from https://content.oss.deltares.nl/delft3d4/Delft3D-FLOW_User_Manual.pdf
- Demetillo, A. T., Japitana, M. V., & Taboada, E. B. (2019). A system for monitoring water quality in a large aquatic area using wireless sensor network technology. *Sustainable Environment Research*, *29*(1), 1–9. <https://doi.org/10.1186/s42834-019-0009-4>
- Deser, C., Lehner, F., Rodgers, K. B., Ault, T., Delworth, T. L., DiNezio, P. N., et al. (2020). Insights from earth system model initial-condition large ensembles and future prospects. *Nature Climate Change*, *10*(4), 277–286. <https://doi.org/10.1038/s41558-020-0731-2>
- Dietze, M. C., Fox, A., Beck-Johnson, L. M., Betancourt, J. L., Hooten, M. B., Jarnevich, C. S., et al. (2018). Iterative near-term ecological forecasting: Needs, opportunities, and challenges. *Proceedings of the National Academy of Sciences*, *115*(7), 1424–1432. <https://doi.org/10.1073/pnas.1710231115>
- Di Nunno, F., Zhu, S., Ptak, M., Sojka, M., & Granata, F. (2023). A stacked machine learning model for multi-step ahead prediction of lake surface water temperature. *Science of the Total Environment*, *890*, 164323. <https://doi.org/10.1016/j.scitotenv.2023.164323>
- Diogo, P. A., Fonseca, M., Coelho, P. S., Mateus, N. S., Almeida, M. C., & Rodrigues, A. (2008). Reservoir phosphorus sources evaluation and water quality modeling in a transboundary watershed. *Desalination*, *226*(1–3), 200–214. <https://doi.org/10.1016/j.desal.2007.01.242>
- Dokulil, M. T., Teubner, K., & Jagsch, A. (2006). Climate change affecting hypolimnetic water temperatures in deep alpine lakes. *Internationale Vereinigung für theoretische und angewandte Limnologie: Verhandlungen*, *29*(3), 1285–1288. <https://doi.org/10.1080/03680770.2005.11902889>
- Duka, M. A., Shintani, T., & Yokoyama, K. (2021). Thermal stratification responses of a monomictic reservoir under different seasons and operation schemes. *Science of the Total Environment*, *767*, 144423. <https://doi.org/10.1016/j.scitotenv.2020.144423>

- Duraibabu, D. B., Leen, G., Toal, D., Neue, T., Lewis, E., & Dooly, G. (2017). Underwater depth and temperature sensing based on fiber optic technology for marine and fresh water applications. *Sensors*, *17*(6), 1228. <https://doi.org/10.3390/s17061228>
- Edinger, J. E., Duttweiler, D. W., & Geyer, J. C. (1968). The response of water temperatures to meteorological conditions. *Water Resources Research*, *4*(5), 1137–1143. <https://doi.org/10.1029/WR004i005p01137>
- Edmundson, J. A., & Mazumder, A. (2002). Regional and hierarchical perspectives of thermal regimes in subarctic, Alaskan lakes. *Freshwater Biology*, *47*(1), 1–17. <https://doi.org/10.1046/j.1365-2427.2002.00775.x>
- Eggers, K., & Tetzlaff, G. (1978). A simple model for describing the heat balance of a shallow lake with application to Lake Chad. *Boundary-Layer Meteorology*, *15*(2), 205–214. <https://doi.org/10.1007/BF00121922>
- Eiben, A. E., Hinterding, R., & Michalewicz, Z. (1999). Parameter control in evolutionary algorithm. *IEEE Transactions on Evolutionary Computation*, *3*(2), 124–141. <https://doi.org/10.1109/4235.771166>
- Ellis, G. (2008). Opposing the multiverse. *Astronomy and Geophysics*, *49*(2), 2–33. https://doi.org/10.1111/j.1468-4004.2008.49229_1.x
- Even-Dar, E., Mannor, S., & Mansour, Y. (2006). Action elimination and stopping conditions for the multi-armed bandit and reinforcement learning problems. *Journal of Machine Learning Research*, *7*, 1079–1105. <https://doi.org/10.1109/IROS.2013.6696415>
- Fairall, C., Bradley, E. F., Godfrey, J., Wick, G., Edson, J. B., & Young, G. (1996). Cool-skin and warm-layer effects on sea surface temperature. *Journal of Geophysical Research*, *101*(C1), 1295–1308. <https://doi.org/10.1029/95JC03190>
- Fang, X., & Stefan, H. G. (1996). Long-term lake water temperature and ice cover simulations/measurements. *Cold Regions Science and Technology*, *24*(3), 289–304. [https://doi.org/10.1016/0165-232X\(95\)00019-8](https://doi.org/10.1016/0165-232X(95)00019-8)
- Fang, X., & Stefan, H. G. (2009). Simulations of climate effects on water temperature, dissolved oxygen, and ice and snow covers in lakes of the contiguous us under past and future climate scenarios. *Limnology & Oceanography*, *54*(6part2), 2359–2370. https://doi.org/10.4319/lo.2009.54.6_part_2.2359
- Feldbauer, J., Ladwig, R., Mesman, J. P., Moore, T. N., Zündorf, H., Berendonk, T. U., & Petzoldt, T. (2022). Ensemble of models shows coherent response of a reservoir's stratification and ice cover to climate warming. *Aquatic Sciences*, *84*(4), 1–17. <https://doi.org/10.1007/s00027-022-00883-2>
- Fenocchi, A., Rogora, M., Morabito, G., Marchetto, A., Sibilla, S., & Dresti, C. (2019). Applicability of a one-dimensional coupled ecological-hydrodynamic numerical model to future projections in a very deep large lake (Lake Maggiore, Northern Italy/southern Switzerland). *Ecological Modelling*, *392*, 38–51. <https://doi.org/10.1016/j.ecolmodel.2018.11.005>
- Fenocchi, A., Rogora, M., Sibilla, S., Ciampittiello, M., & Dresti, C. (2018). Forecasting the evolution in the mixing regime of a deep subalpine lake under climate change scenarios through numerical modelling (Lake Maggiore, Northern Italy/Southern Switzerland). *Climate Dynamics*, *51*(9), 3521–3536. <https://doi.org/10.1007/s00382-018-4094-6>
- Feuchtmayr, H., Thackeray, S. J., Jones, I. D., De Ville, M., Fletcher, J., James, B., & Kelly, J. (2012). Spring phytoplankton phenology—patterns and drivers of change consistent among lakes in the same climatological region? *Freshwater Biology*, *57*(2), 331–344. <https://doi.org/10.1111/j.1365-2427.2011.02671.x>
- Fichot, C. G., Matsumoto, K., Holt, B., Gierach, M. M., & Tokos, K. S. (2019). Assessing change in the overturning behavior of the Laurentian Great Lakes using remotely sensed lake surface water temperatures. *Remote Sensing of Environment*, *235*, 111427. <https://doi.org/10.1016/j.rse.2019.111427>
- Fisher, H. B., List, E. J., Koh, R. C., Imberger, J., & Brooks, N. H. (Eds.). (1979). *Mixing in inland and coastal waters*. Academic Press. <https://doi.org/10.1016/B978-0-08-051177-1.50001-5>
- Flaim, G., Eccel, E., Zeileis, A., Toller, G., Cerasino, L., & Obertegger, U. (2016). Effects of re-oligotrophication and climate change on lake thermal structure. *Freshwater Biology*, *61*(10), 1802–1814. <https://doi.org/10.1111/fwb.12819>
- Ford, D. E., & Stefan, H. G. (1980). Thermal predictions using integral energy model. *Journal of the Hydraulics Division*, *106*(1), 39–55. <https://doi.org/10.1061/JYCEAJ.0005358>
- Fukushima, T., Matsushita, B., & Sugita, M. (2022). Quantitative assessment of decadal water temperature changes in Lake Kasumigaura, a shallow turbid lake, using a one-dimensional model. *Science of the Total Environment*, *845*, 157247. <https://doi.org/10.1016/j.scitotenv.2022.157247>
- Gaillard, R., Perroud, M., Goyette, S., & Kasparian, J. (2022). Multi-column modelling of lake Geneva for climate applications. *Scientific Reports*, *12*(1), 1–12. <https://doi.org/10.1038/s41598-021-04061-6>
- Gal, G., Yael, G., Noam, S., Moshe, E., & Schlögl, D. (2020). Ensemble modeling of the impact of climate warming and increased frequency of extreme climatic events on the thermal characteristics of a sub-tropical lake. *Water*, *12*(7), 1982. <https://doi.org/10.3390/w12071982>
- Gamag, S., & Samarabandu, J. (2020). Deep learning methods in network intrusion detection: A survey and an objective comparison. *Journal of Network and Computer Applications*, *169*, 102767. <https://doi.org/10.1016/j.jnca.2020.102767>
- Gaudard, A., Råman Vinnå, L., Bärenbold, F., Schmid, M., & Bouffard, D. (2019). Toward an open access to high-frequency lake modeling and statistics data for scientists and practitioners—The case of swiss lakes using simstrat v2.1. *Geoscientific Model Development*, *12*(9), 3955–3974. <https://doi.org/10.5194/gmd-12-3955-2019>
- Gaudard, A., Schwefel, R., Vinnå, L. R., Schmid, M., Wüest, A., & Bouffard, D. (2017). Optimizing the parameterization of deep mixing and internal seiches in one-dimensional hydrodynamic models: A case study with simstrat v1.3. *Geoscientific Model Development*, *10*(9), 3411–3423. <https://doi.org/10.5194/gmd-10-3411-2017>
- GCOS-244. (2022). *The 2022 GCOS implementation plan*. World Meteorological Organization.
- GCOS-245. (2022). *The 2022 GCOS ECV requirements*. World Meteorological Organization.
- Gerten, D., & Adrian, R. (2000). Climate-driven changes in spring plankton dynamics and the sensitivity of shallow polymictic lakes to the North Atlantic Oscillation. *Limnology & Oceanography*, *45*(5), 1058–1066. <https://doi.org/10.4319/lo.2000.45.5.1058>
- Gharari, S., Hrachowitz, M., Fenicia, F., Gao, H., & Savenije, H. (2014). Using expert knowledge to increase realism in environmental system models can dramatically reduce the need for calibration. *Hydrology and Earth System Sciences*, *18*(12), 4839–4859. <https://doi.org/10.5194/hess-18-4839-2014>
- Golub, M., Thiery, W., Marcé, R., Pierson, D., Vanderkelen, I., Mercado-Bettin, D., et al. (2022). A framework for ensemble modelling of climate change impacts on lakes worldwide: The ISIMIP lake sector. *Geoscientific Model Development*, *15*(11), 4597–4623. <https://doi.org/10.5194/gmd-15-4597-2022>
- Goudsmit, G.-H., Burchard, H., Peeters, F., & Wüest, A. (2002). Application of *k-ε* turbulence models to enclosed basins: The role of internal seiches. *Journal of Geophysical Research*, *107*(C12), 23-1. <https://doi.org/10.1029/2001JC000954>
- Goyette, S., & Perroud, M. (2012). Interfacing a one-dimensional lake model with a single-column atmospheric model: Application to the deep Lake Geneva, Switzerland. *Water Resources Research*, *48*(4), W04507. <https://doi.org/10.1029/2011WR011223>
- Grant, L., Vanderkelen, I., Gudmundsson, L., Tan, Z., Perroud, M., Stepanenko, V. M., et al. (2021). Attribution of global lake systems change to anthropogenic forcing. *Nature Geoscience*, *14*(11), 849–854. <https://doi.org/10.1038/s41561-021-00833-x>

- Gu, H., Jin, J., Wu, Y., Ek, M. B., & Subin, Z. M. (2015). Calibration and validation of lake surface temperature simulations with the coupled WRF-lake model. *Climatic Change*, *129*(3–4), 471–483. <https://doi.org/10.1007/s10584-013-0978-y>
- Guinot, V., & Gourbesville, P. (2003). Calibration of physically based models: Back to basics? *Journal of Hydroinformatics*, *5*(4), 233–244. <https://doi.org/10.2166/hydro.2003.0020>
- Gula, J., & Peltier, W. R. (2012). Dynamical downscaling over the Great Lakes Basin of North America using the WRF regional climate model: The impact of the Great Lakes system on regional greenhouse warming. *Journal of Climate*, *25*(21), 7723–7742. <https://doi.org/10.1175/JCLI-D-11-00388.1>
- Guo, S., Wang, F., Zhu, D., Ni, G., & Chen, Y. (2022). Evaluation of the WRF-lake model in the large dimictic reservoir: Comparisons with field data and another water temperature model. *Journal of Hydrometeorology*, *23*(8), 1227–1244. <https://doi.org/10.1175/JHM-D-21-0220.1>
- Guo, S., Zhu, D., & Chen, Y. (2023a). Improvement and evaluation of the latest version of WRF-lake at a deep riverine reservoir. *Advances in Atmospheric Sciences*, *40*(4), 1–15. <https://doi.org/10.1007/s00376-022-2180-5>
- Guo, S., Zhu, D., & Chen, Y. (2023b). Modelling and analyzing a unique phenomenon of surface water temperature rise in a tropical, large, riverine reservoir. *Water Resources Management*, *37*(4), 1711–1727. <https://doi.org/10.1007/s11269-023-03450-y>
- Gupta, H. V., Beven, K. J., & Wagener, T. (2006). Model calibration and uncertainty estimation. In *Encyclopedia of hydrological sciences*. <https://doi.org/10.1002/0470848944.hsa138>
- Gutiérrez, J. M., Maraun, D., Widmann, M., Huth, R., Hertig, E., Benestad, R., et al. (2019). An intercomparison of a large ensemble of statistical downscaling methods over Europe: Results from the VALUE perfect predictor cross-validation experiment. *International Journal of Climatology*, *39*(9), 3750–3785. <https://doi.org/10.1002/joc.5462>
- Häkanson, L. (1996). A new, simple, general technique to predict seasonal variability of river discharge and lake temperature for lake ecosystem models. *Ecological Modelling*, *88*(1), 157–181. [https://doi.org/10.1016/0304-3800\(95\)00083-6](https://doi.org/10.1016/0304-3800(95)00083-6)
- Hamilton, D. P., & Schladow, S. (1997). Prediction of water quality in lakes and reservoirs. Part I—Model description. *Ecological Modelling*, *96*(1), 91–110. [https://doi.org/10.1016/S0304-3800\(96\)00062-2](https://doi.org/10.1016/S0304-3800(96)00062-2)
- Hampton, S. E., Izmet'eva, L. R., Moore, M. V., Katz, S. L., Dennis, B., & Silow, E. A. (2008). Sixty years of environmental change in the world's largest freshwater lake—Lake Baikal, Siberia. *Global Change Biology*, *14*(8), 1947–1958. <https://doi.org/10.1111/j.1365-2486.2008.01616.x>
- Hamrick, J. M. (1992). A three-dimensional environmental fluid dynamics computer code: Theoretical and computational aspects. <https://doi.org/10.21220/V5TT6C>
- Handberg, R., & Campante, T. L. (2011). Bayesian peak-bagging of solar-like oscillators using MCMC: A comprehensive guide. *Astronomy & Astrophysics*, *527*, A56. <https://doi.org/10.1051/0004-6361/201015451>
- Hao, Z., Li, W., Wu, J., Zhang, S., & Hu, S. (2023). A novel deep learning model for mining nonlinear dynamics in lake surface water temperature prediction. *Remote Sensing*, *15*(4), 900. <https://doi.org/10.3390/rs15040900>
- Hart, J. K., & Martinez, K. (2006). Environmental sensor networks: A revolution in the earth system science? *Earth-Science Reviews*, *78*(3–4), 177–191. <https://doi.org/10.1016/j.earscirev.2006.05.001>
- He, W., Wang, H., Zhang, J., Xu, H., & Xiao, Y. (2023). Diurnal variation characteristics of thermal structure in a deep reservoir and the effects of selective withdrawal. *Journal of Environmental Management*, *333*, 117459. <https://doi.org/10.1016/j.jenvman.2023.117459>
- Heddam, S., Ptak, M., & Zhu, S. (2020). Modelling of daily lake surface water temperature from air temperature: Extremely randomized trees (ERT) versus air2water, MARS, M5Tree, RF and MLPNN. *Journal of Hydrology*, *588*, 125130. <https://doi.org/10.1016/j.jhydrol.2020.125130>
- Hegerl, G. C., Brönnimann, S., Schurer, A., & Cowan, T. (2018). The early 20th century warming: Anomalies, causes, and consequences. *Wiley Interdisciplinary Reviews: Climate Change*, *9*(4), e522. <https://doi.org/10.1002/wcc.522>
- Henderson-Sellers, B. (1982). A simple formula for vertical eddy diffusion coefficients under conditions of nonneutral stability. *Journal of Geophysical Research*, *87*(C8), 5860–5864. <https://doi.org/10.1029/JC087iC08p05860>
- Henderson-Sellers, B. (1984). Development and application of “USED”: A hydroclimate lake stratification model. *Ecological Modelling*, *21*(4), 233–246. [https://doi.org/10.1016/0304-3800\(84\)90061-9](https://doi.org/10.1016/0304-3800(84)90061-9)
- Henderson-Sellers, B. (1985). New formulation of eddy diffusion thermocline models. *Applied Mathematical Modelling*, *9*(6), 441–446. [https://doi.org/10.1016/0307-904X\(85\)90110-6](https://doi.org/10.1016/0307-904X(85)90110-6)
- Henderson-Sellers, B. (1986). Calculating the surface energy balance for lake and reservoir modeling: A review. *Reviews of Geophysics*, *24*(3), 625–649. <https://doi.org/10.1029/RG024i003p00625>
- Henriksen, H. J., Schneider, R., Koch, J., Ondracek, M., Trolborg, L., Seidenfaden, I. K., et al. (2023). A new digital twin for climate change adaptation, water management, and disaster risk reduction (hip digital twin). *Water*, *15*(1), 25. <https://doi.org/10.3390/w15010025>
- Herb, W. R., & Stefan, H. G. (2004). Temperature stratification and mixing dynamics in a shallow lake with submersed macrophytes. *Lake and Reservoir Management*, *20*(4), 296–308. <https://doi.org/10.1080/07438140409354159>
- Hipsey, M. R., Bruce, L. C., Boon, C., Busch, B., Carey, C. C., Hamilton, D. P., et al. (2019). A general Lake Model (GLM 3.0) for linking with high-frequency sensor data from the global lake ecological observatory network (GLEON). *Geoscientific Model Development*, *12*(1), 473–523. <https://doi.org/10.5194/gmd-12-473-2019>
- Hipsey, M. R., Gal, G., Arhonditsis, G. B., Carey, C. C., Elliott, J. A., Frassl, M. A., et al. (2020). A system of metrics for the assessment and improvement of aquatic ecosystem models. *Environmental Modelling & Software*, *128*, 104697. <https://doi.org/10.1016/j.envsoft.2020.104697>
- Hodges, B. R., & Dallimore, C. (2001). *Estuary and lake computer model: ELCOM science manual code version 2.0.0*. Centre for Water Research, University of Western Australia.
- Hodges, B. R., Imberger, J., Saggio, A., & Winters, K. B. (2000). Modeling basin-scale internal waves in a stratified lake. *Limnology & Oceanography*, *45*(7), 1603–1620. <https://doi.org/10.4319/lo.2000.45.7.1603>
- Hondzo, M., & Stefan, H. G. (1993). Lake water temperature simulation model. *Journal of Hydraulic Engineering*, *119*(11), 1251–1273. [https://doi.org/10.1061/\(ASCE\)0733-9429\(1993\)119:11\(1251\)](https://doi.org/10.1061/(ASCE)0733-9429(1993)119:11(1251))
- Hondzo, M., You, J., Taylor, J., Bartlet, G., & Voller, V. R. (2022). Measurement and scaling of lake surface skin temperatures. *Geophysical Research Letters*, *49*(6), e2021GL093226. <https://doi.org/10.1029/2021GL093226>
- Hook, S. J., Prata, F. J., Alley, R. E., Abtahi, A., Richards, R. C., Schladow, S. G., & Palmarsson, S. (2003). Retrieval of lake bulk and skin temperatures using along-track scanning radiometer (ATSR-2) data: A case study using lake Tahoe, California. *Journal of Atmospheric and Oceanic Technology*, *20*(4), 534–548. [https://doi.org/10.1175/1520-0426\(2003\)20\(534:ROLBAS\)2.0.CO;2](https://doi.org/10.1175/1520-0426(2003)20(534:ROLBAS)2.0.CO;2)
- Hostetler, S. W., & Bartlein, P. J. (1990). Simulation of lake evaporation with application to modeling lake level variations of Harney-Malheur Lake, Oregon. *Water Resources Research*, *26*(10), 2603–2612. <https://doi.org/10.1029/WR026i010p02603>
- Huang, C., Li, Y., & Yao, X. (2020). A survey of automatic parameter tuning methods for metaheuristics. *IEEE Transactions on Evolutionary Computation*, *24*(2), 201–216. <https://doi.org/10.1109/TEVC.2019.2921598>
- Huang, L., Timmermann, A., Lee, S.-S., Rodgers, K. B., Yamaguchi, R., & Chung, E.-S. (2022). Emerging unprecedented lake ice loss in climate change projections. *Nature Communications*, *13*(1), 1–12. <https://doi.org/10.1038/s41467-022-33495-3>

- Hui, Y., Zhu, Z., & Atkinson, J. F. (2018). Mass balance analysis and calculation of wind effects on heat fluxes and water temperature in a large lake. *Journal of Great Lakes Research*, 44(6), 1293–1305. <https://doi.org/10.1016/j.jglr.2018.09.003>
- Hupfer, M., & Lewandowski, J. (2008). Oxygen controls the phosphorus release from lake sediments—A long-lasting paradigm in limnology. *International Review of Hydrobiology*, 93(4–5), 415–432. <https://doi.org/10.1002/iroh.200711054>
- Hutchinson, G. E., & Löffler, H. (1956). The thermal classification of lakes. *Proceedings of the National Academy of Sciences*, 42(2), 84–86. <https://doi.org/10.1073/pnas.42.2.84>
- Hutorowicz, A. (2020). Baseline water temperature: Estimation of the annual cycle of surface water temperature in lakes in North-Central Poland over the 1951–1968 period. *Water*, 12(12), 3574. <https://doi.org/10.3390/w12123574>
- Imberger, J. (1985). The diurnal mixed layer 1. *Limnology & Oceanography*, 30(4), 737–770. <https://doi.org/10.4319/lo.1985.30.4.0737>
- Imberger, J., & Patterson, J. C. (1981). A dynamic reservoir simulation model—DYRESM: 5. In H. B. Fischer (Ed.), *Transport models/inland & coastal waters* (pp. 310–361). Academic Press. <https://doi.org/10.1016/B978-0-12-258152-6.50014-2>
- Imberger, J., & Patterson, J. C. (1989). Physical limnology. In *Advances in applied mechanics* (Vol. 27, p. 30). Elsevier. [https://doi.org/10.1016/S0065-2156\(08\)70199-6](https://doi.org/10.1016/S0065-2156(08)70199-6)
- Imboden, D. M., & Wüest, A. (1995). Mixing mechanisms in lakes. In A. Lerman, D. Imboden, & J. Gat (Eds.), *Physics and chemistry of lakes* (pp. 83–138). Springer. <https://doi.org/10.1007/978-3-642-85132-2>
- Irani Rahaghi, A., Lemmin, U., Sage, D., & Barry, D. A. (2019). Achieving high-resolution thermal imagery in low-contrast lake surface waters by aerial remote sensing and image registration. *Remote Sensing of Environment*, 221, 773–783. <https://doi.org/10.1016/j.rse.2018.12.018>
- Ishikawa, M., Gonzalez, W., Golyjeswski, O., Sales, G., Rigotti, J. A., Bleninger, T., et al. (2022). Effects of dimensionality on the performance of hydrodynamic models for stratified lakes and reservoirs. *Geoscientific Model Development*, 15(5), 2197–2220. <https://doi.org/10.5194/gmd-15-2197-2022>
- Izmeteva, L. R., Moore, M. V., Hampton, S. E., Ferwerda, C. J., Gray, D. K., Woo, K. H., et al. (2016). Lake-wide physical and biological trends associated with warming in Lake Baikal. *Journal of Great Lakes Research*, 42(1), 6–17. <https://doi.org/10.1016/j.jglr.2015.11.006>
- Jane, S. F., Mincer, J. L., Lau, M. P., Lewis, A. S. L., Stetler, J. T., & Rose, K. C. (2023). Longer duration of seasonal stratification contributes to widespread increases in lake hypoxia and anoxia. *Global Change Biology*, 29(4), 1009–1023. <https://doi.org/10.1111/gcb.16525>
- Jankowski, T., Livingstone, D. M., Buhler, H., Forster, R., & Niederhauser, P. (2006). Consequences of the 2003 European heat wave for lake temperature profiles, thermal stability, and hypolimnetic oxygen depletion: Implications for a warmer world. *Limnology & Oceanography*, 51(2), 815–819. <https://doi.org/10.4319/lo.2006.51.2.0815>
- Jansen, J., Woolway, R. I., Kraemer, B. M., Albergel, C., Bastviken, D., Weyhenmeyer, G. A., et al. (2022). Global increase in methane production under future warming of lake bottom waters. *Global Change Biology*, 28(18), 5427–5440. <https://doi.org/10.1111/gcb.16298>
- Jia, T., Yang, K., Peng, Z., Tang, L., Duan, H., & Luo, Y. (2022). Review on the change trend, attribution analysis, retrieval, simulation, and prediction of lake surface water temperature. *IEEE Journal of Selected Topics in Applied Earth Observations and Remote Sensing*, 15, 6324–6355. <https://doi.org/10.1109/JSTARS.2022.3188788>
- Jia, X., Willard, J. D., Karpatne, A., Read, J., Zwart, J., Steinbach, M., & Kumar, V. (2019). Physics guided RNNs for modeling dynamical systems: A case study in simulating lake temperature profiles. In *Proceedings of the 2019 SIAM international conference on data mining (SDM)* (pp. 558–566). <https://doi.org/10.1137/1.9781611975673.63>
- Jia, X., Willard, J. D., Karpatne, A., Read, J. S., Zwart, J. A., Steinbach, M., & Kumar, V. (2021). Physics-guided machine learning for scientific discovery: An application in simulating lake temperature profiles. *ACM/IMS Transactions on Data Science*, 2(3), 1–26. <https://doi.org/10.1145/3447814>
- Jin, Y. (2011). Surrogate-assisted evolutionary computation: Recent advances and future challenges. *Swarm and Evolutionary Computation*, 1(2), 61–70. <https://doi.org/10.1016/j.swevo.2011.05.001>
- Jöhnk, K., & Umlauf, L. (2001). Modelling the metalimnetic oxygen minimum in a medium sized alpine lake. *Ecological Modelling*, 136(1), 67–80. [https://doi.org/10.1016/S0304-3800\(00\)00381-1](https://doi.org/10.1016/S0304-3800(00)00381-1)
- Jöhnk, K. D., Huisman, J., Sharples, J., Sommeijer, B., Visser, P. M., & Stroom, J. M. (2008). Summer heatwaves promote blooms of harmful cyanobacteria. *Global Change Biology*, 14(3), 495–512. <https://doi.org/10.1111/j.1365-2486.2007.01510.x>
- Kangur, K., Ginter, K., Kangur, A., Kangur, P., & Möls, T. (2020). How did the late 1980s climate regime shift affect temperature-sensitive fish population dynamics: Case study of vendace (*Coregonus albula*) in a large north-temperate lake. *Water*, 12(10), 2694. <https://doi.org/10.3390/w12102694>
- Kangur, K., Tammiksaar, E., & Pauly, D. (2021). Using the “mean temperature of the catch” to assess fish community responses to warming in a temperate lake. *Environmental Biology of Fishes*, 105(10), 1–9. <https://doi.org/10.1007/s10641-021-01114-7>
- Kara, E. L., Hanson, P., Hamilton, D., Hipsey, M. R., McMahon, K. D., Read, J. S., et al. (2012). Time-scale dependence in numerical simulations: Assessment of physical, chemical, and biological predictions in a stratified lake at temporal scales of hours to months. *Environmental Modelling & Software*, 35, 104–121. <https://doi.org/10.1016/j.envsoft.2012.02.014>
- Karpatne, A., Atluri, G., Faghmous, J. H., Steinbach, M., Banerjee, A., Ganguly, A., et al. (2017). Theory-guided data science: A new paradigm for scientific discovery from data. *IEEE Transactions on Knowledge and Data Engineering*, 29(10), 2318–2331. <https://doi.org/10.1109/TKDE.2017.2720168>
- Kettle, H., Thompson, R., Anderson, N. J., & Livingstone, D. M. (2004). Empirical modeling of summer lake surface temperatures in southwest Greenland. *Limnology & Oceanography*, 49(1), 271–282. <https://doi.org/10.4319/lo.2004.49.1.0271>
- Khazaei, B., Nasir, F. B., & Bravo, H. R. (2023). Impacts of tributary inflows on the circulation and thermal regime of the Green Bay estuary of Lake Michigan. *Journal of Hydraulic Engineering*, 149(5), 05023002. <https://doi.org/10.1061/JHEND8.HYENG-13239>
- Kim, S. K., & Choi, S.-U. (2021). Assessment of the impact of selective withdrawal on downstream fish habitats using a coupled hydrodynamic and habitat modeling. *Journal of Hydrology*, 593, 125665. <https://doi.org/10.1016/j.jhydrol.2020.125665>
- Kirillin, G., Leppäranta, M., Terzhevik, A., Granin, N., Bernhardt, J., Engelhardt, C., et al. (2012). Physics of seasonally ice-covered lakes: A review. *Aquatic Sciences*, 74(4), 659–682. <https://doi.org/10.1007/s00027-012-0279-y>
- Kirillin, G., & Shatwell, T. (2016). Generalized scaling of seasonal thermal stratification in lakes. *Earth-Science Reviews*, 161, 179–190. <https://doi.org/10.1016/j.earscirev.2016.08.008>
- Klein, I., Dietz, A. J., Gessner, U., Galayeva, A., Myrzakhmetov, A., & Kuenzer, C. (2014). Evaluation of seasonal water body extents in Central Asia over the past 27 years derived from medium-resolution remote sensing data. *International Journal of Applied Earth Observation and Geoinformation*, 26, 335–349. <https://doi.org/10.1016/j.jag.2013.08.004>
- Kobler, U., Wüest, A., & Schmid, M. (2018). Effects of lake–reservoir pumped-storage operations on temperature and water quality. *Sustainability*, 10(6), 1968. <https://doi.org/10.3390/su10061968>
- Kobler, U. G., & Schmid, M. (2019). Ensemble modelling of ice cover for a reservoir affected by pumped-storage operation and climate change. *Hydrological Processes*, 33(20), 2676–2690. <https://doi.org/10.1002/hyp.13519>

- Kolås, E. H., Mo-Bjørkelund, T., & Fer, I. (2022). Turbulence measurements from a light autonomous underwater vehicle. *Ocean Science*, 18(2), 389–400. <https://doi.org/10.5194/os-18-389-2022>
- Kong, X., Determann, M., Andersen, T. K., Barbosa, C. C., Dadi, T., Janssen, A. B., et al. (2023). Synergistic effects of warming and internal nutrient loading interfere with the long-term stability of lake restoration and induce sudden re-eutrophication. *Environmental Science & Technology*, 57(9), 4003–4013. <https://doi.org/10.1021/acs.est.2c07181>
- Korbmacher, R., & Todeaux, A. (2022). Review of pedestrian trajectory prediction methods: Comparing deep learning and knowledge-based approaches. *IEEE Transactions on Intelligent Transportation Systems*, 23(12), 24126–24144. <https://doi.org/10.1109/TITS.2022.3205676>
- Kraemer, B. M., Anneville, O., Chandra, S., Dix, M., Kuusisto, E., Livingstone, D. M., et al. (2015). Morphometry and average temperature affect lake stratification responses to climate change. *Geophysical Research Letters*, 42(12), 4981–4988. <https://doi.org/10.1002/2015GL064097>
- Kraemer, B. M., Pilla, R. M., Woolway, R. I., Anneville, O., Ban, S., Colom-Montero, W., et al. (2021). Climate change drives widespread shifts in lake thermal habitat. *Nature Climate Change*, 11(6), 521–529. <https://doi.org/10.1038/s41558-021-01060-3>
- Kraus, E., & Turner, J. (1967). A one-dimensional model of the seasonal thermocline II. The general theory and its consequences. *Tellus*, 19(1), 98–106. <https://doi.org/10.3402/tellusa.v19i1.9753>
- Kundu, P., & Cohen, I. M. (2012). *Fluid mechanics* (5th ed.). Elsevier.
- Kurz, S., De Gerssem, H., Galetzka, A., Klaedtke, A., Liebsch, M., Loukrezis, D., et al. (2022). Hybrid modeling: Towards the next level of scientific computing in engineering. *Journal of Mathematics in Industry*, 12(1), 1–12. <https://doi.org/10.1186/s13362-022-00123-0>
- Ladwig, R., Furusato, E., Kirillin, G., Hinkelmann, R., & Hupfer, M. (2018). Climate change demands adaptive management of urban lakes: Model-based assessment of management scenarios for Lake Tegel (Berlin, Germany). *Water*, 10(2), 186. <https://doi.org/10.3390/w10020186>
- Ladwig, R., Hanson, P. C., Dugan, H. A., Carey, C. C., Zhang, Y., Shu, L., et al. (2021). Lake thermal structure drives interannual variability in summer anoxia dynamics in a eutrophic lake over 37 years. *Hydrology and Earth System Sciences*, 25(2), 1009–1032. <https://doi.org/10.5194/hess-25-1009-2021>
- Ladwig, R., Rock, L. A., & Dugan, H. A. (2021). Impact of salinization on lake stratification and spring mixing. *Limnology and Oceanography Letters*, 8(1), 93–102. <https://doi.org/10.1002/lol2.10215>
- Lathrop, R. C., Kasprzak, P., Tarvainen, M., Ventelä, A.-M., Keskinen, T., Koschel, R., & Robertson, D. M. (2019). Seasonal epilimnetic temperature patterns and trends in a suite of lakes from Wisconsin (USA), Germany, and Finland. *Inland Waters*, 9(4), 471–488. <https://doi.org/10.1080/20442041.2019.1637682>
- Lawrence, D. M., Fisher, R. A., Koven, C. D., Oleson, K. W., Swenson, S. C., Bonan, G., et al. (2019). The community land model version 5: Description of new features, benchmarking, and impact of forcing uncertainty. *Journal of Advances in Modeling Earth Systems*, 11(12), 4245–4287. <https://doi.org/10.1029/2018MS001583>
- Layden, A., Merchant, C., & MacCallum, S. (2015). Global climatology of surface water temperatures of large lakes by remote sensing. *International Journal of Climatology*, 35(15), 4464–4479. <https://doi.org/10.1002/joc.4299>
- León, L., Lam, D., Schertzer, W., Swayne, D., & Imberger, J. (2007). Towards coupling a 3D hydrodynamic lake model with the Canadian regional climate model: Simulation on Great Slave Lake. *Environmental Modelling & Software*, 22(6), 787–796. <https://doi.org/10.1016/j.envsoft.2006.03.005>
- Leoni, B., Spreafico, M., Patelli, M., Soler, V., Garibaldi, L., & Nava, V. (2019). Long-term studies for evaluating the impacts of natural and anthropic stressors on limnological features and the ecosystem quality of Lake Iseo. *Advances in Oceanography and Limnology*, 10(2), 2694. <https://doi.org/10.4081/aiol.2019.8622>
- Leppäranta, M. (1993). A review of analytical models of sea-ice growth. *Atmosphere-Ocean*, 31(1), 123–138. <https://doi.org/10.1080/07055900.1993.9649465>
- Levenberg, K. (1944). A method for the solution of certain problems in least squares. *Quarterly of Applied Mathematics*, 2(2), 164–168. <https://doi.org/10.1090/qam/1944-02-02>
- Lewis, A. S., Rollinson, C. R., Allyn, A. J., Ashander, J., Brodie, S., Brookson, C. B., et al. (2022). The power of forecasts to advance ecological theory. *Methods in Ecology and Evolution*, 14(3), 746–756. <https://doi.org/10.1111/2041-210X.13955>
- Lewis, W. M. (1983). A revised classification of lakes based on mixing. *Canadian Journal of Fisheries and Aquatic Sciences*, 40(10), 1779–1787. <https://doi.org/10.1139/f83-207>
- Li, X., Feng, M., Ran, Y., Su, Y., Liu, F., Huang, C., et al. (2023). Big data in earth system science and progress towards a digital twin. *Nature Reviews Earth & Environment*, 4(5), 319–332. <https://doi.org/10.1038/s43017-023-00409-w>
- Li, Y., Acharya, K., Chen, D., & Stone, M. (2010). Modeling water ages and thermal structure of lake mead under changing water levels. *Lake and Reservoir Management*, 26(4), 258–272. <https://doi.org/10.1080/07438141.2010.541326>
- Lin, S., Boegman, L., Shan, S., & Mulligan, R. (2022). An automatic lake-model application using near-real-time data forcing: Development of an operational forecast workflow (coastlines) for Lake Erie. *Geoscientific Model Development*, 15(3), 1331–1353. <https://doi.org/10.5194/gmd-15-1331-2022>
- Lindenschmidt, K. E., Carr, M. K., Sadeghian, A., & Morales-Marin, L. (2019). CE-QUAL-W2 model of dam outflow elevation impact on temperature, dissolved oxygen and nutrients in a reservoir. *Scientific Data*, 6(1), 1–7. <https://doi.org/10.1038/s41597-019-0316-y>
- Liu, H., Yaning, C., Ye, Z., Peng, L., & Zhang, Q. (2019). Recent lake area changes in Central Asia. *Scientific Reports*, 9(1), 16277. <https://doi.org/10.1038/s41598-019-52396-y>
- Liu, W. C., & Chen, W. B. (2012). Prediction of water temperature in a subtropical subalpine lake using an artificial neural network and three-dimensional circulation models. *Computers & Geosciences*, 45, 13–25. <https://doi.org/10.1016/j.cageo.2012.03.010>
- Livingstone, D. M., & Dokulil, M. T. (2001). Eighty years of spatially coherent Austrian lake surface temperatures and their relationship to regional air temperature and the North Atlantic Oscillation. *Limnology & Oceanography*, 46(5), 1220–1227. <https://doi.org/10.4319/lo.2001.46.5.1220>
- Livingstone, D. M., & Imboden, D. M. (1989). Annual heat balance and equilibrium temperature of Lake Aegeri, Switzerland. *Aquatic Sciences*, 51(4), 351–369. <https://doi.org/10.1007/BF00877177>
- Livingstone, D. M., & Lotter, A. F. (1998). The relationship between air and water temperatures in lakes of the Swiss Plateau: A case study with palaeolimnological implications. *Journal of Paleolimnology*, 19(2), 181–198. <https://doi.org/10.1023/A:1007904817619>
- Livingstone, D. M., Lotter, A. F., & Walkery, I. R. (1999). The decrease in summer surface water temperature with altitude in Swiss alpine lakes: A comparison with air temperature lapse rates. *Arctic Antarctic and Alpine Research*, 31(4), 341–352. <https://doi.org/10.1080/15230430.1999.12003319>
- Lopez-Cantu, T., Prein, A. F., & Samaras, C. (2020). Uncertainties in future us extreme precipitation from downscaled climate projections. *Geophysical Research Letters*, 47(9), e2019GL086797. <https://doi.org/10.1029/2019gl086797>
- Ma, Z., Wu, G., Suganthan, P. N., Song, A., & Luo, Q. (2023). Performance assessment and exhaustive listing of 500+ nature-inspired meta-heuristic algorithms. *Swarm and Evolutionary Computation*, 77, 101248. <https://doi.org/10.1016/j.swevo.2023.101248>

- Maberly, S. C., O'Donnell, R. A., Woolway, R. I., Cutler, M. E., Gong, M., Jones, I. D., et al. (2020). Global lake thermal regions shift under climate change. *Nature Communications*, *11*(1), 1–9. <https://doi.org/10.1038/s41467-020-15108-z>
- MacCallum, S. N., & Merchant, C. J. (2012). Surface water temperature observations of large lakes by optimal estimation. *Canadian Journal of Remote Sensing*, *38*(1), 25–45. <https://doi.org/10.5589/m12-010>
- Macintyre, H. L., Heaviside, C., Cai, X., & Phalkey, R. (2021). Comparing temperature-related mortality impacts of cool roofs in winter and summer in a highly urbanized European region for present and future climate. *Environment International*, *154*, 106606. <https://doi.org/10.1016/j.envint.2021.106606>
- Madsen, H., Davidson, T., Hamilton, D., Jeppesen, E., Kjellström, E., Olesen, J., et al. (2014). A framework for testing the ability of models to project climate change and its impacts. *Climatic Change*, *122*(1–2), 271–282. <https://doi.org/10.1007/s10584-013-0990-2>
- Magee, M. R., McIntyre, P. B., Hanson, P. C., & Wu, C. H. (2019). Drivers and management implications of long-term Cisco oxythermal habitat decline in Lake Mendota, WI. *Environmental Management*, *63*(3), 396–407. <https://doi.org/10.1007/s00267-018-01134-7>
- Magee, M. R., & Wu, C. H. (2017). Response of water temperatures and stratification to changing climate in three lakes with different morphometry. *Hydrology and Earth System Sciences*, *21*(12), 6253–6274. <https://doi.org/10.5194/hess-21-6253-2017>
- Maier, H. R., Razavi, S., Kapelan, Z., Matott, L. S., Kasprzyk, J., & Tolson, B. A. (2019). Introductory overview: Optimization using evolutionary algorithms and other metaheuristics. *Environmental Modelling & Software*, *114*, 195–213. <https://doi.org/10.1016/j.envsoft.2018.11.018>
- Mallard, M. S., Nolte, C. G., Bullock, O. R., Spero, T. L., & Gula, J. (2014). Using a coupled lake model with WRF for dynamical downscaling. *Journal of Geophysical Research: Atmospheres*, *119*(12), 7193–7208. <https://doi.org/10.1002/2014JD021785>
- Mao, M., & Xia, M. (2020). Monthly and episodic dynamics of summer circulation in Lake Michigan. *Journal of Geophysical Research: Oceans*, *125*(6), e2019JC015932. <https://doi.org/10.1029/2019JC015932>
- Marcé, R., George, G., Buscarinu, P., Deidda, M., Dunalska, J., de Eyto, E., et al. (2016). Automatic high frequency monitoring for improved lake and reservoir management. *Environmental Science & Technology*, *50*(20), 10780–10794. <https://doi.org/10.1021/acs.est.6b01604>
- Martin, B., Ding, L., Hannoun, I. A., & List, E. J. (2013). Predicting effects of reservoir expansion with three-dimensional modeling: Case study of Los Vaqueros Reservoir. *Lake and Reservoir Management*, *29*(4), 217–232. <https://doi.org/10.1080/10402381.2013.837565>
- Martin, J. L., & McCutcheon, S. C. (1999). *Hydrodynamics and transport for water quality modeling*. Lewis Publishers.
- Martynov, A., Sushama, L., & Laprise, R. (2010). Simulation of temperate freezing lakes by one-dimensional lake models: Performance assessment for interactive coupling with regional climate models. *Boreal Environment Research*, *15*(2), 143–164.
- Martynov, A., Sushama, L., Laprise, R., Winger, K., & Dugas, B. (2012). Interactive lakes in the Canadian regional climate model, version 5: The role of lakes in the regional climate of north America. *Tellus A: Dynamic Meteorology and Oceanography*, *64*(1), 16226. <https://doi.org/10.3402/tellusa.v64i0.16226>
- Mason, L. A., Riseng, C. M., Gronewold, A. D., Rutherford, E. S., Wang, J., Clites, A., et al. (2016). Fine-scale spatial variation in ice cover and surface temperature trends across the surface of the Laurentian Great Lakes. *Climatic Change*, *138*(1–2), 71–83. <https://doi.org/10.1007/s10584-016-1721-2>
- Matuszek, J. E., & Shuter, B. J. (1996). Notes: An empirical method for the prediction of daily water temperatures in the littoral zone of temperate lakes. *Transactions of the American Fisheries Society*, *125*(4), 622–627. [https://doi.org/10.1577/1548-8659\(1996\)125<0622:NAEMFT>2.3.CO;2](https://doi.org/10.1577/1548-8659(1996)125<0622:NAEMFT>2.3.CO;2)
- McCombie, A. M. (1959). Some relations between air temperatures and the surface water temperatures of lakes. *Limnology & Oceanography*, *4*(3), 252–258. <https://doi.org/10.4319/lo.1959.4.3.0252>
- McCormick, M. J., & Fahnenstiel, G. L. (1999). Recent climatic trends in nearshore water temperatures in the St. Lawrence Great Lakes. *Limnology & Oceanography*, *44*(3), 530–540. <https://doi.org/10.4319/lo.1999.44.3.0530>
- McInerney, J. B., Forrest, A. L., Schladow, S. G., & Largier, J. L. (2019). How to fly an autonomous underwater glider to measure an internal wave. In *Oceans 2019 MTS/IEEE Seattle* (pp. 1–8). <https://doi.org/10.23919/OCEANS40490.2019.8962407>
- Meinson, P., Idrizaj, A., Nöges, P., Nöges, T., & Laas, A. (2016). Continuous and high-frequency measurements in limnology: History, applications, and future challenges. *Environmental Reviews*, *24*(1), 52–62. <https://doi.org/10.1139/er-2015-0030>
- Menghani, G. (2023). Efficient deep learning: A survey on making deep learning models smaller, faster, and better. *ACM Computing Surveys*, *55*(12), 1–37. <https://doi.org/10.1145/3578938>
- Mercado-Bettín, D., Clayer, F., Shikhani, M., Moore, T. N., Frías, M. D., Jackson-Blake, L., et al. (2021). Forecasting water temperature in lakes and reservoirs using seasonal climate prediction. *Water Research*, *201*, 117286. <https://doi.org/10.1016/j.watres.2021.117286>
- Merchant, C., Embury, O., Bulgin, C., Block, T., Corlett, G., Fiedler, E., et al. (2019). Satellite-based time-series of sea-surface temperature since 1981 for climate applications. *Scientific Data*, *6*(1), 223. <https://doi.org/10.1038/s41597-019-0236-x>
- Merchant, C., & MacCallum, S. (2018). *Lake surface water temperature ARC-Lake v3 (1995–2012)*. University of Reading. <https://doi.org/10.17864/1947.186>
- Merz, E., Saberski, E., Gilarranz, L. J., Isles, P. D. F., Sugihara, G., Berger, C., & Pomati, F. (2023). Disruption of ecological networks in lakes by climate change and nutrient fluctuations. *Nature Climate Change*, *13*(4), 389–396. <https://doi.org/10.1038/s41558-023-01615-6>
- Mesman, J. P., Stelzer, J. A., Dakos, V., Goyette, S., Jones, I. D., Kasparian, J., et al. (2021). The role of internal feedbacks in shifting deep lake mixing regimes under a warming climate. *Freshwater Biology*, *66*(6), 1021–1035. <https://doi.org/10.1111/fwb.13704>
- Mi, C., Frassl, M. A., Boehrer, B., & Rinke, K. (2018). Episodic wind events induce persistent shifts in the thermal stratification of a reservoir (Rappbode Reservoir, Germany). *International Review of Hydrobiology*, *103*(3–4), 71–82. <https://doi.org/10.1002/iroh.201701916>
- Mi, C., Shatwell, T., Ma, J., Wentzky, V. C., Boehrer, B., Xu, Y., & Rinke, K. (2020). The formation of a metalimnetic oxygen minimum exemplifies how ecosystem dynamics shape biogeochemical processes: A modelling study. *Water Research*, *175*, 115701. <https://doi.org/10.1016/j.watres.2020.115701>
- Minnett, P. J., Smith, M., & Ward, B. (2011). Measurements of the oceanic thermal skin effect. *Deep Sea Research Part II: Topical Studies in Oceanography*, *58*(6), 861–868. <https://doi.org/10.1016/j.dsr2.2010.10.024>
- Mimms, C. K., Shuter, B. J., Davidson, A., & Wang, S. (2018). Factors influencing peak summer surface water temperature in Canada's large lakes. *Canadian Journal of Fisheries and Aquatic Sciences*, *75*(7), 1005–1018. <https://doi.org/10.1139/cjfas-2017-0061>
- Mironov, D. (2008). Parameterization of lakes in numerical weather prediction. description of a lake model (technical report). Retrieved from <https://www.cosmo-model.org/content/model/cosmo/techReports/docs/techReport11.pdf>
- Mironov, D., Heise, E., Kourzeneva, E., Ritter, B., Schneider, N., & Terzhevik, A. (2010). Implementation of the lake parameterisation scheme FLake into the numerical weather prediction model COSMO. *Boreal Environment Research*, *15*, 218–230.
- Missaghi, S., & Hondzo, M. (2010). Evaluation and application of a three-dimensional water quality model in a shallow lake with complex morphology. *Ecological Modelling*, *221*(11), 1512–1525. <https://doi.org/10.1016/j.ecolmodel.2010.02.006>
- Mohseni, O., & Stefan, H. (1999). Stream temperature/air temperature relationship: A physical interpretation. *Journal of Hydrology*, *218*(3), 128–141. [https://doi.org/10.1016/S0022-1694\(99\)00034-7](https://doi.org/10.1016/S0022-1694(99)00034-7)

- Mollema, P. N., & Antonellini, M. (2016). Water and (bio) chemical cycling in gravel pit lakes: A review and outlook. *Earth-Science Reviews*, 159, 247–270. <https://doi.org/10.1016/j.earscirev.2016.05.006>
- Moore, T. N., Mesman, J. P., Ladwig, R., Feldbauer, J., Olsson, F., Pilla, R. M., et al. (2021). LakeEnsemblR: An R package that facilitates ensemble modelling of lakes. *Environmental Modelling & Software*, 143, 105101. <https://doi.org/10.1016/j.envsoft.2021.105101>
- Moras, S., Ayala, A. I., & Pierson, D. C. (2019). Historical modelling of changes in Lake Erken thermal conditions. *Hydrology and Earth System Sciences*, 23(12), 5001–5016. <https://doi.org/10.5194/hess-23-5001-2019>
- Moriassi, D., Arnold, J., Van Liew, M., Bingner, R., Harmel, R., & Veith, T. (2007). Model evaluation guidelines for systematic quantification of accuracy in watershed simulations. *Transactions of the ASABE*, 50(3), 885–900. <https://doi.org/10.13031/2013.23153>
- Mullin, C. A., Kirchhoff, C. J., Wang, G., & Vlahos, P. (2020). Future projections of water temperature and thermal stratification in Connecticut reservoirs and possible implications for cyanobacteria. *Water Resources Research*, 56(11), e2020WR027185. <https://doi.org/10.1029/2020WR027185>
- Munk, W. H., & Anderson, E. R. (1948). Notes on a theory of the thermocline. *Journal of Marine Research*, 7, 276–295.
- Nash, J., & Sutcliffe, J. (1970). River flow forecasting through conceptual models part I—A discussion of principles. *Journal of Hydrology*, 10(3), 282–290. [https://doi.org/10.1016/0022-1694\(70\)90255-6](https://doi.org/10.1016/0022-1694(70)90255-6)
- Niedrist, G., Psenner, R., & Sommaruga, R. (2018). Climate warming increases vertical and seasonal water temperature differences and inter-annual variability in a mountain lake. *Climatic Change*, 151(3), 473–490. <https://doi.org/10.1007/s10584-018-2328-6>
- Noges, P., & Noges, T. (2014). Weak trends in ice phenology of Estonian large lakes despite significant warming trends. *Hydrobiologia*, 731(1), 5–18. <https://doi.org/10.1007/s10750-013-1572-z>
- North, R. P., Livingstone, D. M., Hari, R. E., Köster, O., Niederhauser, P., & Kipfer, R. (2013). The physical impact of the late 1980s climate regime shift on Swiss rivers and lakes. *Inland Waters*, 3(3), 341–350. <https://doi.org/10.5268/IW-3.3.560>
- North, R. P., North, R. L., Livingstone, D. M., Köster, O., & Kipfer, R. (2014). Long-term changes in hypoxia and soluble reactive phosphorus in the hypolimnion of a large temperate lake: Consequences of a climate regime shift. *Global Change Biology*, 20(3), 811–823. <https://doi.org/10.1111/gcb.12371>
- Notaro, M., Zarrin, A., Vavrus, S., & Bennington, V. (2013). Simulation of heavy lake-effect snowstorms across the great lakes basin by RegCM4: Synoptic climatology and variability. *Monthly Weather Review*, 141(6), 1990–2014. <https://doi.org/10.1175/MWR-D-11-00369.1>
- Okubo, A. (1971). Oceanic diffusion diagrams. *Deep-Sea Research and Oceanographic Abstracts*, 18(8), 789–802. [https://doi.org/10.1016/0011-7471\(71\)90046-5](https://doi.org/10.1016/0011-7471(71)90046-5)
- Oleson, K., Lawrence, D. M., Bonan, G. B., Drewniak, B., Huang, M., Koven, C. D., et al. (2013). Technical description of version 4.5 of the community land model (CLM) (No. NCAR/TN-503+STR) (technical report). <https://doi.org/10.5065/D6RR1W7M>
- Olsson, F. (2022). *Impacts of water residence time on lake thermal structure: Implications for management and climate change (Unpublished doctoral dissertation)*. Lancaster University.
- Oreskes, N., Shrader-Frechette, K., & Belitz, K. (1994). Verification, validation, and confirmation of numerical models in the earth sciences. *Science*, 263(5147), 641–646. <https://doi.org/10.1126/science.263.5147.641>
- Osaba, E., Villar-Rodríguez, E., Del Ser, J., Nebro, A. J., Molina, D., LaTorre, A., et al. (2021). A tutorial on the design, experimentation and application of metaheuristic algorithms to real-world optimization problems. *Swarm and Evolutionary Computation*, 64, 100888. <https://doi.org/10.1016/j.swevo.2021.100888>
- Ottosson, F., & Abrahamsson, O. (1998). Presentation and analysis of a model simulating epilimnetic and hypolimnetic temperatures in lakes. *Ecological Modelling*, 110(3), 233–253. [https://doi.org/10.1016/S0304-3800\(98\)00067-2](https://doi.org/10.1016/S0304-3800(98)00067-2)
- Ozdemir, S., Yaqub, M., & Yildirim, S. O. (2023). A systematic literature review on lake water level prediction models. *Environmental Modelling & Software*, 163, 105684. <https://doi.org/10.1016/j.envsoft.2023.105684>
- Pacanowski, R. C., & Philander, S. G. H. (1981). Parameterization of vertical mixing in numerical models of tropical oceans. *Journal of Physical Oceanography*, 11(11), 1443–1451. [https://doi.org/10.1175/1520-0485\(1981\)011<1443:POVMIN>2.0.CO;2](https://doi.org/10.1175/1520-0485(1981)011<1443:POVMIN>2.0.CO;2)
- Patterson, J., Hamblin, P., & Imberger, J. (1984). Classification and dynamic simulation of the vertical density structure of lakes. *Limnology & Oceanography*, 29(4), 845–861. <https://doi.org/10.4319/lo.1984.29.4.0845>
- Perga, M.-E., Bruel, R., Rodriguez, L., Guénand, Y., & Bouffard, D. (2018). Storm impacts on alpine lakes: Antecedent weather conditions matter more than the event intensity. *Global Change Biology*, 24(10), 5004–5016. <https://doi.org/10.1111/gcb.14384>
- Perroud, M., Goyette, S., Martynov, A., Beniston, M., & Annevillec, O. (2009). Simulation of multiannual thermal profiles in deep Lake Geneva: A comparison of one-dimensional lake models. *Limnology & Oceanography*, 54(5), 1574–1594. <https://doi.org/10.4319/lo.2009.54.5.1574>
- Piccolroaz, S. (2016). Prediction of lake surface temperature using the air2water model: Guidelines, challenges, and future perspectives. *Advances in Oceanography and Limnology*, 7(1), 36–50. <https://doi.org/10.4081/aiol.2016.5791>
- Piccolroaz, S., Amadori, M., Toffolon, M., & Dijkstra, H. A. (2019). Importance of planetary rotation for ventilation processes in deep elongated lakes: Evidence from Lake Garda (Italy). *Scientific Reports*, 9(1), 1–11. <https://doi.org/10.1038/s41598-019-44730-1>
- Piccolroaz, S., Calamita, E., Majone, B., Gallice, A., Siviglia, A., & Toffolon, M. (2016). Prediction of river water temperature: A comparison between a new family of hybrid models and statistical approaches. *Hydrological Processes*, 30(21), 3901–3917. <https://doi.org/10.1002/hyp.10913>
- Piccolroaz, S., Fernández-Castro, B., Toffolon, M., & Dijkstra, H. A. (2021). A multi-site, year-round turbulence microstructure atlas for the deep perialpine Lake Garda. *Scientific Data*, 8(1), 1–20. <https://doi.org/10.1038/s41597-021-00965-0>
- Piccolroaz, S., Healey, N., Lenters, J., Schladow, S., Hook, S., Sahoo, G., & Toffolon, M. (2018). On the predictability of lake surface temperature using air temperature in a changing climate: A case study for lake Tahoe (USA). *Limnology & Oceanography*, 63(1), 243–261. <https://doi.org/10.1002/lno.10626>
- Piccolroaz, S., & Toffolon, M. (2013). Deep water renewal in Lake Baikal: A model for long-term analyses. *Journal of Geophysical Research: Oceans*, 118(12), 6717–6733. <https://doi.org/10.1002/2013JC009029>
- Piccolroaz, S., & Toffolon, M. (2018). The fate of Lake Baikal: How climate change may alter deep ventilation in the largest lake on earth. *Climatic Change*, 150(3–4), 181–194. <https://doi.org/10.1007/s10584-018-2275-2>
- Piccolroaz, S., Toffolon, M., & Majone, B. (2013). A simple lumped model to convert air temperature into surface water temperature in lakes. *Hydrology and Earth System Sciences*, 17(8), 3323–3338. <https://doi.org/10.5194/hessd-10-2697-2013>
- Piccolroaz, S., Toffolon, M., & Majone, B. (2015). The role of stratification on lakes' thermal response: The case of Lake Superior. *Water Resources Research*, 51(10), 7878–7894. <https://doi.org/10.1002/2014WR016555>
- Piccolroaz, S., Woolway, R. I., & Merchant, C. J. (2020). Global reconstruction of twentieth century lake surface water temperature reveals different warming trends depending on the climatic zone. *Climatic Change*, 160(3), 427–442. <https://doi.org/10.1007/s10584-020-02663-z>
- Piccolroaz, S., Zhu, S., Ladwig, R., Carrea, L., Oliver, S., Piotrowski, A. P., et al. (2024). Lake water temperature modelling in an ERA of climate change: Data sources, models, and future directions [Dataset]. Zenodo. <https://doi.org/10.5281/zenodo.10489521>

- Piccolroaz, S., Zhu, S., Ptak, M., Sojka, M., & Du, X. (2021). Warming of lowland polish lakes under future climate change scenarios and consequences for ice cover and mixing dynamics. *Journal of Hydrology: Regional Studies*, 34, 100780. <https://doi.org/10.1016/j.ejrh.2021.100780>
- Pilla, R. M., Mette, E. M., Williamson, C. E., Adamovich, B. V., Adrian, R., Anneville, O., et al. (2021). Global data set of long-term summertime vertical temperature profiles in 153 lakes. *Scientific Data*, 8(1), 1–12. <https://doi.org/10.1038/s41597-021-00983-y>
- Pinkel, R., Goldin, M., Smith, J., Sun, O., Aja, A., Bui, M., & Huguen, T. (2011). The Wirewalker: A vertically profiling instrument carrier powered by ocean waves. *Journal of Atmospheric and Oceanic Technology*, 28(3), 426–435. <https://doi.org/10.1175/2010JTECHO805.1>
- Piotrowski, A. P., Napiorkowski, J. J., & Piotrowska, A. E. (2020). Population size in particle swarm optimization. *Swarm and Evolutionary Computation*, 58, 100718. <https://doi.org/10.1016/j.swevo.2020.100718>
- Piotrowski, A. P., Napiorkowski, J. J., & Zhu, S. (2023). Novel air2water model variant for lake surface temperature modeling with detailed analysis of calibration methods. *IEEE Journal of Selected Topics in Applied Earth Observations and Remote Sensing*, 16, 553–569. <https://doi.org/10.1109/JSTARS.2022.3226516>
- Piotrowski, A. P., Napiorkowski, M. J., Napiorkowski, J. J., & Rowinski, P. M. (2017). Swarm intelligence and evolutionary algorithms: Performance versus speed. *Information Sciences*, 384, 34–85. <https://doi.org/10.1016/j.ins.2016.12.028>
- Piotrowski, A. P., Osuch, M., & Napiorkowski, J. J. (2021). Influence of the choice of stream temperature model on the projections of water temperature in rivers. *Journal of Hydrology*, 601, 126629. <https://doi.org/10.1016/j.jhydrol.2021.126629>
- Piotrowski, A. P., Zhu, S., & Napiorkowski, J. J. (2022). Air2water model with nine parameters for lake surface temperature assessment. *Limnologia*, 94, 125967. <https://doi.org/10.1016/j.limno.2022.125967>
- Prats, J., & Danis, P.-A. (2019). An epilimnion and hypolimnion temperature model based on air temperature and lake characteristics. *Knowledge and Management of Aquatic Ecosystems*, 8, 420. <https://doi.org/10.1051/kmae/2019001>
- Preston, A., Hannoun, I. A., List, E. J., Rackley, I., & Tietjen, T. (2014). Three-dimensional management model for Lake Mead, Nevada, Part 1: Model calibration and validation. *Lake and Reservoir Management*, 30(3), 285–302. <https://doi.org/10.1080/10402381.2014.927941>
- Quan, Q., Hao, Z., Xifeng, H., & Jingchun, L. (2020). Research on water temperature prediction based on improved support vector regression. *Neural Computing & Applications*, 34(11), 1–10. <https://doi.org/10.1007/s00521-020-04836-4>
- Rahaghi, A. I., Lemmin, U., Cimatoribus, A., Bouffard, D., Riffler, M., Wunderle, S., & Barry, D. A. (2018). Improving surface heat flux estimation for a large lake through model optimization and two-point calibration: The case of Lake Geneva. *Limnology and Oceanography: Methods*, 16(9), 576–593. <https://doi.org/10.1002/lom3.10267>
- Rainville, L., & Pinkel, R. (2001). Wirewalker: An autonomous wave-powered vertical profiler. *Journal of Atmospheric and Oceanic Technology*, 18(6), 1048–1051. [https://doi.org/10.1175/1520-0426\(2001\)018<1048:WAAWPV>2.0.CO;2](https://doi.org/10.1175/1520-0426(2001)018<1048:WAAWPV>2.0.CO;2)
- Rajula, H. S. R., Verlato, G., Manchia, M., Antonucci, N., & Fanos, V. (2020). Comparison of conventional statistical methods with machine learning in medicine: Diagnosis, drug development, and treatment. *Medicina*, 56(9), 455. <https://doi.org/10.3390/medicina56090455>
- Raman Vinna, L., Wüest, A., Zappa, M., Fink, G., & Bouffard, D. (2018). Tributaries affect the thermal response of lakes to climate change. *Hydrology and Earth System Sciences*, 22, 31–51. <https://doi.org/10.5194/hess-2017-337>
- Ramos, H. M., Kuriqi, A., Coronado-Hernández, O. E., López-Jiménez, P. A., & Pérez-Sánchez, M. (2023). Are digital twins improving urban-water systems efficiency and sustainable development goals? *Urban Water Journal*, 1–13. <https://doi.org/10.1080/1573062X.2023.2180396>
- Rand, J. M., Nanko, M. O., Lykkegaard, M. B., Wain, D., King, W., Bryant, L. D., & Hunter, A. (2022). The human factor: Weather bias in manual lake water quality monitoring. *Limnology and Oceanography: Methods*, 20(5), 288–303. <https://doi.org/10.1002/lom3.10488>
- Read, J. S., Jia, X., Willard, J. D., Appling, A. P., Zwart, J. A., Oliver, S. K., et al. (2019). Process-guided deep learning predictions of lake water temperature. *Water Resources Research*, 55(11), 9173–9190. <https://doi.org/10.1029/2019WR024922>
- Read, J. S., Winslow, L. A., Hansen, G. J., Van Den Hoek, J., Hanson, P. C., Bruce, L. C., & Markfort, C. D. (2014). Simulating 2368 temperate lakes reveals weak coherence in stratification phenology. *Ecological Modelling*, 291, 142–150. <https://doi.org/10.1016/j.ecolmodel.2014.07.029>
- Reichstein, M., Camps-Valls, G., Stevens, B., Jung, M., Denzler, J., Carvalhais, N., & Prabhat (2019). Deep learning and process understanding for data-driven earth system science. *Nature*, 566(7743), 195–204. <https://doi.org/10.1038/s41586-019-0912-1>
- Reinart, A., & Reinhold, M. (2008). Mapping surface temperature in large lakes with modis data. *Remote Sensing of Environment*, 112(2), 603–611. <https://doi.org/10.1016/j.rse.2007.05.015>
- Rempfer, J., Livingstone, D. M., Blodau, C., Forster, R., Niederhauser, P., & Kipfer, R. (2010). The effect of the exceptionally mild European winter of 2006–2007 on temperature and oxygen profiles in lakes in Switzerland: A foretaste of the future? *Limnology & Oceanography*, 55(5), 2170–2180. <https://doi.org/10.4319/lo.2010.55.5.2170>
- Rheinheimer, D. E., Null, S. E., & Lund, J. R. (2015). Optimizing selective withdrawal from reservoirs to manage downstream temperatures with climate warming. *Journal of Water Resources Planning and Management*, 141(4), 04014063. [https://doi.org/10.1061/\(ASCE\)WR.1943-5452.0000447](https://doi.org/10.1061/(ASCE)WR.1943-5452.0000447)
- Rigon, R., Formetta, G., Bancheri, M., Tubini, N., D'Amato, C., David, O., & Massari, C. (2022). Hess opinions: Participatory digital earth twin hydrology systems (darths) for everyone—A blueprint for hydrologists. *Hydrology and Earth System Sciences*, 26(18), 4773–4800. <https://doi.org/10.5194/hess-26-4773-2022>
- Rimet, F., Anneville, O., Barbet, D., Chardon, C., Crepin, L., Domaizon, I., et al. (2020). The Observatory on LAkes (OLA) database: Sixty years of environmental data accessible to the public. *Journal of Limnology*, 79(2), 164–178. <https://doi.org/10.4081/jlimnol.2020.1944>
- Roberts, J. J., Fausch, K. D., Schmidt, T. S., & Walters, D. M. (2017). Thermal regimes of Rocky Mountain lakes warm with climate change. *PLoS One*, 12(7), 1–17. <https://doi.org/10.1371/journal.pone.0179498>
- Robertson, D. (2016). Lake Mendota water temperature secchi depth snow depth ice thickness and meteorological conditions 1894–2007 ver 1. *Environmental Data Initiative*. <https://doi.org/10.6073/pasta/f20f9a644bd12e4b80cb288f1812e935>
- Robertson, D., & Ragotzkie, R. (1990). Changes in the thermal structure of moderate to large sized lakes in response to changes in air temperature. *Aquatic Sciences*, 52(4), 360–380. <https://doi.org/10.1007/BF00879763>
- Robertson, D., Ragotzkie, R., & Magnuson, J. (1992). Lake ice records used to detect historical and future climatic changes. *Climatic Change*, 21(4), 407–427. <https://doi.org/10.1007/BF00141379>
- Rodgers, C. D. (2000). *Inverse methods for atmospheric sounding*. World Scientific. <https://doi.org/10.1142/3171>
- Rodhe, B. (1952). On the relation between air temperature and ice formation in the Baltic. *Geografiska Annaler*, 34(3–4), 175–202. <https://doi.org/10.1080/20014422.1952.11904372>
- Rodi, W. (1984). Turbulence models and their application in hydraulics, International association for Hydraulic Research (IAHR). In *Monograph series, IAHR, Delft*.
- Rodi, W. (1987). Examples of calculation methods for flow and mixing in stratified fluids. *Journal of Geophysical Research*, 92(C5), 5305–5328. <https://doi.org/10.1029/JC092iC05p05305>
- Roemmich, D., & Owens, W. (2000). The Argo project: Observing the global ocean with profiling floats. *Oceanography*, 13(2), 45–50. <https://doi.org/10.5670/oceanog.2000.33>

- Rooney, G. G., Van Lipzig, N., & Thiery, W. (2018). Estimating the effect of rainfall on the surface temperature of a tropical lake. *Hydrology and Earth System Sciences*, 22(12), 6357–6369. <https://doi.org/10.5194/hess-22-6357-2018>
- Rose, K. C., Winslow, L. A., Read, J. S., & Hansen, G. J. A. (2016). Climate-induced warming of lakes can be either amplified or suppressed by trends in water clarity. *Limnology and Oceanography Letters*, 1(1), 44–53. <https://doi.org/10.1002/lol2.10027>
- Sabás, I., Miró, A., Piera, J., Catalan, J., Camarero, L., Buchaca, T., & Ventura, M. (2021). Factors of surface thermal variation in high-mountain lakes of the Pyrenees. *PLoS One*, 16(8), 1–19. <https://doi.org/10.1371/journal.pone.0254702>
- Saber, A., James, D. E., & Hayes, D. F. (2020). Long-term forecast of water temperature and dissolved oxygen profiles in deep lakes using artificial neural networks conjugated with wavelet transform. *Limnology & Oceanography*, 65(6), 1297–1317. <https://doi.org/10.1002/lno.11390>
- Safin, A., Bouffard, D., Ozdemir, F., Ramón, C. L., Runnalls, J., Georgatos, F., et al. (2022). A Bayesian data assimilation framework for lake 3D hydrodynamic models with a physics-preserving particle filtering method using SPUX-MITgcm v1. *Geoscientific Model Development*, 15(20), 7715–7730. <https://doi.org/10.5194/gmd-15-7715-2022>
- Salk, K. R., Venkiteswaran, J. J., Couture, R., Higgins, S. N., Paterson, M. J., & Schiff, S. L. (2022). Warming combined with experimental eutrophication intensifies lake phytoplankton blooms. *Limnology & Oceanography*, 67(1), 147–158. <https://doi.org/10.1002/lno.11982>
- Salmaso, N., Buzzi, F., Cerasino, L., Garibaldi, L., Leoni, B., Morabito, G., et al. (2014). Influence of atmospheric modes of variability on the limnological characteristics of large lakes south of the Alps: A new emerging paradigm. *Hydrobiologia*, 731(1), 31–48. <https://doi.org/10.1007/s10750-013-1659-6>
- Saloranta, T. M., & Andersen, T. (2007). MyLake—A multi-year lake simulation model code suitable for uncertainty and sensitivity analysis simulations. *Ecological Modelling*, 207(1), 45–60. <https://doi.org/10.1016/j.ecolmodel.2007.03.018>
- Schaeffer, B. A., Iames, J., Dwyer, J., Urquhart, E., Salls, W., Rover, J., & Seegers, B. (2018). An initial validation of Landsat 5 and 7 derived surface water temperature for US lakes, reservoirs, and estuaries. *International Journal of Remote Sensing*, 39(22), 7789–7805. <https://doi.org/10.1080/01431161.2018.1471545>
- Schaeffli, B., & Gupta, H. V. (2007). Do nash values have value? *Hydrological Processes*, 21(15), 2075–2080. <https://doi.org/10.1002/hyp.6825>
- Schmid, M., Hunziker, S., & Wüest, A. (2014). Lake surface temperatures in a changing climate: A global sensitivity analysis. *Climatic Change*, 124(1–2), 301–315. <https://doi.org/10.1007/s10584-014-1087-2>
- Schmid, M., & Read, J. (2022). Heat budget of lakes. In T. Mehner & K. Tockner (Eds.), *Encyclopedia of inland waters* (2nd ed., pp. 467–473). Elsevier. <https://doi.org/10.1016/B978-0-12-819166-8.00011-6>
- Schneider, P., Healey, N. C., Hulley, G. C., & Hook, S. J. (2019). Lake surface temperature. In *Taking the temperature of the earth* (pp. 129–150). Elsevier. <https://doi.org/10.1016/B978-0-12-814458-9.00004-6>
- Schneider, P., Hook, S., Radocinski, R., Corlett, G., Hulley, G., Schladow, S., & Steissberg, T. (2009). Satellite observations indicate rapid warming trend for lakes in California and Nevada. *Geophysical Research Letters*, 36(22), L22402. <https://doi.org/10.1029/2009GL040846>
- Schneider, P., & Hook, S. J. (2010). Space observations of inland water bodies show rapid surface warming since 1985. *Geophysical Research Letters*, 37(22), 208–217. <https://doi.org/10.1029/2010GL045059>
- Schwarz, G. (1978). Estimating the dimension of a model. *Annals of Statistics*, 6(2), 461–464. <https://doi.org/10.1214/aos/1176344136>
- Schwindt, S., Medrano, S. C., Mouris, K., Beckers, F., Haun, S., Nowak, W., et al. (2023). Bayesian calibration points to misconceptions in three-dimensional hydrodynamic reservoir modeling. *Water Resources Research*, 59(3), e2022WR033660. <https://doi.org/10.1029/2022WR033660>
- Selker, J. S., Thevenaz, L., Huwald, H., Mallet, A., Luxemburg, W., Van De Giesen, N., et al. (2006). Distributed fiber-optic temperature sensing for hydrologic systems. *Water Resources Research*, 42(12), W12202. <https://doi.org/10.1029/2006WR005326>
- Sepúlveda Steiner, O., Bouffard, D., & Wüest, A. (2019). Convection-diffusion competition within mixed layers of stratified natural waters. *Geophysical Research Letters*, 46(22), 13199–13208. <https://doi.org/10.1029/2019GL085361>
- Sepúlveda Steiner, O., Bouffard, D., & Wüest, A. (2021). Persistence of bioconvection-induced mixed layers in a stratified lake. *Limnology & Oceanography*, 66(4), 1531–1547. <https://doi.org/10.1002/lno.11702>
- Sepúlveda Steiner, O., Forrest, A. L., McInerney, J. B. T., Castro, B. F., Lavanchy, S., Wüest, A., & Bouffard, D. (2023). Spatial variability of turbulent mixing from an underwater glider in a large, deep, stratified lake. *Journal of Geophysical Research: Oceans*, 128(6), e2022JC018913. <https://doi.org/10.1029/2022JC018913>
- Sergeyev, Y. D., Kvasov, D. E., & Mukhametzanov, M. S. (2018). On the efficiency of nature-inspired metaheuristics in expensive global optimization with limited budgets. *Scientific Reports*, 8(1), 453. <https://doi.org/10.1038/s41598-017-18940-4>
- Shabani, A., Zhang, X., Chu, X., & Zheng, H. (2021). Automatic calibration for CE-QUAL-W2 model using improved global-best harmony search algorithm. *Water*, 13(16), 2308. <https://doi.org/10.3390/w13162308>
- Shahriari, B., Swersky, K., Wang, Z., Adams, R. P., & de Freitas, N. (2016). Taking the human out of the loop: A review of Bayesian optimization. *Proceedings of the IEEE*, 104(1), 148–175. <https://doi.org/10.1109/JPROC.2015.2494218>
- Sharma, S., Gray, D. K., Read, J. S., O'reilly, C. M., Schneider, P., Qudrat, A., et al. (2015). A global database of lake surface temperatures collected by in situ and satellite methods from 1985–2009. *Scientific Data*, 2(1), 1–19. <https://doi.org/10.1038/sdata.2015.8>
- Sharma, S., Jackson, D. A., Minns, C. K., & Shuter, B. J. (2007). Will northern fish populations be in hot water because of climate change? *Global Change Biology*, 13(10), 2052–2064. <https://doi.org/10.1111/j.1365-2486.2007.01426.x>
- Sharma, S., Walker, S. C., & Jackson, D. A. (2008). Empirical modelling of lake water-temperature relationships: A comparison of approaches. *Freshwater Biology*, 53(5), 897–911. <https://doi.org/10.1111/j.1365-2427.2008.01943.x>
- Shatwell, T., Thiery, W., & Kirillin, G. (2019). Future projections of temperature and mixing regime of European temperate lakes. *Hydrology and Earth System Sciences*, 23(3), 1533–1551. <https://doi.org/10.5194/hess-23-1533-2019>
- Shinohara, R., Matsuzaki, S. S.-I., Watanabe, M., Nakagawa, M., Yoshida, H., & Kohzu, A. (2023). Heat waves can cause hypoxia in shallow lakes. *Geophysical Research Letters*, 50(8), e2023GL102967. <https://doi.org/10.1029/2023GL102967>
- Shlezinger, N., Whang, J., Eldar, Y., & Dimakis, A. (2023). Model-based deep learning. *Proceedings of the IEEE*, 111(5), 465–499. <https://doi.org/10.1109/JPROC.2023.3247480>
- Shuter, B. J., Schlesinger, D. A., & Zimmerman, A. P. (1983). Empirical predictors of annual surface water temperature cycles in North American lakes. *Canadian Journal of Fisheries and Aquatic Sciences*, 40(10), 1838–1845. <https://doi.org/10.1139/f83-213>
- Smith, D., Hunt, S., Etxaluze, M., Peters, D., Nightingale, T., Mittaz, J., et al. (2021). Traceability of the Sentinel-3 SLSTR Level-1 infrared radiometric processing. *Remote Sensing*, 13(3), 374. <https://doi.org/10.3390/rs13030374>
- Snucins, E., & Gunn, J. (2000). Interannual variation in the thermal structure of clear and colored lakes. *Limnology & Oceanography*, 45(7), 1639–1646. <https://doi.org/10.4319/lo.2000.45.7.1639>
- Soares, L. M. V., & do Carmo Calijuri, M. (2021). Deterministic modelling of freshwater lakes and reservoirs: Current trends and recent progress. *Environmental Modelling & Software*, 144, 105143. <https://doi.org/10.1016/j.envsoft.2021.105143>

- Soares, L. M. V., Silva, T. F. D. G., Vinçon-Leite, B., Eleutério, J. C., Lima, L. C. D., & Nascimento, N. D. O. (2019). Modelling drought impacts on the hydrodynamics of a tropical water supply reservoir. *Inland Waters*, 9(4), 422–437. <https://doi.org/10.1080/20442041.2019.1596015>
- Sommer, T., Carpenter, J. R., Schmid, M., Lueck, R. G., & Wüest, A. (2013). Revisiting microstructure sensor responses with implications for double-diffusive fluxes. *Journal of Atmospheric and Oceanic Technology*, 30(8), 1907–1923. <https://doi.org/10.1175/JTECH-D-12-00272.1>
- Soullignac, F., Anneville, O., Bouffard, D., Chanudet, V., Dambrine, E., Guénand, Y., et al. (2019). Contribution of 3D coupled hydrodynamic–ecological modeling to assess the representativeness of a sampling protocol for lake water quality assessment. *Knowledge and Management of Aquatic Ecosystems*, 42, 420. <https://doi.org/10.1051/kmae/2019034>
- Soullignac, F., Vinçon-Leite, B., Lemaire, B. J., Scarati Martins, J. R., Bonhomme, C., Dubois, P., et al. (2017). Performance assessment of a 3D hydrodynamic model using high temporal resolution measurements in a shallow urban lake. *Environmental Modeling & Assessment*, 22(4), 309–322. <https://doi.org/10.1007/s10666-017-9548-4>
- Stepanenko, V., Jöhnk, K. D., Machulska, E., Perroud, M., Subin, Z., Nordbo, A., et al. (2014). Simulation of surface energy fluxes and stratification of a small boreal lake by a set of one-dimensional models. *Tellus A: Dynamic Meteorology and Oceanography*, 66(1), 21389. <https://doi.org/10.3402/tellusa.v66.21389>
- Stepanenko, V., Mammarella, I., Ojala, A., Miettinen, H., Lykosov, V., & Vesala, T. (2016). Lake 2.0: A model for temperature, methane, carbon dioxide and oxygen dynamics in lakes. *Geoscientific Model Development*, 9(5), 1977–2006. <https://doi.org/10.5194/gmd-9-1977-2016>
- Stepanenko, V., Martynov, A., Jöhnk, K., Subin, Z., Perroud, M., Fang, X., et al. (2013). A one-dimensional model intercomparison study of thermal regime of a shallow, turbid midlatitude lake. *Geoscientific Model Development*, 6(4), 1337–1352. <https://doi.org/10.5194/gmd-6-1337-2013>
- Sterckx, K., Delandmeter, P., Lambrechts, J., Deleersnijder, E., Verburg, P., & Thiery, W. (2023). The impact of seasonal variability and climate change on lake Tanganyika's hydrodynamics. *Environmental Fluid Mechanics*, 23(1), 103–123. <https://doi.org/10.1007/s10652-022-09908-8>
- Straille, D., Jöhnk, K., & Henno, R. (2003). Complex effects of winter warming on the physicochemical characteristics of a deep lake. *Limnology & Oceanography*, 48(4), 1432–1438. <https://doi.org/10.4319/lo.2003.48.4.1432>
- Sturrock, A. M., Winter, T. C., & Rosenberry, D. O. (1992). Energy budget evaporation from Williams lake: A closed lake in north central Minnesota. *Water Resources Research*, 28(6), 1605–1617. <https://doi.org/10.1029/92WR00553>
- Subin, Z. M., Riley, W. J., & Mironov, D. (2012). An improved lake model for climate simulations: Model structure, evaluation, and sensitivity analyses in cesm1. *Journal of Advances in Modeling Earth Systems*, 4(1), M02001. <https://doi.org/10.1029/2011MS000072>
- Sugiyama, N., Kravtsov, S., & Roeber, P. (2018). Multiple climate regimes in an idealized lake–ice–atmosphere model. *Climate Dynamics*, 50(1), 655–676. <https://doi.org/10.1007/s00382-017-3633-x>
- Sungmin, O., Dutra, E., & Orth, R. (2020). Robustness of process-based versus data-driven modeling in changing climatic conditions. *Journal of Hydrometeorology*, 21(9), 1929–1944. <https://doi.org/10.1175/jhm-d-20-0072.1>
- Tan, Z., Yao, H., & Zhuang, Q. (2018). A small temperate lake in the 21st century: Dynamics of water temperature, ice phenology, dissolved oxygen, and chlorophyll a. *Water Resources Research*, 54(7), 4681–4699. <https://doi.org/10.1029/2017WR022334>
- Tan, Z., Zhuang, Q., & Walter Anthony, K. (2015). Modeling methane emissions from arctic lakes: Model development and site-level study. *Journal of Advances in Modeling Earth Systems*, 7(2), 459–483. <https://doi.org/10.1002/2014MS000344>
- Tayal, K., Jia, X., Ghosh, R., Willard, J. D., Read, J., & Kumar, V. (2022). Invertibility aware integration of static and time-series data: An application to lake temperature modeling. In *Proceedings of the 2022 SIAM international conference on data mining (SDM)* (pp. 702–710). <https://doi.org/10.1137/1.9781611977172.79>
- Thiery, W., Martynov, A., Darchambeau, F., Descy, J.-P., Plisnier, P.-D., Sushama, L., & van Lipzig, N. P. (2014). Understanding the performance of the FLake model over two African Great Lakes. *Geoscientific Model Development*, 7(1), 317–337. <https://doi.org/10.5194/gmd-7-317-2014>
- Thomas, R. Q., Boettiger, C., Carey, C. C., Dietze, M. C., Johnson, L. R., Kenney, M. A., et al. (2022). The NEON ecological forecasting challenge. *Authoria Preprints*. <https://doi.org/10.22541/essoar.167079499.99891914/v1>
- Thomas, R. Q., Figueiredo, R. J., Daneshmand, V., Bookout, B. J., Puckett, L. K., & Carey, C. C. (2020). A near-term iterative forecasting system successfully predicts reservoir hydrodynamics and partitions uncertainty in real time. *Water Resources Research*, 56(11), e2019WR026138. <https://doi.org/10.1029/2019WR026138>
- Tiberti, R., Caroni, R., Cannata, M., Lami, A., Manca, D., Strigaro, D., & Rogora, M. (2021). Automated high frequency monitoring of Lake Maggiore through in situ sensors: System design, field test and data quality control. *Journal of Limnology*, 80(2), 1–19. <https://doi.org/10.4081/jlimnol.2021.2011>
- Toffolon, M., Piccolroaz, S., & Calamita, E. (2020). On the use of averaged indicators to assess lakes' thermal response to changes in climatic conditions. *Environmental Research Letters*, 15(3), 034060. <https://doi.org/10.1088/1748-9326/ab763e>
- Toffolon, M., Piccolroaz, S., Majone, B., Soja, A.-M., Peeters, F., Schmid, M., & Wüest, A. (2014). Prediction of surface temperature in lakes with different morphology using air temperature. *Limnology & Oceanography*, 59(6), 2185–2202. <https://doi.org/10.4319/lo.2014.59.6.2185>
- Toffolon, M., Yousefi, A., & Piccolroaz, S. (2022). Estimation of the thermally reactive layer in lakes based on surface water temperature. *Water Resources Research*, 58(6), e2021WR031755. <https://doi.org/10.1029/2021WR031755>
- Triana, J. S. A., Chu, M. L., Guzman, J. A., Moriasi, D. N., & Steiner, J. L. (2019). Beyond model metrics: The perils of calibrating hydrological models. *Journal of Hydrology*, 578, 124032. <https://doi.org/10.1016/j.jhydrol.2019.124032>
- Trumpickas, J., Shuter, B. J., & Minns, C. K. (2009). Forecasting impacts of climate change on great lakes surface water temperatures. *Journal of Great Lakes Research*, 35(3), 454–463. <https://doi.org/10.1016/j.jglr.2009.04.005>
- Ulloa, H. N., Ramón, C. L., Doda, T., Wüest, A., & Bouffard, D. (2022). Development of overturning circulation in sloping waterbodies due to surface cooling. *Journal of Fluid Mechanics*, 930, A18. <https://doi.org/10.1017/jfm.2021.883>
- Valerio, G., Pilotti, M., Marti, C. L., & Imberger, J. R. (2012). The structure of basin-scale internal waves in a stratified lake in response to lake bathymetry and wind spatial and temporal distribution: Lake Iseo, Italy. *Limnology & Oceanography*, 57(3), 772–786. <https://doi.org/10.4319/lo.2012.57.3.0772>
- Van Cleave, K., Lenters, J. D., Wang, J., & Verhamme, E. M. (2014). A regime shift in lake superior ice cover, evaporation, and water temperature following the warm El Niño winter of 1997–1998. *Limnology & Oceanography*, 59(6), 1889–1898. <https://doi.org/10.4319/lo.2014.59.6.1889>
- Vanderkelen, I., Lipzig, N. P. M., Lawrence, D. M., Droppers, B., Golub, M., Gosling, S. N., et al. (2020). Global heat uptake by inland waters. *Geophysical Research Letters*, 47(12), e2020GL087867. <https://doi.org/10.1029/2020GL087867>
- Van Haren, H., Groenewegen, R., Laan, M., & Koster, B. (2001). A fast and accurate thermistor string. *Journal of Atmospheric and Oceanic Technology*, 18(2), 256–265. [https://doi.org/10.1175/1520-0426\(2001\)018<0256:FAAATS>2.0.CO;2](https://doi.org/10.1175/1520-0426(2001)018<0256:FAAATS>2.0.CO;2)
- Van Haren, H., Groenewegen, R., Laan, M., & Koster, B. (2005). High sampling rate thermistor string observations at the slope of Great Meteor Seamount. *Ocean Science*, 1(1), 17–28. <https://doi.org/10.5194/os-1-17-2005>
- Vecek, N., Crepinsek, M., & Mernik, M. (2017). On the influence of the number of algorithms, problems, and independent runs in the comparison of evolutionary algorithms. *Applied Soft Computing*, 54, 23–45. <https://doi.org/10.1016/j.asoc.2017.01.011>

- Venayagamoorthy, S. K., & Stretch, D. D. (2010). On the turbulent Prandtl number in homogeneous stably stratified turbulence. *Journal of Fluid Mechanics*, *644*, 359–369. <https://doi.org/10.1017/S002211200999293X>
- Vitale, A. J., Perillo, G. M., Genchi, S. A., Arias, A. H., & Piccolo, M. C. (2018). Low-cost monitoring buoys network tracking biogeochemical changes in lakes and marine environments—A regional case study. *Pure and Applied Chemistry*, *90*(10), 1631–1646. <https://doi.org/10.1515/pac-2018-0508>
- Vrugt, J. A., ter Braak, C. J. F., Diks, C. G. H., & Schoups, G. (2013). Hydrologic data assimilation using particle Markov chain Monte Carlo simulation: Theory, concepts and applications. *Advances in Water Resources*, *51*, 457–478. <https://doi.org/10.1016/j.advwatres.2012.04.002>
- Wang, F., Ni, G., Riley, W. J., Tang, J., Zhu, D., & Sun, T. (2019). Evaluation of the WRF lake module (v1.0) and its improvements at a deep reservoir. *Geoscientific Model Development*, *12*(5), 2119–2138. <https://doi.org/10.5194/gmd-12-2119-2019>
- Wang, H., Deng, Y., Yan, Z., Yang, Y., & Tuo, Y. (2023). Thermal response of a deep monomictic reservoir to selective withdrawal of the upstream reservoir. *Ecological Engineering*, *187*, 106864. <https://doi.org/10.1016/j.ecoleng.2022.106864>
- Wang, L., Xu, B., Zhang, C., Fu, G., Chen, X., Zheng, Y., & Zhang, J. (2022). Surface water temperature prediction in large-deep reservoirs using a long short-term memory model. *Ecological Indicators*, *134*, 108491. <https://doi.org/10.1016/j.ecolind.2021.108491>
- Wang, S., He, Y., Hu, S., Ji, F., Wang, B., Guan, X., & Piccolroaz, S. (2021). Enhanced warming in global dryland lakes and its drivers. *Remote Sensing*, *14*(1), 86. <https://doi.org/10.3390/rs14010086>
- Wang, W., Shi, K., Wang, X., Wang, S., Zhang, D., Peng, Y., et al. (2023). A record-breaking extreme heat event caused unprecedented warming of lakes in China. *Science Bulletin*, *68*(6), 578–582. <https://doi.org/10.1016/j.scib.2023.03.001>
- Wang, X., Wang, W., He, Y., Zhang, S., Huang, W., Woolway, R. I., et al. (2023). Numerical simulation of thermal stratification in Lake Qiantao using an improved WRF-Lake model. *Journal of Hydrology*, *618*, 129184. <https://doi.org/10.1016/j.jhydrol.2023.129184>
- Ward, B., Fristedt, T., Callaghan, A. H., Sutherland, G., Sanchez, X., Vialard, J., & Doeschate, A. T. (2014). The Air–Sea Interaction Profiler (ASIP): An autonomous upwardly rising profiler for microstructure measurements in the upper ocean. *Journal of Atmospheric and Oceanic Technology*, *31*(10), 2246–2267. <https://doi.org/10.1175/JTECH-D-14-00010.1>
- Webb, E. A., & Liljedahl, A. K. (2023). Diminishing lake area across the northern permafrost zone. *Nature Geoscience*, *16*(3), 202–209. <https://doi.org/10.1038/s41561-023-01128-z>
- Webb, M. S. (1974). Surface temperatures of Lake Erie. *Water Resources Research*, *10*(2), 199–210. <https://doi.org/10.1029/WR010i002p00199>
- Weber, M., Rinke, K., Hipsey, M., & Boehrer, B. (2017). Optimizing withdrawal from drinking water reservoirs to reduce downstream temperature pollution and reservoir hypoxia. *Journal of Environmental Management*, *197*, 96–105. <https://doi.org/10.1016/j.jenvman.2017.03.020>
- Weinstock, J. (1981). Energy dissipation rates of turbulence in the stable free atmosphere. *Journal of the Atmospheric Sciences*, *38*(4), 880–883. [https://doi.org/10.1175/1520-0469\(1981\)038<0880:EDROTI>2.0.CO;2](https://doi.org/10.1175/1520-0469(1981)038<0880:EDROTI>2.0.CO;2)
- Weise, T., Chiong, R., & Tang, K. (2012). Evolutionary optimization: Pitfalls and booby traps. *Journal of Computer Science and Technology*, *27*(5), 907–936. <https://doi.org/10.1007/s11390-012-1274-4>
- Welander, P. (1982). A simple heat-salt oscillator. *Dynamics of Atmospheres and Oceans*, *6*(4), 233–242. [https://doi.org/10.1016/0377-0265\(82\)90030-6](https://doi.org/10.1016/0377-0265(82)90030-6)
- Wikle, K., & Zammit-Mangion, A. (2023). Statistical deep learning for spatial and spatiotemporal data. *Annual Review of Statistics and Its Application*, *10*(1), 247–270. <https://doi.org/10.1146/annurev-statistics-033021-112628>
- Willard, J. D., Jia, X., Xu, S., Steinbach, M., & Kumar, V. (2022). Integrating scientific knowledge with machine learning for engineering and environmental systems. *ACM Computing Surveys*, *55*(4), 1–37. <https://doi.org/10.1145/3514228>
- Willard, J. D., Read, J. S., Appling, A. P., Oliver, S. K., Jia, X., & Kumar, V. (2021). Predicting water temperature dynamics of unmonitored lakes with meta-transfer learning. *Water Resources Research*, *57*(7), e2021WR029579. <https://doi.org/10.1029/2021WR029579>
- Willard, J. D., Read, J. S., Topp, S., Hansen, G. J. A., & Kumar, V. (2022). Daily surface temperatures for 185,549 lakes in the conterminous United States estimated using deep learning (1980–2020). *Limnology and Oceanography Letters*, *7*(4), 287–301. <https://doi.org/10.1002/lo2.10249>
- Wilson, R. C., Hook, S. J., Schneider, P., & Schladow, S. G. (2013). Skin and bulk temperature difference at Lake Tahoe: A case study on lake skin effect. *Journal of Geophysical Research: Atmospheres*, *118*(18), 10–332. <https://doi.org/10.1002/jgrd.50786>
- Winslow, L. A., Leach, T. H., & Rose, K. C. (2018). Global lake response to the recent warming hiatus. *Environmental Research Letters*, *13*(5), 054005. <https://doi.org/10.1088/1748-9326/aab9d7>
- Winter, T. C., Buso, D. C., Rosenberry, D. O., Likens, G. E., Sturrock, A. J. M., & Mau, D. P. (2003). Evaporation determined by the energy-budget method for Mirror Lake, New Hampshire. *Limnology & Oceanography*, *48*(3), 995–1009. <https://doi.org/10.4319/lo.2003.48.3.0995>
- Wolpert, D. H., & MacReady, W. G. (1997). No free lunch theorems for optimization. *IEEE Transactions on Evolutionary Computation*, *1*, 67–82. <https://doi.org/10.1109/4235.585893>
- Wood, T., Wherry, S., Piccolroaz, S., & Girdner, S. (2023). Future climate-induced changes in mixing and deep oxygen content of a caldera lake with hydrothermal heat and salt inputs. *Journal of Great Lakes Research*, *49*(3), 563–580. <https://doi.org/10.1016/j.jglr.2023.03.014>
- Woolway, R. I. (2023). The pace of shifting seasons in lakes. *Nature Communications*, *14*(1), 2101. <https://doi.org/10.1038/s41467-023-37810-4>
- Woolway, R. I., Huang, L., Sharma, S., Lee, S.-S., Rodgers, K. B., & Timmermann, A. (2022). Lake ice will be less safe for recreation and transportation under future warming. *Earth's Future*, *10*(10), e2022EF002907. <https://doi.org/10.1029/2022EF002907>
- Woolway, R. I., Jennings, E., & Carrea, L. (2020). Impact of the 2018 European heatwave on lake surface water temperature. *Inland Waters*, *10*(3), 322–332. <https://doi.org/10.1080/20442041.2020.1712180>
- Woolway, R. I., Jennings, E., Shatwell, T., Golub, M., Pierson, D. C., & Maberly, S. C. (2021). Lake heatwaves under climate change. *Nature*, *589*(7842), 402–407. <https://doi.org/10.1038/s41586-020-03119-1>
- Woolway, R. I., Jones, I. D., Hamilton, D. P., Maberly, S. C., Muraoka, K., Read, J. S., et al. (2015). Automated calculation of surface energy fluxes with high-frequency lake buoy data. *Environmental Modelling & Software*, *70*, 191–198. <https://doi.org/10.1016/j.envsoft.2015.04.013>
- Woolway, R. I., Jones, I. D., Maberly, S. C., French, J. R., Livingstone, D. M., Monteith, D. T., et al. (2016). Diel surface temperature range scales with lake size. *PLoS One*, *11*(3), 1–14. <https://doi.org/10.1371/journal.pone.0152466>
- Woolway, R. I., Kraemer, B. M., Lenters, J. D., Merchant, C. J., O'Reilly, C. M., & Sharma, S. (2020). Global lake responses to climate change. *Nature Reviews Earth & Environment*, *1*(8), 388–403. <https://doi.org/10.1038/s43017-020-0067-5>
- Woolway, R. I., & Merchant, C. J. (2017). Amplified surface temperature response of cold, deep lakes to inter-annual air temperature variability. *Scientific Reports*, *7*(1), 1–8. <https://doi.org/10.1038/s41598-017-04058-0>
- Woolway, R. I., & Merchant, C. J. (2018). Intralake heterogeneity of thermal responses to climate change: A study of large northern hemisphere lakes. *Journal of Geophysical Research: Atmospheres*, *123*(6), 3087–3098. <https://doi.org/10.1002/2017JD027661>
- Woolway, R. I., & Merchant, C. J. (2019). Worldwide alteration of lake mixing regimes in response to climate change. *Nature Geoscience*, *12*(4), 271–276. <https://doi.org/10.1038/s41561-019-0322-x>

- Woolway, R. I., Sharma, S., Weyhenmeyer, G., Debolskiy, A., Golub, M., Mercado-Bettin, D., et al. (2021). Phenological shifts in lake stratification under climate change. *Nature Communications*, *12*(1), 2318. <https://doi.org/10.1038/s41467-021-22657-4>
- Wu, Y., Huang, A., Yang, X., Qiu, B., Wen, L., Zhang, Z., et al. (2020). Improvements of the coupled WRF-lake model over lake Nam Co, central Tibetan plateau. *Climate Dynamics*, *55*(9–10), 2703–2724. <https://doi.org/10.1007/s00382-020-05402-3>
- Wüest, A., Bouffard, D., Guillard, J., Ibelings, B. W., Lavanchy, S., Perga, M.-E., & Pasche, N. (2021). LÉXPLORE: A floating laboratory on Lake Geneva offering unique lake research opportunities. *Wiley Interdisciplinary Reviews: Water*, *8*(5), e1544. <https://doi.org/10.1002/wat2.1544>
- Xia, W., Shoemaker, C., Akhtar, T., & Nguyen, M.-T. (2021). Efficient parallel surrogate optimization algorithm and framework with application to parameter calibration of computationally expensive three-dimensional hydrodynamic lake PDE models. *Environmental Modelling & Software*, *135*, 104910. <https://doi.org/10.1016/j.envsoft.2020.104910>
- Xiao, C., Lofgren, B. M., Wang, J., & Chu, P. Y. (2016). Improving the lake scheme within a coupled WRF-lake model in the Laurentian Great Lakes. *Journal of Advances in Modeling Earth Systems*, *8*(4), 1969–1985. <https://doi.org/10.1002/2016MS000717>
- Xue, P., Pal, J. S., Ye, X., Lenters, J. D., Huang, C., & Chu, P. Y. (2017). Improving the simulation of large lakes in regional climate modeling: Two-way lake–atmosphere coupling with a 3D hydrodynamic model of the Great Lakes. *Journal of Climate*, *30*(5), 1605–1627. <https://doi.org/10.1175/JCLI-D-16-0225.1>
- Xue, P., Ye, X., Pal, J. S., Chu, P. Y., Kayastha, M. B., & Huang, C. (2022). Climate projections over the Great Lakes region: Using two-way coupling of a regional climate model with a 3-D lake model. *Geoscientific Model Development*, *15*(11), 4425–4446. <https://doi.org/10.5194/gmd-15-4425-2022>
- Yang, B., Wells, M. G., McMeans, B. C., Dugan, H. A., Rusak, J. A., Weyhenmeyer, G. A., et al. (2021). A new thermal categorization of ice-covered lakes. *Geophysical Research Letters*, *48*(3), e2020GL091374. <https://doi.org/10.1029/2020GL091374>
- Yao, F., Livneh, B., Rajagopalan, B., Wang, J., Crétaux, J.-F., Wada, Y., & Berge-Nguyen, M. (2023). Satellites reveal widespread decline in global lake water storage. *Science*, *380*(6646), 743–749. <https://doi.org/10.1126/science.abo2812>
- Yao, H., Samal, N. R., Joehnk, K. D., Fang, X., Bruce, L. C., Pierson, D. C., et al. (2014). Comparing ice and temperature simulations by four dynamic lake models in Harp lake: Past performance and future predictions. *Hydrological Processes*, *28*(16), 4587–4601. <https://doi.org/10.1002/hyp.10180>
- Yeates, P., & Imberger, J. (2003). Pseudo two-dimensional simulations of internal and boundary fluxes in stratified lakes and reservoirs. *International Journal of River Basin Management*, *1*(4), 297–319. <https://doi.org/10.1080/15715124.2003.9635214>
- Yousefi, A., & Toffolon, M. (2022). Critical factors for the use of machine learning to predict lake surface water temperature. *Journal of Hydrology*, *606*, 127418. <https://doi.org/10.1016/j.jhydrol.2021.127418>
- Yu, S., McBride, C. G., Frassl, M. A., Hipsey, M. R., & Hamilton, D. P. (2022). dycdtools: An r package for assisting calibration and visualising outputs of an aquatic ecosystem model. *The R Journal*, *14*(4), 235–251. <https://doi.org/10.32614/RJ-2023-008>
- Zare, F., Elsawah, S., Iwanaga, T., Jakeman, A. J., & Pierce, S. A. (2017). Integrated water assessment and modelling: A bibliometric analysis of trends in the water resource sector. *Journal of Hydrology*, *552*, 765–778. <https://doi.org/10.1016/j.jhydrol.2017.07.031>
- Zhao, G., Li, Y., Zhou, L., & Gao, H. (2022). Evaporative water loss of 1.42 million global lakes. *Nature Communications*, *13*(1), 3686. <https://doi.org/10.1038/s41467-022-31125-6>
- Zhao, H., Li, J., Yuan, Q., Lin, L., Yue, L., & Xu, H. (2022). Downscaling of soil moisture products using deep learning: Comparison and analysis on Tibetan Plateau. *Journal of Hydrology*, *607*, 127570. <https://doi.org/10.1016/j.jhydrol.2022.127570>
- Zhong, Y., Notaro, M., Vavrus, S. J., & Foster, M. J. (2016). Recent accelerated warming of the Laurentian Great Lakes: Physical drivers. *Limnology & Oceanography*, *61*(5), 1762–1786. <https://doi.org/10.1002/lno.10331>
- Zhu, S., Di Nunno, F., Ptak, M., Sojka, M., & Granata, F. (2023). A novel optimized model based on NARX networks for predicting thermal anomalies in polish lakes during heatwaves, with special reference to the 2018 heatwave. *Science of the Total Environment*, *905*, 167121. <https://doi.org/10.1016/j.scitotenv.2023.167121>
- Zhu, S., Nyarko, E. K., & Hadzima-Nyarko, M. (2018). Modelling daily water temperature from air temperature for the Missouri River. *PeerJ*, *6*, e4894. <https://doi.org/10.7717/peerj.4894>
- Zhu, S., Piotrowski, A. P., Ptak, M., Napiorkowski, J. J., Dai, J., & Ji, Q. (2021). How does the calibration method impact the performance of the air2water model for the forecasting of lake surface water temperatures? *Journal of Hydrology*, *597*, 126219. <https://doi.org/10.1016/j.jhydrol.2021.126219>
- Zhu, S., Ptak, M., Choiński, A., & Wu, S. (2020). Exploring and quantifying the impact of climate change on surface water temperature of a high mountain lake in Central Europe. *Environmental Monitoring and Assessment*, *192*, 1–11. <https://doi.org/10.1007/s10661-019-7994-y>
- Zhu, S., Ptak, M., Yaseen, Z. M., Dai, J., & Sivakumar, B. (2020). Forecasting surface water temperature in lakes: A comparison of approaches. *Journal of Hydrology*, *585*, 124809. <https://doi.org/10.1016/j.jhydrol.2020.124809>
- Zhu, Y., Cheng, J., Cui, Z. X., Zhu, Q., Ying, L., & Liang, D. (2023). Physics-driven deep learning methods for fast quantitative magnetic resonance imaging: Performance improvements through integration with deep neural networks. *IEEE Signal Processing Magazine*, *40*(2), 116–128. <https://doi.org/10.1109/MSP.2023.3236483>
- Zouabi-Aloui, B., Adelana, S. M., & Gueddari, M. (2015). Effects of selective withdrawal on hydrodynamics and water quality of a thermally stratified reservoir in the southern side of the Mediterranean sea: A simulation approach. *Environmental Monitoring and Assessment*, *187*(5), 1–19. <https://doi.org/10.1007/s10661-015-4509-3>